AD_____

Award Number: DAMD17-98-1-8620

TITLE: Bioenergetic Defects and Oxidative Damage in Transgenic Mouse Models of Neurodegenerative Disorders

PRINCIPAL INVESTIGATOR: Susan E. Browne, Ph.D.

CONTRACTING ORGANIZATION: Weill Medical College of Cornell University
New York, New York 10021

REPORT DATE: May 2004

TYPE OF REPORT: Annual

PREPARED FOR: U.S. Army Medical Research and Materiel Command
Fort Detrick, Maryland 21702-5012

REPORT DOCUMENTATION PAGE

Form Approved
OMB No. 074-0188

1. AGENCY USE ONLY (Leave blank)	2. REPORT DATE	3. REPORT TYPE AND DATES COVERED
	May 2004	Annual (1 May 03 - 30 Apr 04)

4. TITLE AND SUBTITLE
Bioenergetic Defects and Oxidative Damage in Transgenic Mouse Models of Neurodegenerative Disorders

5. FUNDING NUMBERS
DAMD17-98-1-8620

6. AUTHOR(S)
Susan E. Browne, Ph.D.

7. PERFORMING ORGANIZATION NAME(S) AND ADDRESS(ES)
Weill Medical College of Cornell University
New York, New York 10021

E-Mail: Sub2001@med.cornell.edu

8. PERFORMING ORGANIZATION REPORT NUMBER

9. SPONSORING / MONITORING AGENCY NAME(S) AND ADDRESS(ES)
U.S. Army Medical Research and Materiel Command
Fort Detrick, Maryland 21702-5012

10. SPONSORING / MONITORING AGENCY REPORT NUMBER

11. SUPPLEMENTARY NOTES
Original contains color plates. All DTIC reproductions will be in black and white.

12a. DISTRIBUTION / AVAILABILITY STATEMENT
Approved for Public Release; Distribution Unlimited

12b. DISTRIBUTION CODE

13. ABSTRACT (Maximum 200 Words)

The initial three years of this project determined the contributions of bioenergetic defects and oxidative stress to neurodegeneration in Huntington's disease (HD) and amyotrophic lateral sclerosis (ALS), as previously reported. The current report period covers the second year of work on the Consortium project "Mitochondrial Free Radical Generation in Parkinson's Disease", which was appended to the original grant number. This project is to assess *in vivo* whether mitochondria are the source of free radical generation in animal models of Parkinson's disease (PD).

In this period of the study we have continued studies examining the relationship between mitochondrial complex I inhibition and free radical-mediated oxidative damage. Using *in vivo* approaches we are optimizing the doses and time-courses for detection of complex I inhibition and reactive oxygen species (ROS) generation after intracerebral administration of rotenone and pyridaben. We have found increased production of the DNA oxidative damage marker 8-hydroxydeoxyguanosine (8-OHdG) shortly (1 hour) after rotenone injection into rat striatum. Lipid peroxidation and induction of the stress-response marker heme oxygenase-1 follow DNA oxidation, concomitant with complex I inhibition. Due to an unforeseen change in personnel, a no-cost extension of one year was requested, and granted, to complete these studies in the forthcoming year.

14. SUBJECT TERMS	15. NUMBER OF PAGES
Neurotoxin	77
	16. PRICE CODE

17. SECURITY CLASSIFICATION OF REPORT	18. SECURITY CLASSIFICATION OF THIS PAGE	19. SECURITY CLASSIFICATION OF ABSTRACT	20. LIMITATION OF ABSTRACT
Unclassified	Unclassified	Unclassified	Unlimited

Table of Contents

4. INTRODUCTION

The goal of the original three-year grant proposal was to gain insight into the roles of mitochondrial energy metabolism and oxidative stress in the etiology of neuronal degeneration in degenerative diseases, specifically Huntington's disease (HD) and amyotrophic lateral sclerosis (ALS). The results of these studies have previously been reported. In 2002 this proposal was extended by the addition of a second project, entitled "Mitochondrial Free Radical Generation In Parkinson's Disease", which is a constituent (Project III) of a Research Consortium made up of four investigators. This project continues the theme of determining the interactions between energy metabolism and oxidative stress in the etiology of neurodegenerative disorders. The aims are to ascertain *in vivo*: 1) Whether inhibition of a component of the mitochondrial respiratory chain (complex I), implicated in the pathogenesis of Parkinson's disease (PD), induces pathogenesis via free radical generation; and 2) Whether mitochondria are the initial source of these free radicals. Findings may give insight into potential drug targets for PD. These questions are somewhat easier to address by *in vitro* approaches (covered in other projects within the Consortium), given the extreme technical difficulties of discretely measuring purely mitochondrial events *in vivo*. Therefore we are taking an indirect approach, by measuring the time-course and nature of oxidative events caused by toxic insults directed against discrete mitochondrial components. Results for the second year of this consortium project are presented here. *NB:* In the course of this second year the post-doctoral fellow conducting the bulk of these studies left the department. Since it took some time to recruit a replacement, a no-cost extension of one year was requested, and granted, to complete these studies. This report reflects Year 2 studies completed to date. Comprehensive results for all Year 2 studies will be submitted at the end of the extension period.

5. BODY: SUMMARY OF RESEARCH PLAN, AND PROGRESS

A. Overview of Consortium Projects

The overall goals of this grant are to gain insight into the roles of mitochondrial energy metabolism and oxidative stress in the etiology of neuronal damage and death in neurodegenerative disorders. ***This study is Project III of a Consortium consisting of four projects*** (Project I, G. Fiskum PI, Grant # 17-99-1-9483; Project II, T. Sick PI; and Project IV, I. Reynolds PI, Grant # 17-98-1-8628). Projects comprising this consortium used different *in vitro*, *ex vivo,* and *in vivo* approaches to elucidate the specific roles of mitochondria and reactive oxygen species (ROS) in the pathogenesis of Parkinson's disease (PD). **Project III** specifically addresses the contribution of mitochondrial

complex I to ROS generation *in vivo*, by measuring oxidative damage markers in rat brain after inhibiting activity of specific complex I subunits.

Parkinson's Disease, Complex I, and ROS: Oxidative damage and mitochondrial dysfunction, specifically reduced activity of NADH:ubiquinone oxidoreductase (complex I) of the electron transport chain, are well characterized components of Parkinson's disease (PD) etiology. *In vivo* studies show that complex I inhibition in the brain, by MPTP/MPP^+ or rotenone for example, can result in region-specific neuropathologic changes resembling PD. *In vitro* studies implicate mitochondria as a major source of ROS mediating oxidative damage and pinpoint a number of the >45 complex I subunits identified to date as candidate sites for ROS production.

An important step towards understanding the mechanism of region-specific cell damage in PD is to determine *in vivo* whether there is a direct link between abnormal mitochondrial function and the generation of ROS in the disease. We are approaching this question by manipulating the activities of different mitochondrial complex I subunits, using intracerebral delivery of subunit-specific complex I inhibitors in rats. Markers of ROS generation will then be examnied in post-mortem brain tissue, and *in vivo* by microdialysis, and correlated with measures of complex I activity. We will test inhibitors with different specificities for complex I subunits that are encoded both by mitochondrial (mt) DNA (eg. the ND1 subunit), or by nuclear (n) DNA (eg. the PSST subunit). We will thus determine if selectively altering certain functional components of complex I affects either its activity, and/or ROS generation. By limiting the intervention to a mitochondrial component, and by measuring ROS production shortly after the mitochondrial insult, we will ascertain if generated ROS derive from mitochondria rather than other cellular origins.

Complex I: Structure, Function and ROS Generation: NADH-ubiquinone oxido-reductase (complex I) is the first and largest enzyme complex of the mitochondrial respiratory (or "electron transport") chain. The overall function of complex I is to transfer one pair of electrons from NADH to flavin mono-nucleotide (FMN), and ultimately to ubiquinone (UQ), whilst simultaneously pumping hydrogen ions out of the mitochondrial matrix into the inter-membrane space. Complex I has a molecular mass of approximately 900-1000 kDa and comprises at least 45 subunits (Bourges et al., 2004), 7 of which are encoded by mtDNA (ND1-ND6, ND4L), and the remainder by nDNA. Subunits are organised into an L-shape structure consisting of a hydrophobic membrane arm embedded into the inner mitochondrial membrane (IMM), and a hydrophilic peripheral arm aligned perpendicular to the IMM and directed into the mitochondrial matrix. The peripheral arm has two fractions; a flavoprotein (FP) where electron transfer begins, and iron-sulphur (Fe-S) clusters (N)

several of which act as redox groups that facilitate electron transfer. Binding sites for NADH and FMN are found on the peripheral arm. The membrane arm is comprised of at least 24 nDNA-encoded subunits, the 7 mtDNA subunits, and possibly two Fe-S clusters (Okun et al., 1999).

The electron carrier NADH enables entry of electrons into complex I. There are two well defined binding sites for NADH in eukaryotes, the 51kDa and 39kDa subunits. It is believed the 39kDa subunit is required to maintain stability of the redox group "X" , facilitating electron transfer (Schulte et al., 2001). Electron input occurs via the FMN prosthetic group and the Fe-S clusters (Rasmussen et al., 2001). The 'catalytic core' of complex I is comprised of the PSST, TYKY, NUOD, ND1 and ND5 subunits (Schuler et al., 2001). PSST is a 23-kDa subunit containing one binding site for Fe-S cluster N2. It plays a vital role in electron transfer by functionally coupling N2 to CoQ (Schuler et al., 1999). The binding of CoQ is the final stage in electron transfer via complex I and an important function of the membrane arm. The actual quinone binding site has not been equivocally proven, and different studies suggest it is encoded by the ND1 and ND4 proteins (Triepels et al., 2001), or a hydrophilic 49-kDa/NUOD subunit located at the interface of the peripheral and membrane arms (Darrouzet et al., 1998). The TYKY subunit is proposed to bind two tetranuclear Fe-S clusters (N6a and N6b) that form the novel redox groups found in complex I. TYKY is part of a special class of 8Fe-ferredoxins and works as an electrical driving unit for the proton pump (Rasmussen et al., 2001).

B. Research Goals: "*Mitochondrial Free Radical Generation In Parkinson's Disease*"

YEAR 1:

AIM 1: Characterization of the regional and temporal development of complex I inhibition in specific brain regions at time points after administration of subunit-specific complex I inhibitors to rats:

(i) Stereotactic unilateral intracerebral injection of rotenone, DCCD, or pyridaben into the region of the substantia nigra of anesthetized rats; and vehicle into the contraleteral hemisphere. Rats will be sacrificed and brain tissue harvested at multiple time-points post-injection.

(ii) Spectrophotometric measurement of complex I activity, citrate synthase activity (a marker for mitochondrial number), and protein levels in post-mortem tissue from the striatum, nigra, cortex and cerebellum.

YEARS 1 AND 2:

AIM 2: Characterization of the regional and temporal development of cerebral oxidative damage after administration of rotenone, DCCD and pyridaben to rats.

(i) HPLC measurement of oxidative damage markers at time-points before and after complex inhibition (time-points and regions determined in 1) by:

a) HPLC detection of brain levels of DNA damage product 8-hydroxy-deoxyguanosine (8-OHdG),

b) HPLC and immunohistochemical detection of lipid peroxidation marker malondialdehyde in affected brain regions.

YEAR 2:

AIM 3: Assessment of levels of free radical markers in striatal exracellular fluid (ECF) microdialysates before and after inhibiting subunit activity, at time-points elucidated in (i), by:

a) HPLC detection of hydroxyl (OH^-) radical levels in microdialysates from striatum, by measuring the extent of conversion of salicylate (i.p. injection) to DHBA by OH^- (DHBA detected in dialysate).

b) HPLC detection of microdialysate levels of the DNA damage product 8-OHdG; and

c) Immunocytochemical localization of 8-OHdG throughout brains of inhibitor-treated rats.

d) Completion of oxidative damage studies begun in year 1.

NB: The Goals of this study were modified in Year1 by: 1) Removal of DCCD as a test substrate, due to its extreme toxicity to humans, combined with its ease of systemic penetration (via skin, eyes, inhalation); 2) Change in the injection site of the inhibitors. Preliminary studies to optimize the injections into the substantia nigra (SN) in rats showed pronounced inter-animal variability (due to the small size of this brain region), and substantial mechanical damage in the overlying brain regions. Since the primary aim of this study does not require selective targeting of dopaminergic nigro-straital projections, injections were targeted instead to the striatum - a larger brain region that allows more reproducible needle placement without affecting multiple other brain regions.

C. RESULTS

All studies used male Lewis rats, 250-300g at the commencement of studies. For stereotactic drug injection into the brain, rats are anesthetized with a cocktail of ketamine (100mg/kg) and xylazine (10mg/kg). Rats are placed in a Kopf stereotactic frame, and body temperature maintained at 37°C by means of a heating pad.

C1) *Summary of Year 1 Results (Reported in 2003)*

AIM 1: In the first year of this project we reported the dose-response effects of rotenone (6, 20, 60 and 120 μM) on Complex I activity, 1hr after intra-striatal injection. Complex I activity was measured in striatum, cortex and cerebellum of rotenone and vehicle (DMSO/polyethylene glycol (PEG) cocktail)-injected animals (measured spectrophotometrically, and normalized to activity of the mitochondrial matrix enzyme citrate synthase, to control for mitochondrial number in the preparation). 120μM rotenone produced the largest decrease in complex I activity. Complex I impairment, measured at multiple time-points up to 24 hours after intra-striatal injection, showed maximal enzyme inhibition at 8 and 24 hours post-rotenone (120μM) injection.

AIM 2 *(This goal was to be carried out over both years of the consortium project).*

HPLC and immunohistochemical characterization of the nature, and time-course, of oxidative damage arising after intra-striatal injections of Complex I inhibitors:

Year 1 Results: We completed immunohistochemical assessment of the effects of rotenone insult on levels of the lipid peroxidation makers malondialdehyde (MDA) and 8-iso-prostaglandin F2 (PgF2), and the oxidative stress response marker heme oxygenase-1 (HO-1), 8h and 24h after intra-striatal administration of rotenone (120μmol in 3μl) or vehicle (DMSO/PEG). Results showed increased staining for all three markers in rotenone-injected striatum, compared with the vehicle-injected contralateral striatum in the same animals, both at 8h and at 24h post-injection. The pattern and approximate numbers of positively stained cells for each marker did not differ markedly between the two time points, suggesting that the maximal initial effect on oxidation may be achieved by 8 hours. Malondialdehyde-positive cells were most prominent in the immediate vicinity of the lesion/injection site following rotenone. Iso-prostaglandin F2 showed an intermediate level of staining, but affected a larger area of striatum than malondialdehyde, while heme oxygenase-1 positive cells were the most abundant of all the markers examined, present in the largest striatal volume.

C2) YEAR 2: PROGRESS AND RESULTS

AIM 1-*Continued.* Experimental findings in Year 1 left some outstanding questions which required clarification. These led to a several additional experiments, conducted in Year 2, discussed below:

(a) ***Try to improve lesion reproducibility by changing rotenone administration route:*** We carried out pilot experiments using an alternative route of rotenone administration, namely intracerebroventricular (i.c.v.) administration, in an attempt to rapidly generate striatal lesions without inducing the mechanical damage inherent to stereotactic injections. Preliminary results using

i.c.v. injection of 120µM rotenone were extremely variable in terms of lesion size and complex I inhibition, and therefore this administration route was not pursued.

(b) ***Attempt to improve the measurement of Complex I activity changes by inhibitors, using Complex I quantitative histochemistry:*** We encountered many problems with the variability of complex I measurements in brain tissue using the spectrophotometric assay approach. This has proved to be extremely time consuming, and tissue consuming. One particular confound is that the inhibitors used are likely not affecting complex I activity throughout the entire striatum, and therefore any changes in discrete areas of striatum may be masked in our spectrophotometric assays of complex I activity that use whole striatum. Therefore we performed further time course studies on the effects of rotenone (120µM, intrastriatal injection) on complex I activity, this time using a histochemistry approach with quantitative densitometry, to localize regions of striatum in which complex I was impaired, and to quantify activity changes within these areas.

Rats were sacrificed at 1, 4, and 8 hours after unilateral injection of rotenone into one striatum (120µM, 3µl, n=6/gp), and vehicle (3µl DMSA/PEG) into the contralateral striatum. Brains were removed and frozen in isopentane at -43°C, cut into 10µm-thick coronal cryostat sections, and processed for complex I histochemistry with densitometry according to the methods of Jung *et al.* (2002) and Higgins and Greenamyre (1996), respectively. This procedure is a colorimetric assay that measures a change in color of nitro blue tetrazolium (NBT) in response to NADH oxidation by complex I. The amount of complex I activity is extrapolated from the optical density (OD) of the colored product in discrete brain regions, over a given time period. The technique requires comparison of relative enzyme products between sections, and therefore tissue sections must be processed simultaneously under identical conditions.

The areas where NADH oxidation occurred following injections were easily delineated within the striatum, as shown in Figure 1. Rotenone produced a decrease in complex I activity (increased density in this inverse exposure) in a larger area of the striatum than vehicle. Relative optical densities in affected regions are shown in Table 1, presented as the difference in optical densities between vehicle-injected and rotenone-injected striata. The extent of rotenone's effect on complex I was minimal 1h post-injection, but increased with time, and was highest 8h post-injection (Table 1). We are still in the process of optimizing incubation conditions to take advantage of this procedure in other experiments.

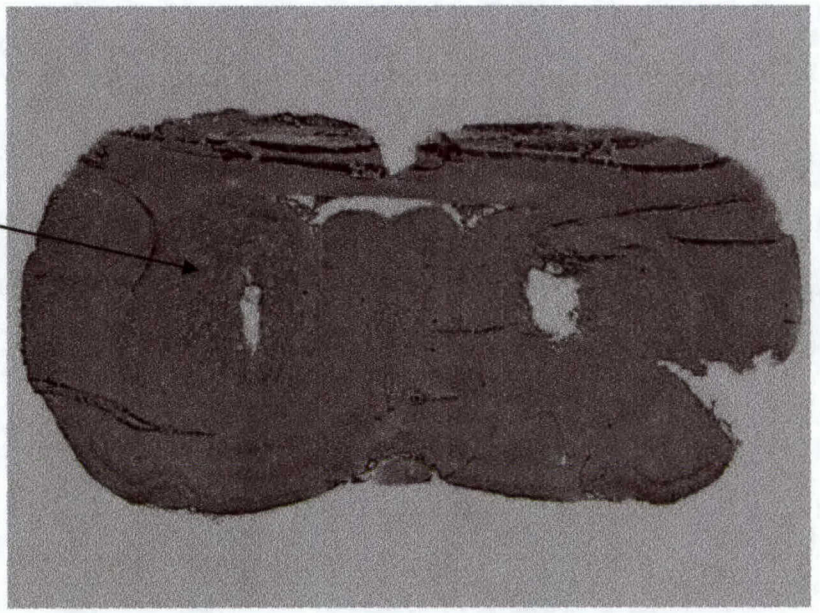

Fig 1: A representative section showing complex I activity histochemistry after injection of 120µM rotenone (left hemisphere) or vehicle (right hemisphere) into the striatum. In this "inverse" phase image a 'ring' of increased intensity appears around the rotenone injected hemisphere, compared to the vehicle-injected hemisphere where a slight increase is evident only in the area of mechanical damage immediately around the needle tract and injection site.

Table 1: The extent of NADH oxidation following intrastriatal injections. Mean difference values reflect the differences in ODs between vehicle and rotenone-injected hemispheres, measured in the same sections, at each time point (n=4-6/rats gp).

Time post-injection	**Mean Difference**	***p*-Value**
1 hour	0.009	*0.6376*
4 hours	*0.017*	*0.1595*
8 hours	*0.048*	*0.7727*

***(c)* We have also commenced experiments to determine the optimum dosing regimes for pyridaben.**

(i) ***HPLC Measurement of Tissue MDA Levels:*** We used HPLC to measure tissue levels of malondialdehyde (MDA, lipid peroxidative damage marker) in the striatum, cortex and cerebellum of rats that had received bilateral intrastriatal injections of rotenone (120µM, 3µl), or vehicle (DMSO/PEG, 3µl). Rats were sacrificed at 1, 4, and 8h after rotenone, and 8h after vehicle injection (n=6/gp). Non-injected rats (n=6) were used as baseline controls.

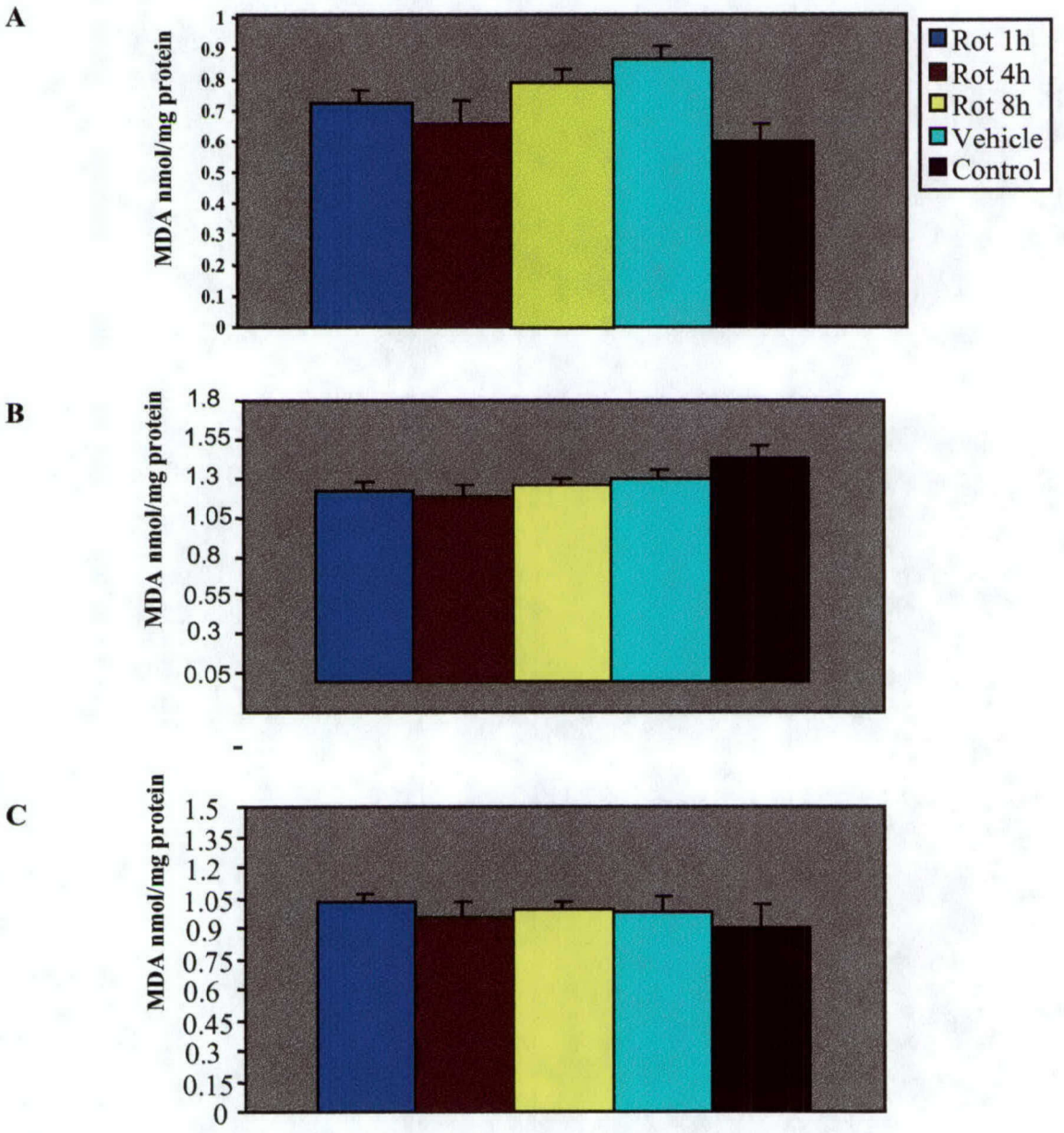

Figure 2: MDA measurements in homogenate preparations from (A) striatum, (B) cerebral cortex, and (C) cerebellum of rotenone, vehicle and un-injected rats. Data presented as mean +/- SEM (nmol/mg protein), $p>0.05$ (ANOVA, n=6/group).

Brains were removed, regions dissected out, tissue frozen in isopentane at -43°C and stored at -80°C. For HPLC analysis, tissues were homogenized in 40% ETOH. MDA in the sample was reacted with thiobarbituric acid (TBA, 42mM), in the presence of butylated hydroxytoluene (BHT, 0.05% in ETOH) and 0.44M phosphoric acid (H_3PO_4), for detection of the MDA-TBA product by the method of Agarwal and Chase (2002). MDA content was extrapolated relative to an MDA standard (Sigma, St. Louis, MO). Results for striatum, cortex and cerebellum are presented in Figure 2. MDA levels were not significantly altered in any of the regions examined up to 8h after rotenone injection. These findings contrast with our previous observations in striatum of increased MDA immunoreactivity at the site of rotenone injection, evident at 8 and 24h post-injection. We hypothesise that this discrepancy results from the fact that increased MDA immunoreactivity was restricted to an area of striatum in close proximity to the needle tract, suggesting that in this time frame MDA generation is restricted to regions close to the core area of complex I inhibition. Hence, we would not expect to detect MDA elevations in either the cortex or cerebellum, and any changes in striatum may be masked by the relatively large amount of striatal tissue sampled with respect to the area in which MDA generation is elevated.

(ii) ***Immunocytochemical assessment of oxidative damage markers in the striatum immediately after rotenone injection.*** We extended the studies begun in Year 1 of this project, which examined MDA, F2 isoprostane, and HO-1 immunostaining 8 and 24h after rotenone injection. In Year 2 we examined levels of these markers, in addition to and the DNA oxidation marker 8-hydroxydeoxyguanosine (8-OHdG), in rat striatum 1, 2 and 4h after unilateral stereotaxic intra-striatal injections of rotenone (120µM, 3µl), and vehicle (DMSO/PEG) into the contralateral striatum. Rats were perfused with 4% paraformaldehyde, their brains removed and post-fixed in paraformaldehyde for 24 hours, transferred to 70% ETOH, and then paraffin embedded. Coronal (30µm) sections were cut with a microtome. Sections were immunostained as follows:

a) *Malondialdehyde (MDA):* Rabbit anti-malondialdehyde-modified protein (kindly provided by Dr. Craig Thomas, Hoechst Marion Roussel), diluted 1:1,000.

b) *8-iso-prostaglandin F2 (PgF2)*: Rabbit anti-Pg F2 (Assay Designs Inc., Ann Arbor, MI), 1: 1,000.

c) *Heme oxygenase-1 (HO-1)*: Rabbit anti-HO-1 (StressGen, British Columbia, Canada), 1: 3,000.

d) *8-OHdG:* Mouse anti-8-OHdG (Vector Laboratories (Burlingame, CA, USA), diluted 1:500.

Haematoxylin and eosin (H&E) staining was used to delineate the the lesion in each animal.

Results are shown in Figure 3.

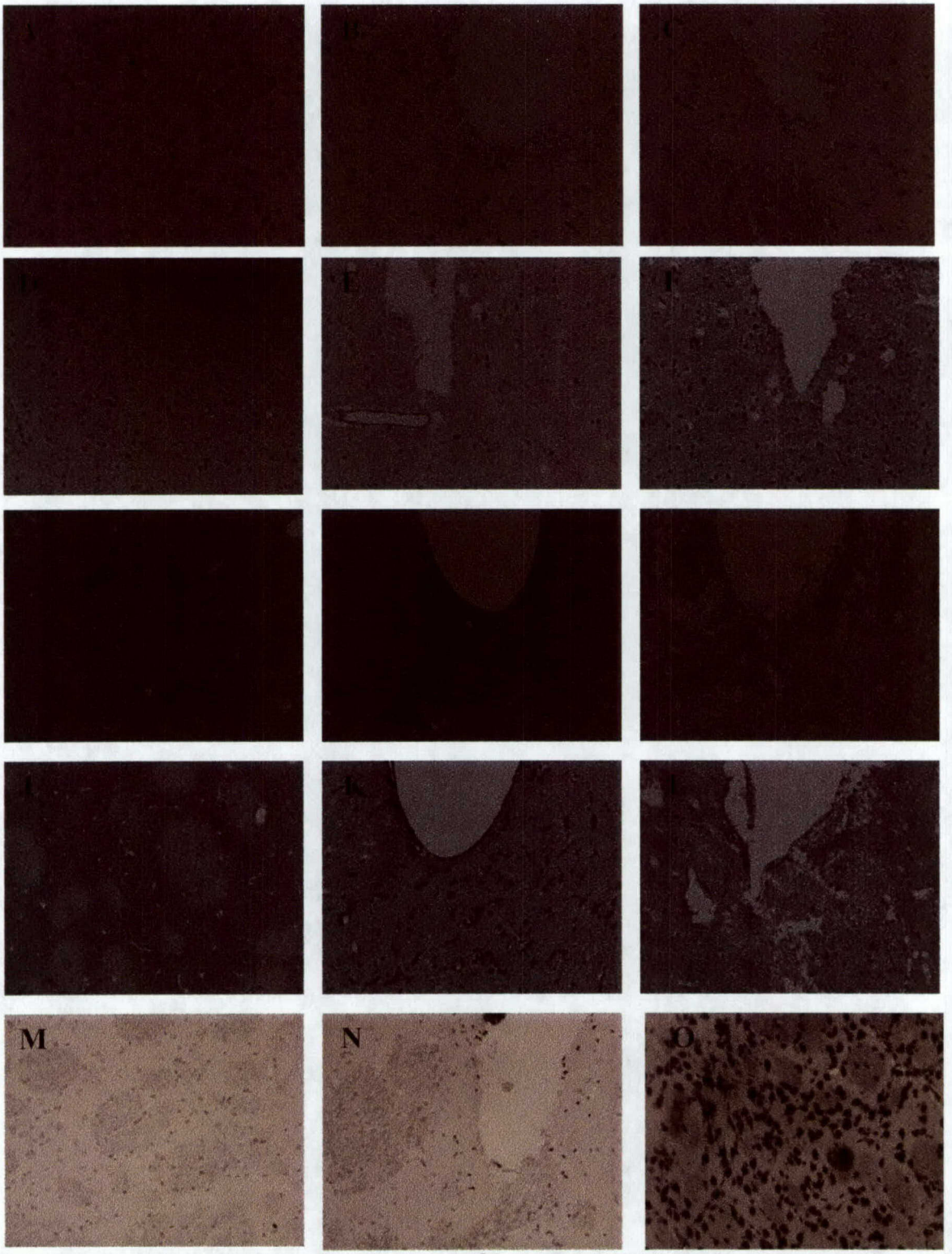

Fig 3: Immunohistochemical staining for oxidative damage markers in serial sections from the striatum of control (uninjected), vehicle, or rotenone injected animals, one hour post-injection. Left panels, a representative control rat; Center panels, Vehicle-treated; Right panels, representative sections from a rotenone-injected rat. **A-C:** Haematoxylin and eosin (H&E) staining. **D-F:** MDA; **G-I: F2-**Isoprostane; **J-L:** HO-1; **M-O:** 8-OHdG. After local administration of rotenone acute formation of 8-OHdG is seen indicating marked DNA oxidation. Local injection of rotenone did not propagate formation of oxidative markers for lipid peroxidation (MDA or F2-Isoprostane), or the stress-response element HO-1. Scale bar = 100μm

In contrast to the elevations in lipid peroxidation (MDA, PgF2) and oxidative stress (HO-1) markers by 8h post-rotenone, reported previously, these markers were unaltered acutely (1h) after rotenone injection. The DNA damage marker 8-OHdG, however, was markedly upregulated 1h after rotenone injection compared to levels in both vehicle-injected and control (uninjected) rats. The nature of the 8-OHdG effect is shown at higher magnification in Figure 4, which illustrates the concentration of 8-OHdG immunostaining within cell nuclei, rather than cytosol, consistent with DNA localization. These observations suggest that DNA oxidation is induced extremely rapidly after inhibition of complex I by rotenone, whereas other stress responses are relatively delayed. Results implicate ROS generation as a rapid and therefore potentially pathogenic consequence of rotenone administration.

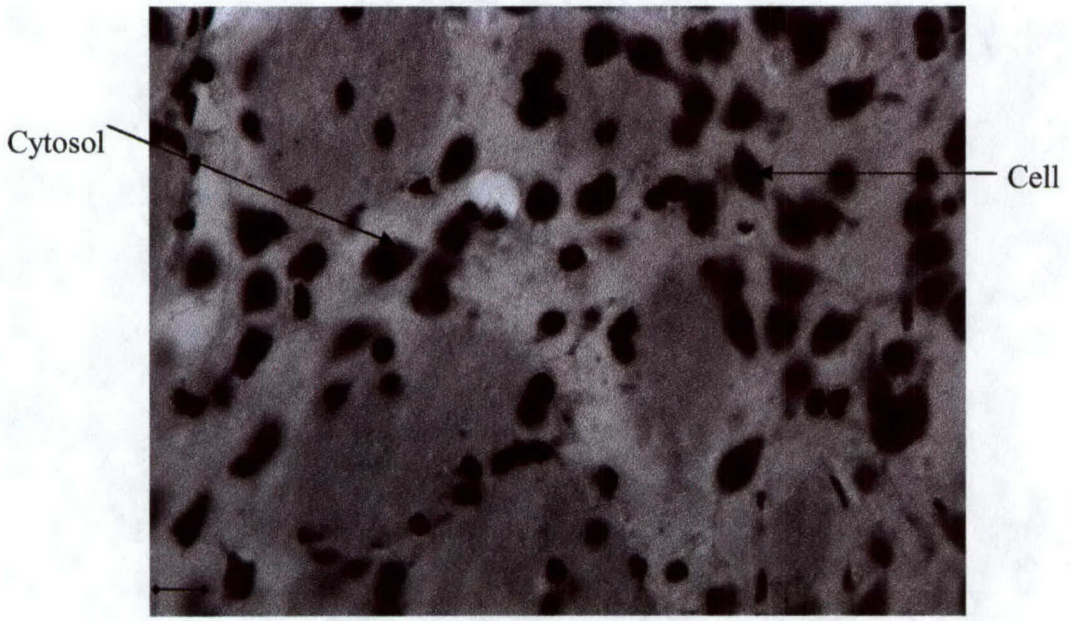

Figure 4: Magnification of plate O of Figure 3, above, demonstrating 8-0HdG localization to cell nuclei following rotenone injection into rat striatum. Scale bar = 50μm.

D. Discussion: During the second year of this study we endeavored to improve the reproducibility of complex I inhibition/lesions induced by rotenone. To this end we tested different rotenone administration routes, and different assays for qualitatively and quantitatively assessing complex I activity in rat brains. While alternative administration route proved unsatisfactory, the histochemical assay of complex I activity yielded some additional information with regards to the extent of tissue in which complex I activity is compromised at different time points after rotenone, but still needs to be refined. The major finding from Year 2 is that the complex I inhibitor rotenone induces oxidative damage extremely rapidly after introduction into tissue, with elevated levels of the DNA damage marker 8-OHdG evident as soon as 1h after rotenone injection. Damage to other cellular elements, including lipids, is slower, but is evident by 8h post-injection. We are currently assessing oxidative damage markers at intermediate time points after rotenone. We also began experiments to determine the optimum doses of pyridaben required for complex I inhibition.

The studies in the second year of this study were handicapped by the unforeseen move of the research fellow conducting the bulk of these studies, 6 months into the study. We had begun training this individual in the microdialysis procedure required for Aim 3 of these studies, but studies had to be curtailed when they left. We therefore requested a one year no-cost extension to allow us to hire another fellow, train them in microdialysis, and perform the studies in Aim 3. The results of these studies will be reported in the next annual progress report.

6. KEY RESEARCH ACCOMPLISHMENTS

- Development and characterization of the histochemical/densitometric assay of complex I activity in post-mortem rat brain sections.
- Demonstration of the area of complex I inactivation by rotenone in rat striatum, using the histochemical procedure.
- Demonstration of the temporal development of complex I activity impairments after intrastriatal rotenone injection, using the histochemical procedure.
- Testing of intracerebroventricular adminstration of rotenone to rats as a possible alternative route of inhibitor administration, to improve reproducibility of striatal complex I inhibition; and subsequent dismissal of this approach.

- Demonstration of extremely early elevations in a marker of oxidative damage to DNA (8-OHdG) in the striatum of rotenone-injected rats (evident by 1h post-injection; earliest time-point examined to date).
- Demonstration that although lipid peroxidation markers (malondialdehyde and 8-iso-prostaglandin F2) are elevated around the site of rotenone insult in rat striatum by 8h post-injection (previously shown), these markers are induced *after* DNA damage is evident (ie. they are not evident 1h post-injection).
- Demonstration that induction of the cell stress marker heme oxygenase 1 following rotenone insult in rat striatum (previously reported), follows DNA damage (ie. not evident at 1h post- injection).
- The finding that increased generation of the lipid peroxidation marker MDA locally around the site of rotenone injection 8h post-injection (reported previously), is not reflected in an overall elevation of striatal MDA levels measured by HPLC. We hypothesize this is most likely due to the discrete localization of any MDA production induced by rotenone, which may be masked in the whole-striatum homogenate preparation used for HPLC studies.

7. REPORTABLE OUTCOMES (June 2003-May 2004)

Manuscripts

Browne SE* and Beal MF. The Energetics of Huntington's Disease. *Neurochem. Res* (2004) 29: 531-46.

Petrucelli L, Dickson D, Kehoe K, Taylor J, Synder H, Kim J, Grover A, McGowan E, Prihar G, De Lucia M, Lewis J, Dillmann WH, **Browne SE**, Hall AE, Voellmy R, Dawson T, Wolozin B, Hardy J and Hutton M. CHIP and Hsp70 Regulate Tau Ubiquitination, Degradation and Aggregation. (2004) *Hum Molec Gen.* 13:703-14

Klivenyi P, Starkov AA, Calingasan NY, Gardian G, **v SE,** Yang, L, Bubber P, Gibson GE, Patel MS, Beal MF. Mice deficient in dihydrolipoamide dehydrogenase show increased vulnerability to MPTP, malonate and 3-nitropropionic acid neurotoxicity. (2004) *J. Neurochem.* 88: 1352-60.

Yang LC, Sugama S, Lorenzl S, **Browne SE**, Gregorio J, Chirichigno J, Joh TH, Beal MF, Albers DS. Minocycline exacerbates MPTP toxicity in an *in vivo* model of Parkinson's disease. *J. Neurosci. Res* (2003) 74: 278-85.

Klivenyi P, Ferrante RJ, Gardian G, **Browne S**, Chabrier P-E, Beal MF. Neuroprotective effects of BN82451 in a transgenic mouse model of Huntington's disease. *J. Neurochem.* (2003) 86: 267-272.

Browne SE, Yang L, Berger SE, DiMauro J-PP, Fuller SW, Beal MF. Metabolic changes in the G93A mouse model of familial amyotrophic lateral sclerosis precede pathologic changes. *J. Neuroscience* (2003) *Submitted.*

Book Chapter

1. **Browne SE.** Huntington's Disease. In: *Manual of Neuropsychiatric Disorders*. (2004) F Tarazi and J Schetz, Eds. *Humana Press. In press.*

Conference Abstracts

1. McConoughey SJ, **Browne SE**. (2004) Glut1 and Glut3 transporters in Huntingtin mutant mice. Forum of European Neurosci. *In press.*
2. DiMauro J-PP, McConoughey SJ, Burr HN, **Browne SE**. (2004) Mitochondrial and Energetic Dysfunction in Animal Models of Huntington's Disease. Intl. Soc. Neurochem. *Submitted.*
3. **Browne SE**, DiMauro J-PP, Albrecht RJ, Burr HN. (2003) The evolution of metabolic defects in a knock-in mutant mouse model of Huntingtons disease. Soc. Neurosci. Abs. 29: 130.12
4. Saydoff JA, Liu LS, Brenneman D, Garcia RAG, Hu ZY, Cardin S, Gonzalez A, von Borstel RW, Beal MF, **Browne SE**. (2003) Uridine prodrug PN401 is neuroprotective in the R6/2 and N171-82Q mouse models of Huntington's disease. Soc. Neurosci. Abs. 29: 130.11
5. Kim S-Y, Marekov L, Bubber P, **Browne S**, Stavrovskaya I, Son JH, Beal MF, Blass JP, Gibson GE, Cooper AJL. (2003) Mitochondrial Aconitase as a Transglutaminase Target: Implication for Mitochondrial Dysfunction in Huntington Brain. Soc. Neurosci. Abs. 29: 130.5
6. Choi D, Kim Y, Lorenzl S, Yang L, Sugama S, **Browne SE**, Beal F, Joh T. (2003) Attenuation of MPTP-elicited degeneration of SN DA neurons in MMP-3 null mice. Soc. Neurosci. Abs. 29: 409.14
7. Kwong JQ, Begum H, **Browne SE**, Beal MF, Kaplitt MG, Manfredi G. (2003) RNAi-Mediated inhibition of mutated htt in Huntington's disease models. Soc. Neurosci. Abs. 29: 208.18
8. Calingasan NY, Klivenyi P, Gardian G, Chen J, **Browne SE**, Beal MF. (2003) Dihydrolipoamide dehydrogenase (DLD) deficiency increases the vulnerability of mouse brain to mitochondrial toxins. Soc. Neurosci. Abs. 29: 732.2
9. Burr H, DiMauro J-PP, Gregorio J, **Browne SE**. (2003) [^{14}C]-2-Deoxyglucose in vivo autoradiographic studies reveal alterations in cerebral metabolism precede pathologic changes in two mutant mouse models of Huntingtin's disease. Brain 03 & Brain/PET 03, J.CBF Metab. 23 (Supp. 1): 585.

Invited Presentations

June 5th 2003 University of Edinburgh, SCOTLAND, UK,

Department of Neuroscience Seminar Series.
"The Cerebral Energetics of Huntington's Disease".

November 17th 2003 Farber Institute for Neuroscience, Research Seminar
Thomas Jefferson University Medical College, Philadelphia, PA, USA.
"CNS Energetics and SOD1 in ALS Pathogenesis".

December 2nd 2003 McLean Hospital, Neuroscience Seminar.
Harvard Medical School, Belmont, MA, USA.
"CNS Metabolism and the pathogenesis of ALS."

March 19th 2004 Mayo Clinic Seminar Series,
Mayo Jacksonville, Jacksonville, FL, USA.
"CNS Energy Metabolism and the Pathogenesis of Huntington's Disease".

8. CONCLUSIONS

The overall goals of this proposal were to gain insight into the roles of CNS energy metabolism defects and oxidative stress in mechanisms of neuronal death and dysfunction in neurodegenerative disorders. Outcomes may impact therapeutic strategies for treatment of both degenerative disorders and neurotoxin exposure. Previous studies in human and animal models have implicated the involvement of mis-metabolism and oxidative damage in the pathogenesis of several neurodegenerative diseases including Parkinson's disease (PD), Huntington's disease (HD), and amyotrophic lateral sclerosis (ALS). This project concentrated largely on using *in vivo* techniques in whole animal models of degenerative disorders to gain insight into disease mechanisms at multiple stages of pathogenesis.

In the first three years of this grant we made substantial progress in characterizing the nature of changes in cerebral energy metabolism seen in theR6/2, N171-82Q and *Hdh* mouse models of HD, both *in vivo* and *in vitro*. We also showed that cerebral glucose metabolism is impaired in the G93A transgenic mouse model of ALS (overexpressing human mutant SOD1) at 60 days of age, and ATP generation is depressed as early as 30 days. Our observations suggest that energetic dysfunction may play an intrinsic role in the pathogenesis of the motor neuron disorder seen in both HD and ALS mouse models, since alterations precede symptomatic and pathological changes in these animals.

In the period of this grant report, we have extended studies into the role of mitochondria, and in particular mitochondrial complex I, as a source of reactive oxygen species (ROS) in PD. We have further characterized the nature of the complex I inhibition induced by rotenone, and have commenced studies with another complex I inhibitor, pyridaben, which shows a different pattern of complex I subunit specificity to rotenone. We have also expanded on our novel observations of

increased free radical-mediated damage after rotenone injection into rat striatum. Notably, we have been able to demonstrate that oxidative damage to DNA is evident as soon as 1h post-rotenone injection. In the concluding experiments of this project, to be performed in the next year, we will further characterize the nature and time course of oxidative damage induced by complex I inhibitors by looking at shorter time-points post-injection, and using microdialysis approaches to measure free radical generation around the sites of inhibitor injections *in vivo*.

9. REFERENCES CITED

Agarwal, R. and S. Chase (2002). Rapid, fluorimetric-liquid chromatographic determination of malondialdehyde in biological samples. *J Chromatography_B* 775: 121-6.

Alam M, Schmidt WJ. (2002) Rotenone destroys dopaminergic neurons and induces parkinsonian symptoms in rats. *Behav Brain Res.* 136:317-24.

Antkiewicz-Michaluk L, Karolewicz B, Romanska I, Michaluk J, Bojarski AJ, Vetulani J. (2003) 1-Methyl-1,2,3,4-tetrahydroisoquinoline protects against rotenone-induced mortality and biochemical changes in rat brain. *Eur J Pharmacol.* 466:263-9.

Betarbet, R., Sherer, T.B., MacKenzie, G., Garcia-Osuna, M., Panov, A.V. and Greenamyre, J.T., (2000). Chronic systemic pesticide exposure reproduces features of Parkinson's disease. *Nat. Neurosci.* 3: 1301–1306.

Bourges I, Ramus C, Mousson De Camaret B, Beugnot R, Remacle C, Cardol P, Hofhaus G, Issartel JP. (2004) Structural organization of mitochondrial human complex I: role of the ND4 and ND5 mitochondria-encoded subunits and interaction with the prohibitin. *Biochem J.* Jul 13 [Epub]

Darrouzet E, I. J., Lunardi J, Dupuis A. (1998). The 49-kDa subunit of NADH-ubiquinone oxidoreductase (Complex I) is involved in the binding of piericidin and rotenone, two quinone-related inhibitors. *Fed Euro Biochem Soc Letts* 431*:* 34-38.

Gonzales S, Erario MA, Tomaro ML. (2002) Heme oxygenase-1 induction and dependent increase in ferritin. A protective antioxidant stratagem in hemin-treated rat brain. *Dev Neurosci.* 24:161-8.

Hatefi Y. (1978) Preparation and properties of NADH: ubiquinone oxidoreductase (complex I). EC 1.6.5.3. *Meth Enzymol.* 53: 11-14.

Higgins DS Jr, Greenamyre JT. (1996) [3H]dihydrorotenone binding to NADH: ubiquinone reductase (complex I) of the electron transport chain: an autoradiographic study. *J Neurosci.* 16:3807-16.

Hoglinger GU, Feger J, Prigent A, Michel PP, Parain K, Champy P, Ruberg M, Oertel WH, Hirsch EC. (2003) Chronic systemic complex I inhibition induces a hypokinetic multisystem degeneration in rats. *J Neurochem.* 84:491-502.

Jung C, Higgins CM, Xu Z. (2002) A quantitative histochemical assay for activities of mitochondrial electron transport chain complexes in mouse spinal cord sections. *J Neurosci Meth.* 114:165-72.

Magnitsky S, Toulokhonova L, Yano T, Sled VD, Hagerhall C, Grivennikova VG, Burbaev DS, Vinogradov AD, Ohnishi T. (2002) EPR characterization of ubisemiquinones and iron-sulfur

cluster N2, central components of the energy coupling in the NADH-ubiquinone oxidoreductase (complex I) in situ. *J Bioenerg Biomembr.* 34:193-208.

Okun JG, L. P., Brandt U (1999). Three classes of inhibitors share a common binding domain in mitochondrial complex I (NADH:ubiquinone oxidoreductase). *J Biol Chem* 274: 2625-30.

Rasmussen TSD, Brors B, Kintscher L, Weiss H, Friedrich T (2001). Identification of two tetranuclear FeS clusters on the ferredoxin-type subunit of NADH:ubiquinone oxidoreductase (complex I). *Biochem.* 40: 6124-31.

Schuler FCJ. (2001) Functional coupling of PSST and ND1 subunits in NADH:ubiquinone oxidoreductase established by photoaffinity labeling. *Biochimica et Biophysica Acta* 1506: 79-87.

Schuler FYT, Di Bernardo S, Yagi T, Yankovskaya V, Singer TP, Casida JE. (1999). NADH-quinone oxidoreductase: PSST subunit couples electron transfer from iron-sulfur cluster N2 to quinone. *PNAS USA* 96: 4149-53.

Schulte U. (2001). Biogenesis of Respiratory Complex 1. *J Bioenerg and Biomembr.* 33: 205-12.

Shepherd D and Garland PB. (1969) Citrate synthase from rat liver. *Meth. Enzymol.* 13: 11-16.

Sherer TB, Kim JH, Betarbet R, Greenamyre JT. (2003) Subcutaneous rotenone exposure causes highly selective dopaminergic degeneration and α-synuclein aggregation. *Exp Neurol.* 179:9-16.

Triepels RH, V. D. H. L., Trijbels JM, Smeitink JA. (2001). Respiratory chain complex I deficiency. *Amer J Med Genet.* 106: 37-45.

10. APPENDIX

a) C.V. for Dr, Browne (PI) attached

b) 5 manuscripts published in the last 12 months are appended:

Browne and Beal. (20044) *Neurochem. Res* (2004) 29: 531-46.

Petrucelli L, et al. (2004) *Hum Molec Gen.* 13:703-14

Klivenyi et al. (2004) *J. Neurochem.* 88: 1352-60.

Yang et al. (2003) *J. Neurosci. Res* 74: 278-85.

Klivenyi et al. (2003) *J. Neurochem.* 86: 267-272.

CURRICULUM VITAE

Name and Title: Susan Elizabeth Browne Ph.D., Assistant Professor.

Date of Birth: 13th December 1966

Academic Address: Neurology and Neuroscience, Weill Medical College of Cornell University, Neurology Dept., A502, 525 E. 68th St., New York NY 10021.

Tel: (212) 746-4672
Fax: (212) 746-8276
E-mail: sub2001@ med. cornell.edu

Education:

1985-1989 B.Sc. (with Honors), Pharmacology. University of Aberdeen, Scotland

1989-1993 Ph.D., Neuroscience. University of Glasgow, Scotland.
"Excitatory amino acid receptor-mediated events in the brain: Quantitative autoradiographic studies."
Supervisor: Prof. James McCulloch, Wellcome Surgical Institute.

Professional Experience:

1993-1996 **Post-Doctoral Research Fellow**, Neurology Research, Massachusetts General Hospital (MGH) and Harvard Medical School (HMS), Boston MA.

1996-1999 **Instructor**, Neurology Research, MGH and HMS, Boston MA.

1997-1999 **Assistant**, Neurology Service, Harvard Medical School, Boston MA.

1999 - Present **Assistant Professor** of Neuroscience, Weill Medical College of Cornell University, New York NY.

2001 - Present **Assistant Professor**, Weill Graduate School of Medical Sciences of Cornell University; Program in Neuroscience.

Grant Support, *PI:*

1998-2004 **USAMRAA: DAMD 7-98-1-8620: *PI***
Neurotoxin Exposure Treatment Research Program:
"Bioenergetic defects and oxidative damage in transgenic mouse models of neurodegenerative disorders".

1997-2005 **Huntington's Disease Society of America: *Co-PI.***
Coalition for the Cure:
"Metabolic defects and oxidative damage in a transgenic mouse model of Huntington's disease."

2000-2002 **Huntington's Disease Society of America: *PI***
"The role of energy metabolism in pathogenesis in transgenic mouse models of HD and another CAG repeat disorder".

Investigator:

1999-2008 **NIH: 1R01 NS39258** (PI: Beal)
'Bioenergetics in animal models of Huntington's Disease"
Investigator

2003-2004 **The AT Childrens Project** (PI: Beal)
Investigator

Fellowships:

1996-1999 **Amyotrophic Lateral Sclerosis Association:**
"An *in vivo* investigation of the cerebral metabolic consequences of motor neuron disease: Measurement of local cerebral glucose utilization in a transgenic mouse model of familial ALS."

1996-1999	**Muscular Dystrophy Association:** "Cerebral energy metabolism in a transgenic mouse model of ALS."
1995	**Sandoz Foundation for Gerontological Research:** "Effect of impairment of mitochondrial energy metabolism and oxidative damage on cerebral glucose metabolism."
1993-1995	**Huntington's Disease Society of America:** "Mitochondrial energy metabolism and oxidative damage in Huntington's disease."
Prizes/Awards:	
1989	Wellcome Trust Ph.D. Studentship
1997	*HDSA / Astra Merck Scholarship* WFN HD Research Meeting, Sydney, Australia.
Teaching:	*Weill Graduate School of Medical Sciences of Cornell University*
2000-present	**Course Director:** "The Neurobiology of Degenerative Diseases". Neuroscience Graduate Program. **Lecturer**: "Molecular Neuropharmacology". Neuroscience and Pharmacology Graduate Program.
2000-2002	**Lecturer:** "Brain and Mind". Neuroanatomy, Weill Medical College.
Students: 2001- 2003	Ph.D. Rotation Supervisor: Christina Higgins; Stephen McConoughey Adriana Galvan , Carl Wonders, B. Med (Australia) Supervisor: Debbie Fried.
Committees and Professional Affiliations:	NINDS Reviewer (2003-) Institutional Animal Care and Use Committee (WMC, 2003-present) British Neuroscience Association UK (1991-present) Society for Neuroscience (1994-present) International Society of Cerebral Blood Flow and Metabolism (1997-) American Society for Neurochemistry (2002-present)
Local Coordinator:	Society for Neuroscience Greater New York Chapter (2004-)
Journal Reviewer:	Brain Research, Eur. J. Neuroscience, Exp. Neurology, J. Cerebral Blood Flow & Metabolism, J. Neurochemistry, J. Neuroscience, Neurobiology of Disease, Stroke.
Techniques: *In Vivo* (rats and mice):	[^{14}C]-2-deoxyglucose autoradiographic measurement of local cerebral metabolic rates for glucose, in conscious rats and mice. [^{14}C]-methylglucose autoradiography. [^{125}I]-MK-801 autoradiography. Stereotactic intracerebral injections: excitotoxin and mitochondrial toxin lesions of discrete brain regions. Mechanical visual pathway lesions by orbital enucleation. Vascular cannulation. Systemic drug administration.
In Vitro: (human and rodent CNS tissue):	Quantitative ligand binding autoradiography, sections and homogenates. Histological lesion analysis. Immunocytochemistry Densitometry. Mitochondrial isolation from tissue. Spectrophotometric metabolic enzyme activity assays. Mitochondrial and nuclear DNA extraction. HPLC detection of oxidative damage products. Oxygraph. ATP synthesis luciferin/luciferase assay. PCR. RT-PCR. Affymetrix gene microarry.

PUBLICATIONS

1. **BROWNE SE*** and Beal MF. The Energetics of Huntington's Disease. *Neurochem. Res* (2004) 29: 531-46.
2. **BROWNE SE,** Roberts II LJ, Dennery PA, Doctrow SR, Beal MF, Barlow C, Levine RL. Treatment with a catalytic antioxidant corrects the neurobehavioral defect in ataxia-telangiectasia mice. (2004) *Free Rad Biol Med.* 36:938-942
3. Petrucelli L, Dickson D, Kehoe K, Taylor J, Synder H, Kim J, Grover A, McGowan E, Prihar G, De Lucia M, Lewis J, Dillmann WH, **BROWNE SE**, Hall AE, Voellmy R, Dawson T, Wolozin B, Hardy J and Hutton M. CHIP and Hsp70 Regulate Tau Ubiquitination, Degradation and Aggregation. (2004) *Hum Molec Gen.* 13:703-14
4. Klivenyi P, Starkov AA, Calingasan NY, Gardian G, **BROWNE SE,** Yang, L, Bubber P, Gibson GE, Patel MS, Beal MF. Mice deficient in dihydrolipoamide dehydrogenase show increased vulnerability to MPTP, malonate and 3-nitropropionic acid neurotoxicity. (2004) *J. Neurochem.* 88: 1352-60.
5. Yang LC, Sugama S, Lorenzl S, **BROWNE SE**, Gregorio J, Chirichigno J, Joh TH, Beal MF, Albers DS. Minocycline exacerbates MPTP toxicity in an *in vivo* model of Parkinson's disease. *J. Neurosci. Res* (2003) 74: 278-85.
6. Klivenyi P, Ferrante RJ, Gardian G, **BROWNE S**, Chabrier P-E, Beal MF. Neuroprotective effects of BN82451 in a transgenic mouse model of Huntington's disease. *J. Neurochem.* (2003) 86: 267-272.
7. Wu AS, Aguirre N, Calingasan NY, **BROWNE SE**, Crow JP, Kiaei M, Beal MF. Iron porphyrin treatment extends survival in a transgenic animal model of amyotrophic lateral sclerosis. *J. Neurochem.* (2003) 85:142-150.
8. **BROWNE SE*,** Beal MF. Toxin-induced mitochondrial dysfunction. *Int Rev Neurobiol.* (2002) 53: 243-79.
9. Andreassen OA, Dedeoglu A, Stanojevic V, Hughes DB, **BROWNE SE**, Leech CA, Ferrante RJ, Habener JF, Beal MF, Thomas MK. Huntington's Disease of the Endocrine Pancreas: Insulin Deficiency and Diabetes Mellitus due to Impaired Insulin Gene Expression. *Neurobiol Dis* (2002) 11:410-424.
10. **BROWNE SE**, Lin L, Mattson A, Georgievska B, Isacson O. Cognitive deficits correlate with sustained cerebral hypometabolism after selective degeneration of the basal forebrain cholinergic system in rats. *Expt. Neurol.* (2001) 170: 36-47.
11. Jeitner TM, Bogdanov MB, Mattson WR, Daikhin Y, Yudkoff M, Folk JE, Steinman L, **BROWNE SE,** Beal MF, Blass JP, Cooper AJL. N(epsilon)-(gamma-L-glutamyl)-L-lysine (GGEL) is increased in cerebrospinal fluid of patients with Huntington's disease. *J Neurochem.* (2001) 79:1109-1112.
12. Andreassen OA, Dedeoglu A, Ferrante RJ, Jenkins BG, Ferrante KL, Thomas M, **BROWNE SE**, Friedlich A, Hersch SM, Borchelt DR, Ross CA, Beal MF. Creatine increases survival and delays motor symptoms in a transgenic animal model of Huntington's disease. *Neurobiol. Ageing.* (2001)) 8: 479-491.
13. Albers DS, Augood SJ, Park LCH, **BROWNE SE**, Martin DM, Adamson J, Hutton M, Standaert DG, Vonsattel JPG, Gibson GE, Beal MF. Frontal lobe dysfunction in PSP: Evidence for oxidative stress and mitochondrial impairment. *J. Neurochem.* (2000). 74: 878-881.
14. **BROWNE SE***, Ferrante RJ, Beal MF. Oxidative stress in Huntington's disease. *Brain Pathol.* (1999) 9: 147-163.
15. **BROWNE SE***, Ayata C, Huang PL, Moskowitz MA, Beal MF. Lack of either endothelial or neuronal nitric oxide synthase isoforms does not differentially affect basal cerebral glucose metabolism in knockout mice. *J. Cereb Blood Flow Metab.* (1999) 19:144-148.
16. **BROWNE SE***. Neurodegenerative disease. *IDrugs* (1999) 2: 4-6.
17. Polidori MC, Mecocci P, **BROWNE SE**, Senin U, Beal MF. Oxidative damage to mitochondrial DNA in Huntington's disease parietal cortex. *Neurosci Lett* (1999) 272:53-6
18. Simon DK, Pulst SM, Sutton JP, **BROWNE SE**, Beal MF, Johns DR. Familial multisystem degeneration with parkinsonism associated with the 11778 mitochondrial DNA mutation. *Neurology* 1999; 53:1787-93.

19. **BROWNE SE**, Bowling AC, Baik MJ, Gurney M,Brown RH Jr., Beal MF. Metabolic dysfunction in familial, but not sporadic, amyotrophic lateral sclerosis. *J. Neurochem.* (1998) 71: 281-287.
20. **BROWNE SE***, Muir J, Robbins TW, Page KJ, Everitt BJ, McCulloch J. The cerebral metabolic effects of manipulating glutamatergic systems within the basal forebrain in conscious rats. *Eur. J. Neurosci.* (1998) 10: 649-663.
21. Matthews RT, Yang L, **BROWNE SE**, Baik MJ, Beal MF. Coenzyme Q_{10} administration increases brain mitochondrial concentrations and exerts neuroprotective effects. *PNAS* (1998) 95: 8892-8897.
22. **BROWNE SE**, Bowling AC, MacGarvey U, Baik MJ, Berger SC, Muqit MMK, Bird ED, Beal MF. Oxidative damage and metabolic dysfunction in Huntington's disease: selective vulnerability of the basal ganglia. *Ann. Neurol.* (1997) 41: 646-653.
23. Ferrante RJ, **BROWNE SE**, Shinobu LA, Bowling AC, Baik MJ, MacGarvey U, Kowall NW, Brown RH Jr, Beal MF. Evidence of increased oxidative damage in both sporadic and familial amyotrophic lateral sclerosis. *J. Neurochem.* (1997) 69: 2064-2074.
24. Beal MF, Ferrante RJ, **BROWNE SE**, Matthews RT, Kowall NW, Brown RH Jr. Increased 3-nitrotyrosine in both sporadic and familial amyotrophic lateral sclerosis. *Ann. Neurol.* (1997) 42: 644-654.
25. Matthews RT, Ferrante RJ, Jenkins BG, **BROWNE SE**, Goetz K, Berger S, Chen IY, Beal MF. Iodoacetate produces striatal excitotoxic lesions. *J. Neurochem.* (1997) 69: 285-289.
26. Schulz JB, Matthews RT, Muqit MMK, **BROWNE SE**, Beal MF. Inhibition of neuronal nitric oxide synthase by 7-nitroindazole protects against MPTP-induced neurotoxicity in mice. *J. Neurochem.* (1995) 64: 936-939.
27. Macrae IM and **BROWNE SE**. Brain structures involved in the hypotensive effects of rilmenidine: evaluation by [^{14}C]2-deoxyglucose autoradiography. *J. Cardiovasc. Pharmacol.* (1995) 26 Suppl 2:S55-58.
28. **BROWNE SE** and Beal MF. Oxidative damage and mitochondrial dysfunction in neurodegen-erative diseases. *Biochem. Soc. Trans.* (1994) 22: 1002-1006.
29. **BROWNE SE** and Macrae IM. Differential patterns of local cerebral glucose utilisation associated with rilmenidine- or B-HT 933-induced hypotension. *Brain Res.* (1994) 666: 216-222.
30. **BROWNE SE** and McCulloch J. AMPA receptor antagonists and local cerebral glucose utilization in the rat. *Brain Res.* (1994) 641: 10-20.
31. Fujisawa H, Dawson D, **BROWNE SE**, MacKay KB, Bullock R, McCulloch J. Pharmacological modification of glutamate neurotoxicity *in vivo*. *Brain Res.* (1993) 629: 73-78.
32. **BROWNE SE**, Horsburgh K, Dewar D, McCulloch J. D-[^{3}H]-Aspartate binding does not map glutamate-releasing neurones in the retino-fugal projection: an autoradiographic comparison with [^{3}H]-cyclohexyladenosine binding. *Molec. Neuropharmacol.* (1991) 1: 129-133.
33. Pertwee RG, **BROWNE SE**, Ross TM, Stretton CD. An investigation of the involvement of GABA in certain pharmacological effects of delta-9-tetrahydrocannabinol. *Pharmacol. Biochem. Behav.* (1991) 40: 581-585.

BOOK CHAPTERS

1. **BROWNE SE.** Huntington's Disease. In: *Manual of Neuropsychiatric Disorders*. (2004) F Tarazi and J Schetz, Eds. *Humana Press. In press.*
2. **BROWNE SE**, Beal MF. Toxin Induced Mitochondrial Dysfunction. In: *Mitochondrial Function and Dysfunction.* AHV Schapira, Ed. *Academic Press* (2002) 241-280.
3. **BROWNE SE**, Beal MF. Huntington's disease. In: Functional Neurobiology of Ageing. PR Hof, CV Mobbs, Eds. *Academic Press* (2000) 711-725.
4. **BROWNE SE**. Mitochondrial dysfunction and oxidative damage in Huntington's disease. In: *Neurodegenerative Diseases: Mitochondria and Free Radicals in Pathogenesis.* MF Beal, I Bodis-Wollner, N Howell Eds. *Wiley-Liss Inc.* (1997) 361-374.

ABSTRACTS (Last 2 Years)

1. McConoughey SJ, **Browne SE**. (2004) Glut1 and Glut3 transporters in Huntingtin mutant mice. *Forum of European Neurosci.* In press.
2. DiMauro J-PP, McConoughey SJ, Burr HN, **Browne SE**. (2004) Cerebral Glucose Utilization Defects precede Pathological Changes in Mouse Models of Huntington's Disease. *Gordon Research Conference: Brain Energy Metabolism and Blood Flow.* Submitted.
3. DiMauro J-PP, McConoughey SJ, Burr HN, **Browne SE**. (2004) Mitochondrial and Energetic Dysfunction in Animal Models of Huntington's Disease. *Intl. Soc. Neurochem.* Submitted.
4. **Browne SE**, DiMauro J-PP, Albrecht RJ, Burr HN. (2003) The evolution of metabolic defects in a knock-in mutant mouse model of Huntingtons disease. *Soc. Neurosci. Abs.* 29: 130.12
5. Saydoff JA, Liu LS, Brenneman D, Garcia RAG, Hu ZY, Cardin S, Gonzalez A, von Borstel RW, Beal MF, **Browne SE**. (2003) Uridine prodrug PN401 is neuroprotective in the R6/2 and N171-82Q mouse models of Huntington's disease. *Soc. Neurosci. Abs.* 29: 130.11
6. Kim S-Y, Marekov L, Bubber P, **Browne S**, Stavrovskaya I, Son JH, Beal MF, Blass JP, Gibson GE, Cooper AJL. (2003) Mitochondrial Aconitase as a Transglutaminase Target: Implication for Mitochondrial Dysfunction in Huntington Brain. *Soc. Neurosci. Abs.* 29: 130.5
7. Choi D, Kim Y, Lorenzl S, Yang L, Sugama S, **Browne SE**, Beal F, Joh T. (2003) Attenuation of MPTP-elicited degeneration of SN DA neurons in MMP-3 null mice. *Soc. Neurosci. Abs.* 29: 409.14
8. Kwong JQ, Begum H, **Browne SE**, Beal MF, Kaplitt MG, Manfredi G. (2003) RNAi-Mediated inhibition of mutated htt in Huntington's disease models. *Soc. Neurosci. Abs.* 29: 208.18
9. Calingasan NY, Klivenyi P, Gardian G, Chen J, **Browne SE**, Beal MF. (2003) Dihydrolipoamide dehydrogenase (DLD) deficiency increases the vulnerability of mouse brain to mitochondrial toxins. *Soc. Neurosci. Abs.* 29: 732.2
10. Burr H, DiMauro J-PP, Gregorio J, **Browne SE**. (2003) [^{14}C]-2-Deoxyglucose *in vivo* autoradiographic studies reveal alterations in cerebral metabolism precede pathologic changes in two mutant mouse models of Huntingtin's disease. *Brain 03 & Brain/PET 03, J.CBF Metab.* 23 (Supp. 1): 585.
11. Gregorio J, DiMauro J-P P, Narr S, Fuller SW, **Browne SE**. Cerebral metabolism defects in HD: Glucose utilization abnormalities in multiple HD mouse models. *Soc. Neurosci. Abs.* (2002) 28: 195.10
12. Kim S-Y, **Browne SE**, Beal MF, Cooper AJ, Blass JP. Differential expression of transglutaminases genes in affected compared to spared regions of huntington brain. *Soc. Neurosci. Abs.* (2002) 28: 92.3
13. Wu AS, Aguirre N, Calingasan NY, **Browne SE**, Crow JP, Kiaei M, Beal MF. Iron porphyrin treatment extends survival in a transgenic animal model of amyotrophic lateral sclerosis. *Soc. Neurosci. Abs.* (2002) 28: 789.1
14. Gregorio J, Burr H, Klivenyi P, Gardian G, von Borstel RW, Saydoff JA, Beal MF, **Browne SE**. Manipulating oxidative damage and energy metabolism: Novel neuroprotectants in HD mouse models. *HDF: Changes, Advances and Good news (CAG)$_n$.* (2002) 18.
15. Kim S-Y, **Browne SE**, Beal MF, Cooper AJ., Blass JP. Transglutaminases in Huntington Brain: Possible Relation to Selective Vulnerability. *American Soc. Neurochem.* (2002)
16. **Browne SE**. Disruptions of cellular energy metabolism in HD: evidence for treatment effects? *Frontiers in Neurodegeneration – Huntington's Disease.* (2002).

INVITED SPEAKER (Last 2 years)

February 1st 2002	Frontiers in Neurodegeneration – Huntington's Disease. Reisensburg, GERMANY. *"Disruptions of cellular energy metabolism in HD: evidence for treatment effects?"*
May 7th 2002	Biochemistry Department Seminar Series University of Maryland, Baltimore, MD, USA. *"Animal Models of Neurodegenerative Disorders: Insights into Pathogenesis"*
July 20-21 2002	Hereditary Disease Foundation, Mary Jennifer Selznick Workshop, Cardiff, WALES, UK. *"Behavioral Assessment in Mouse Models of Huntington's Disease."*
October 16-18 2002	Young ALS Investigator's Workshop Lafayette, PA, USA. *"Cerebral Energy Metabolism in G93A Mice."*
April 15th 2003	American Society for Pharmacology and Experimental Therapeutics, Symposium: Animal Models of Neuropsychiatric Diseases. San Diego, CA, USA. *"Modeling Huntington's Disease in the Mouse: Mechanistic and Therapeutic Insights"*
June 5th 2003	University of Edinburgh, SCOTLAND, UK, Department of Neuroscience Seminar Series. *"The Cerebral Energetics of Huntington's Disease".*
November 17th 2003	Farber Institute for Neuroscience, Research Seminar Thomas Jefferson University Medical College, Philadelphia, PA, USA. *"CNS Energetics and SOD1 in ALS Pathogenesis".*
December 2nd 2003	McLean Hospital, Neuroscience Seminar. Harvard Medical School, Belmont, MA, USA. *"CNS Metabolism and the pathogenesis of ALS."*
March 19th 2004	Mayo Clinic Seminar Series, Mayo Jacksonville, Jacksonville, FL, USA. *"CNS Energy Metabolism and the Pathogenesis of Huntington's Disease".*

APPENDIX 2

Neurochemical Research, Vol. 29, No. 3, March 2004 (© 2004), pp. 531–546

The Energetics of Huntington's Disease*

Susan E. Browne[1,2] and M. Flint Beal[1]

(Accepted August 20, 2003)

Huntington's disease (HD) is a hereditary neurodegenerative disorder that gradually robs sufferers of the ability to control movements and induces psychological and cognitive impairments. This devastating, lethal disease is one of several neurological disorders caused by trinucleotide expansions in affected genes, including spinocerebellar ataxias, dentatorubral-pallidoluysian atrophy, and spinal bulbar muscular atrophy. HD symptoms are associated with region-specific neuronal loss within the central nervous system, but to date the mechanism of this selective cell death remains unknown. Strong evidence from studies in humans and animal models suggests the involvement of energy metabolism defects, which may contribute to excitotoxic processes, oxidative dmage, and altered gene regulation. The development of transgenic mouse models expressing the human HD mutation has provided novel opportunities to explore events underlying selective neuronal death in HD, which has hitherto been impossible in humans. Here we discuss how animal models are redefining the role of energy metabolism in HD etiology.

KEY WORDS: Huntington's disease; Huntingtin; mitochondria; energy metabolism; glucose utilization; genetic models.

INTRODUCTION

Huntington's disease (HD) is an autosomal dominantly inherited neurodegenerative disorder that is characterized by the insidious progressive development of mood disturbances, behavioral changes, involuntary choreiform movements, and cognitive impairments. Onset is most commonly in adulthood, with a typical duration of 15–20 years before premature death.

* Special issue dedicated to Professor John B. Clark.

[1] Departments of Neurology and Neuroscience, Weill Medical College of Cornell University, New York, New York.

[2] Address reprint requests to: Susan E. Browne, Department of Neurology and Neuroscience, A-502, Weill Medical College of Cornell University, 525 East 68th Street, New York, New York, 10021. Tel: 212-746-4672; Fax: (212) 746-8276; E-mail: sub2001@med.cornell.edu

DISCUSSION

The Neuropathologic and Genetic Basis of Huntington's Disease

The motor and behavioral disturbances in HD reflect the selective pattern of cell loss in the brain and the specific neurotransmitter pathways affected. Although it is often regarded as a basal ganglia disease, because the predominant neuropathological feature is progressive caudal to rostral degeneration of the caudate putamen (1), HD is in fact a multisystem disorder. By end stage, when more than 90% of caudate putamen neurons are lost and the striatum is severely atrophic and gliotic, degeneration is also evident in several other brain regions, including the cerebral cortex, globus pallidus (GP), and to a lesser extent thalamus, subthalamic nucleus, nucleus accumbens, substantia nigra, cerebellum, and white matter (1).

GABA-ergic (γ-aminobutyric acid) medium spiny projection neurons, which constitute 80% of striatal neurons, are most vulnerable in HD. The first clinical symptoms of the disease correlate with loss of 30%–40% of striatal dopamine D1 and D2 receptors localized on the medium spiny neurons (2). Within these neurons, GABA co-localizes with enkephalin (ENK), substance-P (SP), dynorphin, or calbindin. Aspiny interneurons containing nicotinamide adenine dinucleotide phosphate diaphorase (NADPH-d), neuropeptide Y (NPY), somatostatin (SS), and nitric oxide synthase (NOS) are relatively spared in HD. ENK-positive spiny neurons projecting to the external segment of the globus pallidus (GPe) degenerate earliest in the disease, preceding SP-containing neurons projecting to the internal segment (GPi) (3). Hence the spontaneous, uncontrolled movements typical of HD appear to result from the disruption of basal ganglia–thalamocortical pathways that regulate movement control (4). The pathological basis of the mood disturbances and personality changes that are often the earliest and most debilitating of the symptoms for patients, are less clear. However, it is likely that cortical neuronal dysfunction before overt cell loss, particularly in prefrontal regions, underlies these traits (5).

The genetic defect in HD is an expansion of an unstable CAG repeat encoding glutamines (Q), close to the 5′ end of the chromosome 4 gene for huntingtin protein (6). Expansion of this trinucleotide stretch to 34–39 CAG repeats in one allele confers risk of developing HD, but above 39 repeats the disease is completely penetrant. Several features of the disease phenotype are influenced by CAG repeat length, including age of onset (7) and the extent of DNA fragmentation in striatal neurons (8). HD also shows the trait of "anticipation" resulting from instability of the repeat size during transmission (9).

Despite knowledge of the HD gene defect, mutant huntingtin's toxic action has not yet been identified. In fact, the function of wildtype huntingtin is not clear either, although it is implicated in developmental apoptosis, neurogenesis, and intracellular trafficking mechanisms (10–13). Evidence points to the mutation inducing a toxic gain of function, rather than causing loss of wildtype huntingtin function, because mice lacking one allele of wildtype huntingtin show little or no pathology (14). Huntingtin is, however, essential for development, as evidenced by the fact that *HD* homologue–null mice die *in utero*. Findings that this phenotype can be completely rescued by crossing into knock-in mice that express a mutant polyglutamine expansion (Hdh^{Q50} mice) imply that huntingtin's normal function persists despite the presence of a pathogenic glutamine repeat (11). Expression levels for huntingtin are also critical, and mice expressing abnormally low levels of murine huntingtin exhibit developmental abnormalities (15).

The preferential vulnerability of striatal neurons in HD is enigmatic and cannot be simply explained in terms of the distribution of abnormal huntingtin, because the gene mutation is expressed throughout the body and does not show a marked selectivity for cerebral regions targeted by the disease process (16,17).

Within the striatum there is some evidence suggesting differential distribution between distinct neuronal populations (18–20), but it appears more likely that vulnerability to degeneration is conferred by another property of striatal neurons. At the neuronal level, huntingtin protein is widely expressed throughout cells, with a largely cytoplasmic distribution in perikarya, axons, dendrites, and some nerve terminals. Mutant huntingtin contains several cleavage sites for caspases and proteases (21), and as the disease progresses, N-terminal fragments of huntingtin form ubiquitinated protein aggregates in neuronal nuclei (neuronal intranuclear inclusions [NII]) and in dystrophic neurites (cytoplasmic inclusions [CI]). These aggregates have been identified in both HD brain and in the brains of multiple mouse lines expressing mutant huntingtin (22–26). The question of whether huntingtin aggregates are directly toxic is still a matter of debate, although the current weight of opinion favors a lack of involvement or even a neuroprotective role (27,28). Nuclear localization of mutant htt, however, does seem to be necessary for cell damage. One study demonstrated that transfecting mouse clonal cells with either full-length or truncated huntingtin containing mutant CAG repeat lengths induced toxicity along with the formation of both nuclear and cytosolic inclusions, whereas huntingtin with wild-type CAG repeats remained within the cytoplasm and was inert (29). Inhibiting caspase activity with Z-VAD-FMK increased cell survival but had no effect on either NII or CI number, implying that neuronal death is independent of aggregate formation in this model. In addition, introducing a nuclear export signal to mutant huntingtin abrogates toxicity *in vitro* (30). A provokative corollary to this issue is a recent report suggesting that nuclear localization of mutant huntingtin only occurs in nondividing cells, perhaps contributing to the neuronal selectivity of huntingtin toxicity (31).

Although mutant huntingtin's initial toxic trigger remains elusive, experimental evidence supports roles for several different detrimental cell pathways at some stage of the degenerative process within targeted neurons. These include apoptotic cascades, excitotoxicity, the possibility of huntingtin aggregate toxicity, and pernicious effects of huntingtin protein–protein interactions, putatively via

transglutaminase-catalyzed polyglutamine interactions with glutamines, lysines, and polyamines in other proteins (32–34). The latter is a particularly intriguing hypothesis, because huntingtin has been shown to have an affinity for many proteins critically involved in cell survival, including BDNF, glyceraldehyde 3-phosphate dehydrogenase (GAPDH), calmodulin, caspase-3, α-adaptin, and a number of transcription factors, including Sp1, CBP, and p53 (32,35–38).

Another prominent component of HD pathogenesis is altered energy metabolism. Energetic defects in the HD population have been chronicled for many years; however, the specific role of impaired metabolism and mitochondrial defects in cell death pathways is still unclear. Are metabolic defects a primary event inducing cell death cascades, or are they secondary to another cellular defect? And if they are causative, how does mutant huntingtin trigger this effect? Can huntingtin directly influence mitochondrial function, or are mitochondrial defects the result of intranuclear events? The purpose of this review is to address the current status of knowledge on the role of energetic defects in cell death processes in HD, and how metabolic compromise can influence other detrimental cellular processes that are implicated in the disease. A brief review of historical evidence for metabolic defects in HD patients is presented, and the remainder of this review will concentrate more on the groundbreaking evidence gained in recent years from genetic models of the disease.

Bioenergetic Defects Are a Profound Feature of Huntington's Disease

The first hypotheses of energetic impairments in HD arose from observations of pronounced weight loss in patients, despite sustained caloric intake (39). Weight loss does not correlate with chorea, suggesting it is an insidious event resulting from the disease mutation rather than secondary to hyperactivity (40). Then positron emission tomography (PET) studies revealed that glucose metabolism in the basal ganglia and cerebral cortex is markedly reduced in symptomatic HD patients (5,41,42). Furthermore, the extent of caudate hypometabolism correlates well with declines in clinical test scores for bradykinesia, rigidity, dementia, and functional capacity. Similarly, putaminal hypometabolism predicts the extent of chorea and defects in eye movements, whilst hypometabolism in the thalamus correlates with the degree of dystonia in patients (5,43). Reduced cerebral functional activity in symptomatic patients may simply reflect neuronal loss, but more compelling evidence for a potential causative role of energetic defects comes from findings that striatal hypometabolism precedes the bulk of tissue loss and occurs in asymptomatic at-risk subjects (44–46). Approximately 50% of gene-positive mutation carriers exhibit metabolic defects years before the onset of clinical symptoms (46,47). In addition, patients suffering psychological disturbances and mood changes often exhibit cortical hypometabolism before the onset of motor symptoms (5). The involvement of a defect in glycolysis has also been suggested by findings that symptomatic HD patients have elevated lactate production in the basal ganglia and occipital cortex, detected by proton nuclear magnetic resonance (^{1}H-NMR) imaging (48,49). Interestingly, this abnormal lactate generation can be ameliorated by treatment with the metabolic cofactor coenzyme Q_{10} (50). NMR spectroscopy has also revealed marked increases in cerebrospinal fluid (CSF) pyruvate content and reductions in muscle phosphocreatine (PCr)/creatine and ATP/phosphocreatine ratios in symptomatic patients (50–52).

Consequently, biochemical studies in HD postmortem tissue have revealed alterations in the activity of several key components of oxidative phosphorylation and the tricarboxylic acid (TCA) cycle in brain regions targeted in HD. Pyruvate dehydrogenase activity is decreased in basal ganglia and hippocampus, and striatal oxygen consumption is reduced in HD patients (53). Activities of complexes II, III, and IV of the electron transport chain are markedly and selectively reduced in caudate and putamen of advanced grade (3 and 4) HD patients (54,55). Impaired complex I activity has been reported in muscle from HD patients but appears to be unaffected in brain (54,56,57). However, findings that respiratory chain enzyme activities are unchanged in presymptomatic and early-stage HD patients suggests that these enzymatic changes are secondary to the pathogenic process (58), a hypothesis largely supported by observations in mutant mouse models of HD (discussed below). The most profound enzyme defect detected in HD to date is the dramatic reduction in activity of the TCA cycle enzyme aconitase in affected brain regions and muscle ($>-70\%$; 59). Sites of metabolic abnormalities in HD are summarized in Figure 1. Interestingly, mitochondrial abnormalities and metabolic defects are also features of other trinucleotide repeat diseases including SCA1, SCA2, and SCA3, adding fuel to speculation that energetic defects play common roles in these disorders and may be directly linked to the polyglutamine defect (60,61).

GAPDH is another metabolic enzyme that has been implicated in HD pathogenesis, on the basis of the propensity for polyglutamines to bind the enzyme (35). Glycolytic activity of GAPDH, however, was

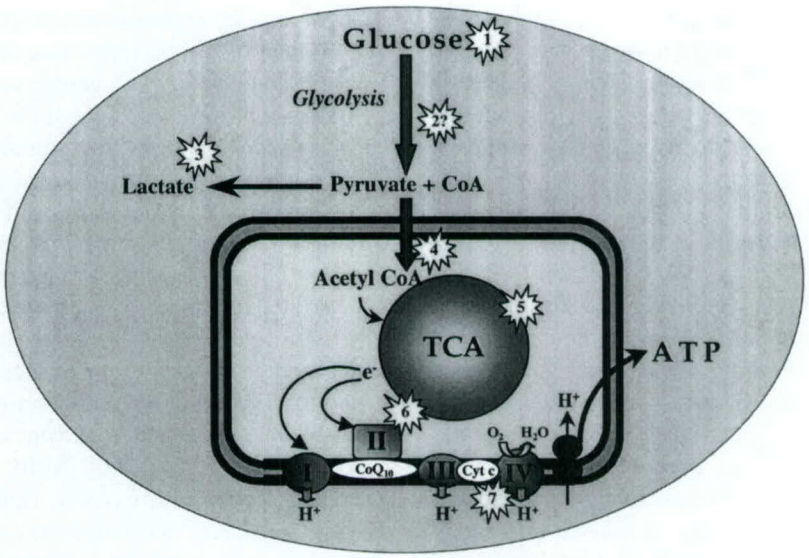

Fig. 1. A schematic representation of the sites of impairments in the glucose metabolic pathway identified to date in neurons of HD patients, and, in some cases, in mutant mouse models. *Sites:* 1, Glucose uptake; 2, glyceraldehyde-3-phosphate dehydrogenase, GAPDH (glycolytic dysfunction not proven); 3, lactate production increased; 4, pyruvate dehydrogenase; 5, aconitase; 6, succinate dehyrogenase; 7, cytochrome oxidase.

found to be conserved throughout the brain in late stage HD (54). This does not rule out the possibility that other actions of this promiscuous molecule are affected in the disease, including effects on microtubule-mediated intracellular trafficking or apoptosis. Recent reports have subsequently shown that the subcellular localization of GAPDH is altered by mutant huntingtin expression, with increased nuclear localization in both human fibroblasts and in neurons from a transgenic mouse model (62–64). The appearance of an abnormal high molecular weight form of GAPDH in fibroblast nuclei has also been associated with decreased glycolytic activity (62).

Mitochondrial Toxins Mimic Huntington's Disease

The relevance of succinate dehydrogenase (SDH) defects to the HD phenotype is underscored by the fact that mitochondrial toxins that selectively inhibit succinate dehydrogenase in the TCA cycle and complex II, namely 3-nitropropionic acid (3-NP) and malonate, induce striatal-selective lesions in humans, rodents, and primates that closely resemble those seen in HD (65,66). Systemic 3-NP intoxication in humans induces basal ganglia lesions visible by CT-scans, localized principally to the putamen but sometimes extending to the caudate, that are associated with multiple cognitive symptoms, including acute encephalopathies and coma, and motor abnormalities (65). Systemic administration of 3-NP to both rodents and primates produces age-dependent striatal lesions that are strikingly similar to those seen in HD (67,68). In primates, chronic 3-NP administration produces selective striatal lesions characterized by a depletion of calbindin neurons with sparing of NADPH-d neurons, and proliferative changes in the dendrites of spiny neurons. Animals also show both spontaneous and apomorphine-inducible choreiform movement disorders resembling those in HD (66). 3-NP basal ganglia lesions in rats are associated with elevated lactate levels, similar to the increased lactate production seen in HD patients (69). Inhibition of cerebral SDH activity by 3-NP has been demonstrated *in vivo* in a number of studies. 3-NP markedly inhibits SDH activity within 2 h of intraperitoneal administration in rodents, producing 50%–70% reductions in SDH activity throughout the brain (68; Browne and Beal, unpublished observations), consistent with the degree of complex II-III deficiency reported in HD striatum in postmortem studies (54). Interestingly, the neurodegenerative sequelae of systemic administration of the toxin are largely restricted to the striatum, despite its relatively homogeneous distribution and uniform reduction in SDH activity throughout the brain (68; Browne and Beal, unpublished observations). This observation appears to once again underscore the vulnerability of striatal neurons to metabolic stress.

Genetic Models of Huntington's Disease: How Do Energetic Defects Evolve?

The discovery of the gene mutation in HD and the subsequent generation of animal models expressing this mutation has transformed studies into HD etiology, by conferring the ability to map early events in the disease and track the development of pathologic processes relative to disease symptoms. The mutant HD gene has now been expressed in a number of different organisms, including *Caenorhabditis elegans,* drosophila, mice, and rats (28,37,70,71). Although lower organisms may provide reasonable models for rapid screening of potential therapeutic agents, rodent models are proving most useful for examining the contributions of different cellular mechanisms of disease and for testing the efficacy of putative therapeutics.

Multiple mouse models of HD now exist, falling into three broad categories: (i) Mice expressing exon-1 fragments of human huntingtin gene (*HD*) containing polyglutamine mutations (in addition to both alleles of murine wildtype huntingtin [*hdh*]). (ii) Mice expressing the full-length human *HD* gene (plus murine *hdh*). and (iii) Mice with pathogenic CAG repeats inserted into the existing CAG expansion in murine *hdh.* These models vary in terms of the site of transgene incorporation, promoter used, gene expression levels, CAG repeat length, copy number, and background mouse strain used. As a result, mouse phenotypes vary greatly between lines, as demonstrated in Table I (10,24,25,72–79). Most notably, although all models exhibit some features typical of HD (invariably including huntingtin protein aggregate formation at some stage), not all models develop striatal neuronal death. This phenomenon seems to depend ultimately on the context in which the huntingtin mutation is expressed (as demonstrated elegantly in [80]). However, some generalities can be drawn from surveying the available mouse lines. Firstly, mice require longer CAG repeats than humans to elicit pathogenic events, putatively because of their relatively short life spans. Second, age of onset of disease phenotype is accelerated by expressing gene fragments and is faster with shorter fragments. Similarly, mouse life span is more rapidly curtailed by expressing shorter fragments. In contrast, expression of longer fragments or full-length huntingtin seems to be associated with the development of neuronal death patterns more closely resembling human HD pathology. However, age of phenotype onset, aggregate formation, and cell death are all slower in full-length models (including knock-in mice) compared with fragment models. Within each of these subsets, longer CAG repeats accelerate all phenotypes.

Do Energetic Defects Contribute to Pathogenesis in Mouse Huntington's Disease Models?

The most prominent metabolic alterations in HD patients are weight loss and region-specific alterations in cerebral glucose use, cerebral lactate levels, and the activities of mitochondrial enzymes involved in glucose metabolism. These parameters are gradually being systematically investigated in different mouse HD models, and a temporal profile of pathogenic events is slowly emerging.

Reduced body weight and brain weight are features of mice expressing fragments of human huntingtin (e.g., R6/2 and N171-82Q) but are not so typical of full-length htt models (25,72). Alterations in cerebral glucose utilization, however, are early events in different HD mouse lines (81,82). Using quantitative 2-deoxyglucose densitometry in awake, freely moving mice, we found that glucose use changes occur presymptomatically in HD mouse brains. In contrast to most reports in humans, the first detected alterations in mouse lines are marked elevations in glucose use in multiple forebrain regions. Most interestingly, this hypermetabolism occurs before any evidence of pathological changes, aggregate formation, or symptoms in these animals. This observation has now been recapitulated in two distinctly different HD mutant mouse models, Hdh^{Q92} and Hdh^{Q111} knock-in mice expressing mutant CAG expansions in the murine homologue *HD* gene (11) and N171-82Q mice expressing a fragment of human huntingtin gene containing 82 CAGs (25). Hdh^{Q50} and Hdh^{Q92} mice do not develop an overt behavioral phenotype, but Hdh^{Q111} mice show striatal-specific cell loss around 24 months of age (83). Further, nuclear retention of full-length htt is seen long before cell death (~12 weeks) and occurs selectively in striatal medium spiny neurons. Increased CAG repeat length in this line is associated with acceleration of neuronal intranuclear inclusion (NII) formation, evident by 10 months of age in Hdh^{Q111} mice and by 15 months in Hdh^{Q92}, but NII are not seen in Hdh^{Q50} mice (26,83). In contrast, N171-82Q mice that express a fragment of human huntingtin develop a behavioral phenotype more closely reminiscent of HD, developing weight loss, gait abnormalities, impaired motor performance on a rotarod apparatus, systemic glucose intolerance, and NII formation by 3–4 months of age, before premature death at around 4.5–6 months (25).

Glucose use studies were performed in HD mice before the onset of symptoms or NII formation (4-month-old Hdh^{Q50}, Hdh^{Q92}, and Hdh^{Q111} mice, and 2-month-old N171-82Q mice), and in Hdh^{Q92} mice post-NII formation (15 months). Widespread increases in forebrain glucose

Table 1. Transgenic and Knock-in Mouse Models of Huntington's Disease

Mouse Lines	Q	Tremor, rotarod, clasping	Symptom onset (age/wk)	Weight loss	Energy defects	NII formation (age/wk)	Neuronal loss (age/wk)	Comments	Life span (age/wk)
HD Exon 1 Fragment									
R6/2[72,22]	144	✓	8	✓	✓	3.5	Atrophy	*R6/2:* Diabetes,	13–21
R6/1	115	✓	15–20	X	N/D	20	(Stri, CTX)	seizures, "dark"	32–40
Constitutive promoter, 1.9 kb								neurons, htt in mitochondria, mitochondria degeneration	
C57B16/CBA									
N171[25]									
Mouse prion promoter	82	✓	12	✓	✓	12–16	Stri, CTX	*82Q:* Glucose intolerance,	18–24
171aa	44	X	–	X	X	None	–	apoptosis	Normal
C57B1/6J × C3H/HEJ	18	X	–	X	X	None	–		Normal
HD100, HD46[73]									
Rat NSE promoter	100	✓	12–16	X	N/D	CTX, Stri	Stri-few (32)	Dysmorphic dendrites,	N/D
3 kb	46	X	–	X	N/D		–	increased $[Ca^{2+}]_i$	N/D
SJL/B6								after NMDA	
Tet-Off[74]									
CamKIIa-tTA	94	✓	10 *p.e.*	X	N/D	4 *p.e.*	Atrophy (Stri)	Reversible aggregate	N/D
Tet-Off promoter			(in 50%)					appearance, gliosis	
C57B1/6J × CBA								and receptor changes.	
Full-Length Transgenic									
YAC[24]	72	✓	12	✓	N/D*	60	Stri (52)	Impaired Ca^{2+} handling	N/D
1–2 copies	48	X	42	X	N/D*	None	None	by mitochondria	N/D
FVB/N	18	X	–	X	N/D*	None	None		Normal
HD89[75]									
CMV promoter	89	✓	16	X	N/D*	12 (Few, Stri, CTX)	Stri, CTX-few	Striatal glisosis, apoptosis,	52–60 (+/+)
2–22 copies	48	X	16	X	N/D*		None	dendritic changes	72–80 (+/−)
FVB/N	16	X	–	X	N/D*				Normal
Murine Trageted									
Hdh Knockin[11, 26]	111	X	None	X	✓	40	Stri (80–96)	cAMP impairments	96 (+/+)
Constitutive promoter	92	X	None	X	✓	60	None		Normal
CD1 × 129Sv	50	X	None	X	X	None	None		Normal
CAG Knock-in[76]									
Constitutive promoter	94	X	X	N/D	N/D	None	None	NMDA sensitivity,	N/D
C57B16/J × 129Sv	71	X	X	N/D	N/D	None	None	hypokinesia (16 wk)	N/D
Hdh 150Q[77]									
Constitutive promoter	150	✓	25 (+/+)	✓	N/D	40 (Stri, Nuc Accum)	N/D	Gliosis in striatum,	N/D
C57B1/6J × 129/O1a			60 (+/−)		N/D			some seizures	
Hdh4/6 Knockin[78]									
Constitutive promoter	80	X	None	N/D	N/D	>46	None	Aggression (12 wk)	N/D
C57B1/6J × FVB/N	72	X	None	N/D	N/D	None	None		N/D
HD/Hdh Chimera[79]									
Constitutive promoter	80	X	N/D	N/D	N/D	None	None	Gliosis, CAG instability	N/D
Exon 1/intron 1 fragments									
C57B1/6J × ICR									

Note: The models listed reflect those reported by 5/2003.

*ND**, no changes found in respiratory chain enzyme activities in symptomatic mice; other metabolic parameters have not yet been determined.

aa, Amino acid; CTX, cortex; htt, huntingtin protein; N/D, not determined to date; Nuc. accum, nucleus accumbens; *p.e.*, post-expression; Q, glutamine; Stri, striatum; Tet, tetracycline.

use levels were evident in 4-month-old Hdh^{Q92} and Hdh^{Q111} mice (but not Hdh^{Q50}), and in 2-month-old N171-82Q mice. Notably, glucose use changes in *Hdh* mice were exacerbated in mice with longer CAG repeats and in homozygote versus heterozygote mice, suggesting the extent of increased cerebral glucose demand in CAG length-dependent and gene dosage–dependent (81,82). In older Hdh^{Q111} mice, striatal glucose use was depressed, suggestive of neuronal dysfunction before cell loss. Increases in glucose uptake before any pathological changes suggest that cells have increased their glucose demand to fulfill functional requirements, perhaps as a result of impaired activity of specific metabolic enzymes, uncoupling of mitochondria, or increased dependence on glycolysis. Notably, there is one report in humans of elevated cortical glucose use in presymptomatic HD gene-carriers (47). Limited observations in humans perhaps reflect a lack of studies involving early enough imaging to detect subtle, region-specific presymptomatic hypermetabolism. Another point of interest is that glucose use changes are not restricted to brain regions especially susceptible to degeneration (i.e., the cortex and striatum). This observation supports suggestions that selective loss of striatal neurons may be associated with their apparent vulnerability to metabolic stress.

To determine the principal sites at which metabolism is impaired, studies are in progress to examine the functional capacities of multiple components of the glucose metabolic pathway in these and other HD mice. Additional models include R6/2 mice expressing a human *HD* N-terminal fragment and transgenics expressing full-length human mutant *HD* with its constitutive regulatory elements in a YAC construct (see Table I). R6/2 mice (with 144–170 CAGs) were the first mutant HD mice developed and therefore are the best characterized to date (22,72). Mice have an extremely short life span (generally 13–17 weeks) and develop (in chronological order) NII (~3–4 weeks), gait abnormalities, rotarod impairments, glucose intolerance, body weight loss, brain weight loss, diabetes, striatal atrophy (6–10 weeks), and cerebral neurotransmitter receptor alterations (notably metabotropic glutamate and dopamine alterations around 12 weeks of age) (22,72,76). YAC72Q transgenics show a more slowly progressing phenotype, the earliest abnormality reported to date being impaired calcium handling by 4–5 months of age (24,84). Mice go on to develop NII, and some striatal and cortical cell loss, but live a normal life span. Initial metabolic findings in these models suggest that ATP synthesis may be impaired in N171-82Q and R6/2 mice (Browne, Beal, and Yang, unpublished observations). Interestingly, we found that activities of mitochondrial enzyme complexes II and IV (known to be defective in late-stage HD) are normal in both *Hdh* and N171-82Q mice (82). This finding seems to be typical of multiple HD mouse models (58), with only one exception to date, a report of reduced aconitase and complex II activities in late-stage R6/2 mice (85).

Does Mutant Huntingtin Directly Interact with Mitochondria? Evidence from Genetic Models

The studies described thus far are suggestive of an early role for mitochondrial defects in HD etiology, but until recently a direct link between the huntingtin mutation and mitochondrial function has been lacking. However, evidence is gradually emerging that the mutant protein may directly interact with neuronal mitochondria. One study has systematically examined histological parameters in four different mouse lines (R6/2, R6/1, N171-82Q, and Hdh150CAG mice) and found evidence of degenerated mitochondria in striata in late-stage symptomatic mice (80). These degenerating mitochondria were most prominent in the R6/2 line and notably could be detected before other marked pathological changes within neurons (at about 8–10 weeks of age) and concomitant with symptom onset in these animals. The degeneration is typified by mitochondrial swelling, disruption of the cristae and mitochondrial membranes, and eventual condensation and lysosomal engulfment. Moreover, this report provides the first evidence of a direct interaction of huntingtin protein with mitochondria, by demonstrating the localization of huntingtin N-terminal antibody EM48 immunogold particles both within degenerating mitochondria, and on their surfaces, in R6/2 mouse brain (80). Although R6/2 mice show evidence of striatal atrophy and neuronal shrinkage, there is little detectable striatal cell loss by the time of their premature death at 13–17 weeks of age (22). In contrast, N171-82Q mice show much more marked striatal and cortical-specific neuronal degeneration by end stage. This cell death appears to be largely via apoptotic mechanisms, and there is evidence that mitochondrial cytochrome *c* release is involved, triggering caspase-9 activation (34,80). Another study has reported the association of full-length mutant huntingtin with the surface of mitochondria in YAC-72Q transgenic mice (84).

Functional changes in mitochondria caused by mutant huntingtin have also recently been shown by the demonstration that polyglutamines can influence mitochondrial calcium handling. Panov et al. (86) exposed

mitochondria isolated from rat liver and human lymphoblasts to glutathione *S*-transferase fusion proteins containing polyglutamine tracts of different lengths. Pathogenic polyglutamine constructs (62Q) slightly decreased mitochondrial membrane potential and rendered mitochondria more vulnerable to Ca^{2+}-induced depolarization than mitochondria incubated with wild-type polyglutamine residues (19Q and 0Q). This impairment in calcium handling in the presence of only pathological-length polyglutamines implies that the polyglutamine stretch in mutant huntingtin may alter membrane depolarization, making cells more vulnerable to excitotoxic injury and the consequences of permeability transition. However, results to date give little insight into the regional vulnerability of striatal and cortical CNS neurons in HD. One potential explanation is that a combined effect of huntingtin-mediated increased vulnerability and region-specific alterations in ATP generation underlie regional susceptibility.

Enhancing Metabolism is Protective in Huntington's Disease: Indirect Evidence of Energetic Defects

Circumstantial evidence that energetic defects contribute to neurodegenerative processes in HD is provided by findings that agents that enhance energy production in the brain exert beneficial effects. NMR measurements of lactate production in humans and in rodent mitochondrial toxin models suggest that coenzyme Q_{10} and creatine are neuroprotective, putatively via enhancing cerebral energy metabolism (50,69). Oral administration of CoQ_{10} ameliorated elevated lactate levels seen in the cortex of HD patients, an effect that was reversible on withdrawal of the agent (50). CoQ_{10}, which also has antioxidant effects, also improves symptoms in some other mitochondria-associated disorders, including MELAS and Kearns Sayre syndrome, reducing CSF and serum lactate and pyruvate levels, and enhancing mitochondrial enzyme activities in platelets (87,88). Furthermore, CoQ_{10} attenuates neurotoxicity induced by the mitochondrial toxins MPTP and malonate in animal models (89,90), and was found to increase survival and delay symptom onset in two genetic mouse models of HD (R6/2 and N171–82Q) (91,92). These findings led to CoQ_{10} being tested in a 30-month clinical trial in early-stage HD patients, both in combination with the weak NMDA receptor antagonist remacemide, and alone (93). Although this multiarm trial did not detect a significant ameliorative effect of CoQ_{10}, it did demonstrate a trend toward a protective effect, with treatment slowing the decline in "total functional capacity" of HD patients by 13%. Although findings were not immediately conclusive, results are encouraging and further studies of different doses are planned.

An alternative strategy to enhance cerebral energy metabolism is to increase brain energy stores of the high-energy compound phosphocreatine (PCr) via systemic creatine administration (94,95). Oral creatine treatment successfully attenuated neurotoxicity induced by 3-NP in rats, ameliorating increases in striatal lactate levels and decreases in levels of high-energy phosphate compounds (including ATP) induced by the toxin (69). Furthermore, oral creatine administration has been found to delay disease onset in two HD mouse models, and protect against purkinje cell loss in a transgenic mouse model of another polyglutamine repeat disease, SCA1 (96–98). As a result of these promising effects, creatine's efficacy in HD is currently being assessed in clinical trials. A third approach to modulate energy metabolism therapeutically that has proved efficacious in HD mutant mice, is stimulation of pyruvate dehydrogenase activity by treatment with dichloroacetate (99). Pyruvate dehydrogenase complex activity is impaired in symptomatic R6/2 trangenic mice, but this defect can be reversed with dichloroacetate (DCA) treatment (99). DCA also significantly increased survival, improved motor function, delayed loss of body weight, attenuated the development of striatal neuron atrophy, and prevented diabetes in both the R6/2 and N171–82Q mouse models of HD.

How Are Energetic Changes Deleterious to Neurons in Huntington's Disease?

Excitotoxicity. Impaired energy metabolism, resulting from a toxic action of mutant huntingtin, may be detrimental to cells by inducing excitotoxic damage (100,101). Reduced ATP production can result in cell death directly via disrupting energy-dependent processes. ATP is essential to fuel ionic pumps that generate and maintain ionic and voltage gradients across neuronal membranes, including Na^+/K^+-ATPase pumps that control resting membrane potential and ATPases that regulate intracellular Ca^{2+} levels. Impaired Na^+/K^+-ATPase pump activity may prevent membrane repolarization, resulting in prolonged or inappropriate opening of voltage-dependent ion channels. If severe enough, this partial membrane depolarization can facilitate activation of NMDA receptors by endogenous, normally inert levels of glutamate. In this scenario a concomitant Ca^{2+} influx will occur, triggering nitric oxide synthase (NOS) activation and free radical production. This hypothesis is supported by findings that normally

ambient levels of excitatory amino acids become toxic in the presence of oxidative phosphorylation inhibitors, sodium-potassium pump inhibitors, glucose deprivation, or potassium-induced partial cell membrane depolarization (102–104).

Evidence for excitotoxic processes in HD patients comes primarily from studies of NMDA receptors in HD postmortem tissue. Selective depletion of NMDA receptors has been found in HD striatum, suggesting that neurons bearing NMDA receptors are preferentially vulnerable to degeneration (105). Findings of similar reductions in the striatum of an asymptomatic at-risk patient imply that excitotoxic stress may occur early in the disease process (106). Animal models provide the bulk of evidence for excitotoxicity in HD pathogenesis. Excitotoxic striatal lesions in rats and primates closely resemble those seen in HD brain, with NMDA agonists such as quinolinic acid producing neuronal-specific lesions that show relative sparing of NADPH-diaphorase and parvalbumin-positive neurons typical of HD (89). In primates, quinolinic acid produces striking sparing of NADPH diaphorase neurons, as well as an apomorphine inducible movement disorder (107). In contrast, although AMPA/kainate receptor agonists also produce striatal lesions, they do not replicate the pattern of selective cell loss characteristic of HD.

Excitotoxic processes are also implicated in cell death mediated by mitochondrial toxins that deplete ATP production, including 3-nitropropionic acid (3-NP), 3-acetylpyridine (3-AP), aminooxyacetic acid (AOAA), 1-methyl-4-phenylpyridinium (MPP^+), and malonate (66,90). Systemic administration of 3-NP results in increased binding of tritiated MK-801 (an NMDA receptor channel ligand), consistent with activation of NMDA receptors as a secondary consequence of energy depletion in this model (108). Consequently, 3-NP and malonate lesions can be prevented by prior removal of glutamatergic excitatory corticostriatal inputs by decortication, by glutamate release inhibitors such as riluzole, and by NMDA receptor antagonists including MK-801 (90). Taken together these observations imply that 3-NP toxicity is mediated by secondary excitotoxic mechanisms.

Genetic models of HD also provide evidence of a role for excitotoxic mechanisms in the development of neuronal damage, but findings to date suggest differences between mouse models dependent on the context in which the gene defect is expressed. In YAC-72Q mice, striatal quinolinic acid lesions were exacerbated relative to lesion volumes in wildtype mice, at ages preceding motor symptom onset (109). Cultured neonatal medium spiny neurons expressing the YAC72Q transgene also showed susceptibility to excitotoxic damage induced by NMDA, but not AMPA, which could be abolished by the NMDA receptor NR2B subunit–specific antagonist ifenprodil. NMDA toxicity was also found to be abrogated in cerebellar cells, putatively as a result of their lower levels of NR2B expression (109). The authors therefore hypothesized that regional expression of NR2B subunits may correlate with the severity of neuronal degeneration in HD.

In contrast, another transgenic mouse model that expresses an N-terminal fragment of huntingtin and 46 or 100 CAGs (73) shows no preferential susceptibility to quinolinic acid excitotoxic lesions (110). However, expression of the HD mutation in the context of a shorter gene fragment and longer CAG repeats in R6/2 (145 CAG) and R6/1 (115 CAG) mice conferred resistance to quinolinic acid, malonate, NMDA, and 3-NP toxicity (111,112). One hypothesis to explain the resistance of neurons in these mice is reduced synaptic activity. Dopamine levels in R6/1 mice show 70% depletions in extracellular dopamine relative to wildtype littermate levels (112,113). However, intrastriatal malonate administration in R6/1 mice resulted in a temporary increase in local dopamine release, although lesion volume was reduced by 80% in these animals. In contrast, increased susceptibility to NMDA of R6/2 striatal and cortical neurons has been demonstrated *ex vivo* (76), an observation recapitulated in an *HD* knockin model (76). In another study measuring EPSCs in R6/2 mouse striatal medium spiny neurons, reductions in spontaneous activity were detected at the time of symptom onset in these mice (114). Transmission depression was overt by the time mice become severely impaired (~11–12 weeks of age). The authors demonstrated this to be due to reduced presynaptic events in glutamateric input neurons, implicating defects in the corticostriatal projection pathway in this HD model. The fact that the glutamate release inhibitor riluzole prolongs survival in R6/2 mice (115) reinforces suggestions of an excitotoxic component in this mouse model.

Oxidative Damage. There is evidence that oxidative damage occurs in HD brain and in models of the disorder (54,81,116). Findings in HD patients include increased incidence of DNA strand breaks, exacerbated lipofuscin accumulation (a marker of lipid peroxidation), elevated DNA oxidative damage products such as 8-hydroxydeoxyguanosine (OH^8dG), and increased immunohistochemical staining of oxidative damage products in HD striatum and cortex, including 3-nitrotyrosine (a marker for peroxynitrite-mediated protein nitration), malondialdehyde (marker for oxidative damage to lipids), heme oxygenase (formed during oxidative stress), and OH^8dG (81). Oxidative stress may be a direct mechanism of

huntingtin-linked cellular damage; however, findings that increased oxidative damage to DNA and lipids occurs after symptom onset in the R6/2 transgenic mouse model of HD (117) suggest that it is a downstream event in neuronal dysfunction. It is therefore possible that oxidative damage is induced by energetic defects or secondary excitotoxicity.

Ca^{2+} influx into neurons after activation of excitatory amino acid receptors may trigger increased free radical production via NO-mediated mechanisms, and associated oxidative damage to cellular elements including proteases, lipases, and endonucleases, ultimately leading to cell death (118,119). Direct evidence linking excitotoxicty to free radical generation comes from studies using electron paramagnetic resonance that show that NMDA dose-dependently increases superoxide formation in cultured cerebellar neurons (120). The effects are blocked by NMDA antagonists or removing extracellular Ca^{2+}. This is consistent with findings that exposure of isolated cortical mitochondria to 2.5 μM Ca^{2+}, which is similar to intracellular concentrations induced by excitotoxic stimuli, leads to free radical generation (121). NMDA, kainic acid, and AMPA all stimulate free radical generation in synaptosomes and electron paramagnetic resonance have shown generation of free radicals *in vivo* following systemic kainic acid administration. Further evidence supporting a role for oxidative damage in HD is that the energetic defects seen in HD brain are similar to those induced in cell culture by peroxynitrite, which preferentially inhibits complexes II and III and (to a lesser extent) complex IV activity in the electron transport chain (122).

3-NP toxicity in animals is also associated with increased oxidative damage in the CNS. Hydroxyl (OH^-) free radical production is elevated in the striatum following systemic 3-NP administration, as are levels of the DNA damage marker 8-hydroxy-deoxyguanosine (OH^8dG) and 3-nitrotyrosine (123). Findings that 3-NP-induced lesions and concomitant increases in oxidative damage markers are markedly attenuated in mice overexpressing the superoxide free radical scavenger Cu/Zn superoxide dismutase (SOD1), imply that oxidative free radicals contribute to lesion formation (66). Furthermore, 3-NP striatal lesions are attenuated by free radical spin traps and nitric oxide synthase (NOS) inhibitors (124). In addition, lack of the free radical scavenging enzyme glutathione peroxidase (GSHPx) in knockout mice exacerbates striatal damage and 3-nitrotyrosine elevations caused by systemic administration of 3-NP (66).

Energy Metabolism and Transcriptional Regulation. One potential role for early metabolic alterations in huntingtin-mediated toxicity involves cyclic adenosine 3′,5′-monophosphate (cAMP) signaling. Decreased transcription of genes regulated by cAMP responsive element (CRE) binding protein (CREB) have been implicated in several polyglutamine disorders, including HD. It has been proposed that this decreased transcriptional activity may be due to sequestration of transcriptional coactivators such as CREB binding protein (CBP) and $TAF_{II}130$ into protein aggregates as the disease progresses. This seems unlikely to be the primary step in HD pathogenesis, because evidence shows that NII formation can occur relatively late in the disease process. Also, CBP sequestration cannot explain the dominant reduction in BDNF transcription observed in a *STHdhQ111* striatal cell line, because these cells do not develop inclusions (125). An alternative hypothesis is that a deficiency in cAMP underlies abrogated CRE-mediated gene transcription. cAMP generation is an energy-dependent process, requiring ATP as a precursor, that is reduced in CSF, parietal cortex, and lymphoblastoid cell lines from HD patients (125,126). Furthermore, the adenylate cyclase stimulator forskolin abrogates toxicity induced by expression of mutant huntingtin fragments in PC12 cells (127). In a recent study, Gines et al. (125) used Hdh^{Q111} mice and striatal cell lines to test whether reductions in cAMP link energetic defects with altered CRE signaling in this HD model. cAMP levels were significantly reduced in cortex and striata of these mice by 10 weeks of age, far preceding the formation of nuclear huntingtin aggregates and neuronal death. Further, associated reductions in levels of transcriptionally active phospho-CREB, concomitant with reduced expression of BDNF, were also evident in the cortex of these mice by 5 months of age, indicative of reduced PKA/CREB signaling. These authors went on to suggest that this defect is a result of impaired ATP synthesis induced by the mutant full-length huntingtin, based on observations in a transfected striatal cell line. Notably, mutant huntingtin transfected cells also display elevations in free radical generation and an increased vulnerability to the respiratory chain inhibitor 3-NP.

Changes in cAMP-mediated transcription will have downstream effects on many cell components. One in particular that has gained much interest in HD is brain-derived neurotrophic factor (BDNF). Reduced cAMP-dependent transcription of BDNF is a robust feature of HD pathophysiology. By grades II and III of the disease, BDNF protein and mRNA levels in frontoparietal cortex are halved, and this effect can be mimicked by expressing full-length human mutant huntingtin in a rat CNS parental cell line (128,129). Reduced levels of cortical and striatal BDNF have subsequently been demonstrated in multiple mouse models of HD expressing mutant huntingtin (including R6/2, N171-82Q, *Hdh,* and YAC-72

lines) and are associated with robust alterations in BDNF gene transcription across several different HD mouse lines (125,129–131). In contrast, mice expressing human wild-type huntingtin show increased levels of BDNF. Taken with observations that the striatal pool of BDNF arises from cortical projection neurons, in which huntingtin is widely expressed, it has been suggested that the selective vulnerability of striatal neurons may result from loss of neurotrophic support by BDNF. BDNF also protects neurons against metabolic and excitotoxic insults (132,133) and has been shown to be a promising substrate for cell replacement therapy approaches (134,135). Intrigueingly, a dietary restriction regimen that has been shown to increase BDNF levels in the cerebral cortex, striatum, and hippocampus of mice and rats, was found to increase survival, improve motor performance, ameliorate weight loss, and delay huntingtin aggegate formation and systemic glucose intolerance in R6/2 HD mice (136). The direct protective effect of downregulating metabolic substrates in this manner has yet to be elucidated, but dietary restriction has previously been found to extend life span and is neuroprotective against a number of cell stresses.

Gene profiling studies in HD mouse models also indicate that regulation of several genes involved in mitochondrial function and energy metabolism may be abnormally affected by mutant huntingtin expression. These include creatine kinase, ATP synthase, and subunits of cytochrome *c* oxidase, as well as genes modulating calcium handling and multiple cAMP-regulated genes (130,131,137–139). Although it is tempting to speculate that transcriptional changes in metabolic genes may contribute to HD pathogenesis, caution is warranted in interpreting these observations, because transcriptional changes in a multitude of genes affecting a plethora of different cellular pathways are detected in HD models, of which metabolic components are only a small subset.

Mutant Huntingtin Influences Glucose's Activity as a Signaling Molecule. Another proposed mechanism of cellular damage by mutant huntingtin is disruption of proteosome clearance of ubiquitinated proteins, including mutant huntingtin aggregates. However, clearance of huntingtin may also occur by autophagy. Ravikumar et al. (140) have recently demonstrated that increased intracellular glucose levels are neuroprotective in cultured kidney cells transfected with a mutant huntingtin construct containing 74Q. Reduced huntingtin exon 1 aggregation was also observed. Their results suggest that this is due to increased autophagy as a consequence of dephosphorylation of the authophagy regulator rapamycin (mTOR), concomitant with phosphorylation of glucose to glucose-6-phosphate (140,141). Glucose-mediated regulation of mTOR activity has other implications for cell survival, because it is involved in multible crucial cell processes, including growth and translation of protein transcripts. Further, glucose is also a possible regulator of Akt, which influences cell growth and survival. Cell death in this model is abrogated by overexpression of the GLUT1 astrocytic glucose transporter. This may have direct consequences in HD, as mutant huntingtin exon 1 expression in PC12 cell lines downregulates GLUT1 expression (142), suggesting an intrinsic mechanism of reduced clearance of proteins including huntingtin in HD. This group detected altered expression levels of four genes involved in glucose metabolism in huntingtin transfected PC12 cells (Glut1, Pfkm, Aldolase A, and Enolase), and also demonstrated that augmented expression of Glut1 and Pfkm (another key regulatory protein for glycolysis) rescued both COS7 and SK-N-SH cells from polyglutamine-induced death. These observations raise interesting questions regarding the possible consequences of the initial increases in cerebral glucose uptake detected in mutant mouse models of HD, suggesting that perhaps a feedback loop to remove intracellular mutant huntingtin is set in motion.

CONCLUSION

Studies in human postmortem tissue and *in vivo* imaging techniques have indicated that defects in energy metabolism contribute to neuronal decline at some stage in the HD pathogenesis, but are insufficient to characterize their exact roles. The availability of genetic animal models of the disease is now making it possible to accurately elucidate the nature of this contribution and its importance in modulating mutant huntingtin's toxicity. It is apparent from initial studies that the nature of the genetic model itself affects the pathogenic profile associated with expression of mutant huntingtin, and effects on cerebral energy metabolism vary accordingly. Thus an overview of effects in multiple models is gradually building a picture of how huntingtin's effects on energy metabolism influences pathogenesis of the disease. It is still too early to identify the initial action of mutant huntingtin that triggers selective neuronal dysfunction and cell death pathways, but evidence from both mitochondrial toxin and genetic mouse models suggests that energetic defects occur early in the pathogenic process, and precede overt pathological and symptomatic markers of disease onset. Further, there are tantalizing reports that mutant huntingtin may itself have a direct

interaction with mitochondria and that modulating energy metabolism can affect gene transcription.

ACKNOWLEDGMENT

Studies into glucose metabolism and oxidative metabolism in HD mouse models were supported by grants from the Department of Defense (Browne PI, DAMD17-98-1-8620) and the Huntington's Disease Society of America Coalition for the Cure (Beal and Browne PIs).

REFERENCES

1. Vonsattel, J. P. G. and DiFiglia, M. 1998. Huntington disease. J. Neuropathol. Exp. Neurol. 57:369–384.
2. Andrews, T. C., Weeks, R. A., Turjanski, N., Gunn, R. N., Watkins, L. H., Sahakian, B., Hodges, J. R., Rosser, A. E., Wood, N. W., and Brooks, D. J. 1999. Huntington's disease progression: PET and clinical observations. Brain 122:2353–2363.
3. Beal, M. F., Ellison, D. W., Mazurek, M. F., Swartz, K. J., Malloy, J. R., Bird, E. D., and Martin, J. B. 1988. A detailed examination of substance P in pathologically graded cases of Huntington's disease. J. Neurol. Sci. 84:51–61.
4. Albin, R. L., Reiner, A., Anderson, K. D., Penney, J. B., and Young, A. B. 1990. Striatal and nigral neuron subpopulations in rigid Huntington's disease: Implications for the functional anatomy of chorea and rigidity-akinesia. Ann. Neurol. 27:357–365.
5. Kuwert, T., Lange, H. W., Langer, K.-J., Herzog, H., Aulich, A., and Feinendegen, L. E. 1990. Cortical and subcortical glucose consumption measured by PET in patients with Huntington's disease. Brain 113:1405–1423.
6. The Huntington's Disease Collaborative Research Group. 1993. A novel gene containing a trinucleotide repeat that is expanded and unstable on Huntington's disease chromosome. Cell 72:971–983.
7. MacDonald, M. E., Vonsattel, J.-P., Shrinidhi, J., Couropmitree, N. N., Cupples, L. A., Bird, E. D., Gusella, J. F., Myers, R. H. 1999. Evidence for the GluR6 gene associated with younger onset age of Huntington's disease. Neurology 53:1330–1332.
8. Butterworth, N. J., Williams, L., Bullock, J. Y., Love, D. R., Faull, R. L., and Dragunow, M. 1998. Trinucleotide (CAG) repeat length is positively correlated with the degree of DNA fragmentation in Huntington's disease striatum. Neuroscience 87:49–53.
9. Ross, C. A. 1995. When less is more: Pathogenesis in glutamine repeat neurodegenerative diseases. Neuron 15:493–496.
10. DiFiglia, M., Sapp, E., Chase, K., Schwarz, C., Meloni, A., Young, C., Martin, E., Vonsattel, J.-P., Carraway, R., Reeves, S. A., Boyce, F. M., and Aronin, N. 1995. Huntingtin is a cytoplasmic protein associated with vesicles in human and rat brain neurons. Neuron 14:1075–1081.
11. White, J. K., Auerbach, W., Duyao, M. P., Vonsattel, J.-P., Gusella, J. F., Joyner, A. L., and MacDonald, M. E. 1997. Huntingtin function is required for mouse brain development and is not impaired by the Huntington's disease CAG expansion mutation. Nat. Genet. 17:404–410.
12. Rigamonti, D., Bauer, J. H., De-Fraja, C., Conti, L., Sipione, S., Sciorati, C., Clementi, E., Hackam, A., Hayden, M. R., Li, Y., Cooper, J. K., Ross, C. A., Govoni, S., Vincenz, C., and Cattaneo, E. 2000. Wild-type huntingtin protects from apoptosis upstream of caspase-3. J. Neurosci. 20:3705–3713.
13. Hoffner, G., Kahlem, P., and Dijan, P. 2002. Perinuclear localization of huntingtin as a consequence of its binding to microtubules through an interaction with beta-tubulin: Relevance to Huntington's disease. J. Cell Sci. 115:941–948.
14. Duyao, M. P., Auerbach, A. B., Persichetti, F., Barnes, G. T., McNeil, S. M., Ge, P., Vonsattel, J.-P., Gusella, J. F., Joyner, A. L., and MacDonald, M. E. 1995. Inactivation of the mouse Huntington's disease gene homolog Hdh. Science 269:407–410.
15. Auerbach, W., Hurlbert, M. S., Hilditch-Maguire, P., Wadghiri, Y. Z., Wheeler, V. C., Cohen, S. I., Joyner, A. L., MacDonald, M. E., and Turnbull, D. H. 2001. The HD mutation causes progressive lethal neurological disease in mice expressing reduced levels of huntingtin. Hum. Mol. Genet. 10:2515–2523.
16. Sharp, N. H., Love, S. J., Schilling, G., Li, S.-H., Li, X.-J., Bao, J., Wagster, M. V., Kotzuk, J. A., Steiner, J. P., Lo, A., Hedreen, J., Sisodia, S., Snyder, S. H., Dawson, T. M., Ryugo, D. K., and Ross, C. A. 1995. Widespread expression of the Huntington's disease gene (IT-15) protein product. Neuron 14:1065–1074.
17. Sapp, E., Schwarz, C., Chase, K., Bhide, P. G., Young, A. B., Penney, J., Vonsattel, J. P., Aronin, N., and DiFiglia, M. 1997. Huntingtin localization in brains of normal and Huntington's disease patients. Ann. Neurol. 42:604–612.
18. Ferrante, R. J., Gutekunst, C. A., Persichetti, F., McNeil, S. M., Kowall, N. W., Gusella, J. F., MacDonald, M. E., Beal, M. F., and Hersch, S. M. 1997. Heterogeneous topographic and cellular distribution of huntingtin expression in the normal human neostriatum. J. Neurosci. 17:3052–3063.
19. Fusco, F. R., Chen, Q., Lamoreaux, W. J., Figueredo-Cardenas, G., Jiao, Y., Coffman, J. A., Surmeier, D. J., Honig, M. G., Carlock, L. R., and Reiner, A. 1999. Cellular localization of huntingtin in striatal and cortical neurons in rats: Lack of correlation with neuronal vulnerability in Huntington's disease. J. Neurosci. 19: 1189–1202.
20. Meade, C. A., Deng, Y. P., Fusco, F. R., Del Mar, N., Hersch, S., Goldowitz, D., and Reiner, A. 2002. Cellular localization and development of neuronal intranuclear inclusions in striatal and cortical neurons in R6/2 transgenic mice. J. Comp. Neurol. 449:241–269.
21. Lunkes, A., Lindenberg, K. S., Ben-Haiem, L., Weber, C., Devys, D., Landwehrmeyer, G. B., Mandel, J.-L., and Trottier, Y. 2002. Proteases acting on mutant huntingtin generate cleaved products that differentially build up cytoplasmic and nuclear inclusions. Mol. Cell 10:259–269.
22. Davies, S. W., Turmaine, M., Cozens, B., DiFiglia, M., Sharp, A., Ross, C. A., Scherzinger, E., Wanker, E. E., Mangiarini, L., and Bates, G. 1997. Formation of neuronal intranuclear inclusions (NII) underlies the neurological dysfunction in mice transgenic for the HD mutation. Cell 90:537–548.
23. DiFiglia, M., Sapp, E., Chase, K. O., Davies, S. W., Bates, G. P., Vonsattel, J.-P., and Aronin, N. 1997. Aggregation of huntingtin in neuronal intranuclear inclusions and dystrophic neurites in brain. Science 277:1990–1993.
24. Hodgson, J. G., Agopyan, N., Gutekunst, C.-A., Leavitt, B. R., LePiane, F., Singaraja, R., Smith, D. J., Bissada, N., McCutchoon, K., Nasir, J., Jamot, L., Li, X.-J., Rosemond, E., Roder, J. C., Phillips, A. G., Rubin, E. M., Hersch, S. M., and Hayden, M. R. 1999. A YAC mouse model for Huntington's disease with full-length mutant huntingtin, cytoplasmic toxicity, and selective striatal neurodegeneration. Neuron 23:1–20.
25. Schilling, G., Bacher, M. W., Sharp, A. H., Jinnah, H. A., Duyao, K., Kotzuk, J. A., Slunt, H. H., Ratovitski, T., Cooper, J. A., Jenkins, N. A., et al. 1999. Intranuclear inclusions and neuritic aggregates in transgenic mice expressing a mutant N-terminal fragment of huntingtin. Hum. Mol. Genet. 8:397–407.
26. Wheeler, V. C., White, J. K., Gutekunst, C. A., Vrbanac, V., Weaver, M., Li, X. J., Li, S. H., Yi, H., Vonsattel, J. P., Gusella, J. F., Hersch, S., Auerbach, W., Joyner, A. L., and MacDonald, M. E. 2000. Long glutamine tracts cause nuclear localization of a novel form of huntingtin in medium spiny striatal neurons in HdhQ92 and HdhQ111 knock-in mice. Hum. Mol. Genet. 9:503–513.
27. Saudou, F., Finkbeiner, S., Devys, D., and Greenberg, M. E. 1998. Huntingtin acts in the nucleus to induce apoptosis but death does not correlate with the formation of intranuclear inclusions. Cell 95:55–66.

28. Rubinsztein, D. C. 2002. Lessons from animal models of Huntington's disease. Trends Gen. 18:202–209.
29. Kim, M., Lee, H. S., LaForet, G., McIntyre, C., Martin, E. J., Chang, P., Kim, T. W., Williams, M., Reddy, P. H., Tagle, D., Boyee, F. M., Won, L., Heller, A., Aronin, N., and DiFiglia, M. 1999. Mutant huntingtin expression in clonal striatal cells: Dissociation of inclusion formation and neuronal survival by caspase inhibition. J. Neurosci. 19:964–73.
30. Peters, M. F., Nucifora, F. C. Jr., Kushi, J., Seaman, H. C., Cooper, J. K., Herring, W. J., Dawson, V. L., Dawson, T. M., and Ross, C. A. 1999. Nuclear targeting of mutant Huntingtin increases toxicity. Mol. Cell Neurosci. 14:121–128.
31. Martin-Aparicio, E., Avila, J., and Lucas, J. J. 2002. Nuclear localization of N-terminal mutant huntingtin is cell cycle dependent. Eur. J. Neurosci. 16:355–359.
32. Cooper, A. J. L., Sheu, K.-F. R., Burke, J. R., Onodera, O., Strittmatter, W. J., Roses, A. D., and Blass, J. P. 1997. Transglutaminase-catalyzed inactivation of glyceraldehyde 3-phosphate dehydrogenase and α-ketoglutarate dehydrogenase complex by polyglutamine domains of pathological length. Proc. Natl. Acad. Sci. USA 94:12604–12609.
33. Cooper, A. J., Sheu, K. F., Burke, J. R., Strittmatter, W. J., Gentile, V., Peluso, G., and Blass, J. P. 1999. Pathogenesis of inclusion bodies in (CAG)n/Qn-expansion diseases with special reference to the role of tissue transglutaminase and to selective vulnerability. J. Neurochem. 72:889–899.
34. Hickey, M. A. and Chesselet, M. F. 2003. Apoptosis in Huntington's disease. Prog. Neuropsychopharmacol. Biol. Psychiatry 27:255–265.
35. Burke, J. R., Enghild, J. J., Martin, M. E., Jou, Y.-S., Myers, R. M., Roses, A. D., Vance, V. M., and Strittmatter, W. J. 1996. Huntingtin and DRPLA proteins selectively interact with the enzyme GAPDH. Nat. Med. 2:347–350.
36. Aronin, N., Kim, M., Laforet, G., and DiFiglia, M. 1999. Are there multiple pathways in the pathogenesis of Huntington's disease? Phil. Trans. R. Soc. Lond. 354:995–1003.
37. Steffan, J. S., Bodai, L., Pallos, J., Poelman, M., McCampbell, A., Apostol, B. L., Kazantsev, A., Schmidt, E., Zhu, Y. Z., Greenwald, M., Kurokawa, R., Housman, D. E., Jackson, C. R., Marsh, J. L., and Thompson, L. M. 2001. Histone deacetylase inhibitors arrest polyglutamine-dependent neurodegeneration in Drosophila. Nature 413:739–743.
38. Dunah, A. W., Jeong, H., Griffin, A., Kim, Y. M., Standaert, D. G., Hersch, S. M., Mouradian, M. M., Young, A. B., Tanese, N., and Krainc, D. 2002. Sp1 and TAFII130 transcriptional activity disrupted in early Huntington's disease. Science 296:2238–2243.
39. O'Brien, C. F., Miller, C., Goldblatt, D., Welle, S., Forbes, G., Lipinski, B., Panzik, J., Peck, R., Plumb, S., Oakes, D., Kurlan, R., and Shoulson, I. 1990. Extraneural metabolism in early Huntington's disease. Ann. Neurol. 28:300–301.
40. Djousse, L., Knowlton, B., Cupples, L. A., Marder, K., Shoulson, I., and Myers, R. H. 2002. Weight loss in early stage of Huntington's disease. Neurology 59:1325–1330.
41. Andrews, T. C. and Brooks, D. J. 1998. Advances in the understanding of early Huntington's disease using the functional imaging techniques of PET and SPET. Mol. Med. Today 4:532–539.
42. Kuhl, D. E., Markham, C. H., Metter, E. J., Riege, W. H., Phelps, M. E., and Mazziotta, J. C. 1985. Local cerebral glucose utilization in symptomatic and presymptomatic Huntington's disease. Res. Publ. Assoc. Res. Nerv. Men. Dis. 63:199–209.
43. Berent, S., Giordani, B., Lehtinen, S., Markel, D., Penney, J. B., Buchtel, H. A., Starosta Rubinstein, S., Hichwa, R., and Young, A. B. 1988. Positron emission tomographic scan investigations of Huntington's disease: Cerebral metabolic correlates. Ann. Neurol. 23:541–546.
44. Grafton, S. T., Mazziotta, J. C., Pahl, J. J., St George-Hyslop, P., Haines, J. L., Gusella, J., Hoffman, J. M., Baxter, L. R., and Phelps, M. E. 1992. Serial changes of cerebral glucose metabolism and caudate size in persons at risk for Huntington's disease. Arch. Neurol. 49:1161–1167.
45. Kuwert, T., Lange, H. W., Boecker, H., Titz, H., Herzog, H., Aulich, A., Wang, B. C., Nayak, U., and Feinendegen, L. E. 1993. Striatal glucose consumption in chorea-free subjects at risk of Huntington's disease. J. Neurol. 241:31–36.
46. Antonini, A., Leenders, K. L., Spiegel, R., Meier, D., Vontobel, P., Weigell-Weber, M., Sanchez-Pernaute, R., de Yebenez, J. G., Boesiger, P., Weindl, A., and Maguire, R. P. 1996. Striatal glucose metabolism and dopamine D2 receptor binding in asymptomatic gene carriers and patients. Brain 119:2085–2095.
47. Feigin, A., Leenders, K. L., Moeller, J. R., Missimer, J., Kuenig, G., Spetsieris, P., Antonini, A., and Eidelberg, D. 2001. Metabolic network abnormalities in early Huntington's disease: An [(18)F] FDG PET study. J. Nucl. Med. 42:1591–1595.
48. Jenkins, B. G., Koroshetz, W., Beal, M. F., and Rosen, B. 1993. Evidence for an energy metabolism defect in Huntington's disease using localized proton spectroscopy. Neurology 43:2689–2695.
49. Jenkins, B. G., Rosas, H. D., Chen, Y. C., Makabe, T., Myers, R., MacDonald, M., Rosen, B. R., Beal, M. F., and Koroshetz, W. J. 1998. ^{1}H NMR spectroscopy studies of Huntington's disease: Correlations with CAG repeat numbers. Neurology 50:1357–1365.
50. Koroshetz, W. J., Jenkins, B. G., Rosen, B. R., and Beal, M. F. 1997. Energy metabolism defects in Huntington's disease and possible therapy with coenzyme Q_{10}. Ann. Neurol. 41:160–165.
51. Nicoli, F., Vion-Dury, J., Maloteaux, J. M., Delwaide, C., Confort-Gouny, S., Sciaky, M., and Cozzone, P. J. 1993. CSF and serum metabolic profile of patients with Huntington's chorea: A study by high resolution proton NMR spectroscopy and HPLC. Neurosci. Lett. 154:47–51.
52. Lodi, R., Schapira, A. H., Manners, D., Styles, P., Wood, N. W., Taylor, D. J., and Warner, T. T. 2000. Abnormal *in vivo* skeletal muscle energy metabolism in Huntington's disease and dentatorubropallidoluysian atrophy. Ann. Neurol. 48:72–76.
53. Butterworth, J., Yates, C. M., and Reynolds, G. P. 1985. Distribution of phosphate-activated glutaminase, succinic dehydrogenase, pyruvate dehydrogenase, and γ-glutamyl transpeptidase in post-mortem brain from Huntington's disease and agonal cases. J. Neurol. Sci. 67:161–171.
54. Browne, S. E., Bowling, A. C., MacGarvey, U., Baik, M. J., Berger, S. C., Muqit, M. M. K., Bird, E. D., and Beal, M. F. 1997. Oxidative damage and metabolic dysfunction in Huntington's disease: Selective vulnerability of the basal ganglia. Ann. Neurol. 41:646–653.
55. Gu, M., Gash, M. T., Mann, V. M., Javoy-Agid, F., Cooper, J. M., and Schapira, A. H. V. 1996. Mitochondrial defect in Huntington's disease caudate nucleus. Ann. Neurol. 39:385–389.
56. Parker, W. D. Jr., Boyson, S. J., Luder, A. S., and Parks, J. K. 1990. Evidence for a defect in NADH:ubiquinone oxidoreductase (complex I) in Huntington's disease. Neurology 40:1231–1234.
57. Arenas, J., Campos, Y., Ribacoba, R., Martin, M. A., Rubio, J. C., Ablanedo, P., and Cabello, A. 1998. Complex I defect in muscle from patients with Huntington's disease. Ann. Neurol. 43: 397–400.
58. Guidetti, P., Charles, V., Chen, E. Y., Reddy, P. H., Kordower, J. H., Whetsell, W. O. Jr., Schwarcz, R., and Tagle, D. A. 2001. Early degenerative changes in transgenic mice expressing mutant huntingtin involve dendritic abnormalities but no impairment of mitochondrial energy production. Exp. Neurol. 169:340–50.
59. Tabrizi, S. J., Cleeter, M. W., Xuereb, J., Taanman, J. W., Cooper, J. M., and Schapira, A. H. 1999. Biochemical abnormalities and excitotoxicity in Huntington's disease brain. Ann. Neurol. 45:25–32.
60. Mastrogiacomo, F., LaMarche, J., Dozic, S., Lindsay, G., Bettendorff, L., Robitaille, Y., Schut, L., and Kish, S. J. 1996. Immunoreactive levels of alpha-ketoglutarate dehydrogenase subunits in Friedreich's ataxia and spinocerebellar ataxia type 1. Neurodegen. 5:27–33.
61. Matsuishi, T., Sakai, T., Naito, E., Nagamitsu, S., Kuroda, Y., Iwashita, H., and Kato, H. 1996. Elevated cerebrospinal fluid lactate/pyruvate ratio in Machado-Joseph disease. Acta Neurol. Scand. 93:72–75.

62. Mazzola, J. L. and Sirover, M. A. 2001. Reduction of glyceraldehyde-3-phosphate dehydrogenase activity in Alzheimer's disease and in Huntington's disease fibroblasts. J. Neurochem. 76:442–449.
63. Mazzola, J. L. and Sirover, M. A. 2002. Alteration of nuclear glyceraldehyde-3-phosphate dehydrogenase structure in Huntington's disease fibroblasts. Brain Res. Mol. Brain Res. 100:95–101.
64. Senatorov, V. V., Charles, V., Reddy, P. H., Tagle, D. A., and Chuang, D. M. 2003. Overexpression and nuclear accumulation of glyceraldehyde-3-phosphate dehydrogenase in a transgenic mouse model of Huntington's disease. Mol. Cell Neurosci. 22:285–297.
65. Ludolph, A. C., He, F., Spencer, P. S., Hammerstad, J., and Sabri, M. 1990. 3-Nitropropionic acid: Exogenous animal neurotoxin and possible human striatal toxin. Can. J. Neurol. Sci. 18:492–498.
66. Browne, S. E. and Beal, M. F. 2002. Toxin-induced mitochondrial dysfunction. Int. Rev. Neurobiol. 53:243–279.
67. Brouillet, E., Hantraye, P., Ferrante, R. J., Dolan, R., Leroy-Willig, A., Kowall, N. W., and Beal, M. F. 1995. Chronic mitochondrial energy impairment produces selective striatal degeneration and abnormal choreiform movements in primates. Proc. Natl. Acad. Sci. USA 92:7105–7109.
68. Brouillet, E., Guyot, M. C., Mittoux, V., Altairac, S., Conde, F., Palfi, S., and Hantraye, P. 1998. Partial inhibition of brain succinate dehydrogenase by 3-nitropropionic acid is sufficient to initiate striatal degeneration in rat. J. Neurochem. 70:794–805.
69. Matthews, R. T., Yang, L., Jenkins, B. J., Ferrante, R. J., Rosen, B. R., Kaddurah-Daouk, R., and Beal, M. F. 1998. Neuroprotective effects of creatine and cyclocreatine in animal models of Huntington's disease. J. Neurosci. 18:156–163.
70. Faber, P. W., Alter, J. R., MacDonald, M. E., and Hart, A. C. 1999. Polyglutamine-mediated dysfunction and apoptotic death of a Caenorhabditis elegans sensory neuron. Proc. Natl. Acad. Sci. USA 96:179–184.
71. von Horsten, S., Schmitt, I., Nguyen, H. P., Holzmann, C., Schmidt, T., et al. 2003. Transgenic rat model of Huntington's disease. Hum. Mol. Genet. 12:617–24.
72. Mangiarini, L., Sathasivam, K., Seller, M., Cozens, B., Harper, A., Hetherington, C., Lawton, M., Trottier, Y., Lehrach, H., Davies, S. W., and Bates, G. 1996. Exon 1 of the HD gene with an expanded CAG repeat is sufficient to cause a progressive neurological phenotype in transgenic mice. Cell 87:493–506.
73. Laforet, G. A., Sapp, E., Chase, K., McIntyre, C., Boyce, F. M., Campbell, M., Cadigan, B. A., Warzeeki, L., Tagle, D. A., Reddy, P. H., Cepeda, C., Calvert, C. R., Jokel, E. S., Klapstein, G. J., Ariano, M. A., Levine, M. S., DiFiglia, M., and Aronin, N. 2001. Changes in cortical and striatal neurons predict behavioral and electrophysiological abnormalities in a transgenic murine model of Huntington's disease. J. Neurosci. 21: 9112–9123.
74. Yamamoto, A., Lucas, J. J., and Hen, R. 2000. Reversal of neuropathy and motor dysfunction in a conditional model of Huntington's disease. Cell 101:57–66.
75. Reddy, P. H., Williams, M., Charles, V., Garrett, L., Pike-Buchanan, L., Whetsell, W. O. Jr., Miller, G., and Tagle, D. A. 1998. Behavioural abnormalities and selective neuonal loss in HD transgenic mice expressing mutated full-length HD cDNA. Nat. Genet. 20:198–202.
76. Levine, M. S., Klapstein, G. J., Koppel, A., Gruen, E., Cepeda, C., Vargas, M. E., Jokel, E. S., Carpenter, E. M., Zanjani, H., Hurst, R. S., Efstratiadis, A., Zeitlin, S., and Chesselet, M. F. 1999. Enhanced sensitivity to N-methyl-D-aspartate receptor activation in transgenic and knockin mouse models of Huntington's disease. J. Neurosci. Res. 58:515–532.
77. Lin, C. H., Tallaksen-Greene, S., Chien, W. M., Cearley, J. A., Jackson, W. S., Crouse, A. B., Ren, S., Li, X. J., Albin, R. L., and Detloff, P. J. 2001. Neurological abnormalities in a knock-in mouse model of Huntington's disease. Hum. Mol. Genet. 10: 137–144.
78. Shelbourne, P. F., Killeen, N., Hevner, R. F., Johnston, H. M., Tecott, L., Lewandoski, M., Ennis, M., Ramirez, L., Li, Z., Iannicola, C., Littman, D. R., and Myers, R. M. 1999. A Huntington's disease CAG expansion at the murine Hdh locus is unstable and associated with behavioural abnormalities in mice. Hum. Mol. Genet. 8: 763–774.
79. Ishiguru, H., Yamada, K., Sawada, H., Nishii, K., Ichino, N., Sawada, M., Kurosawa, Y., Matsushita, N., Kobayashi, K., Goto, J., Hashida, H., Masuda, N., Kanazawa, I., and Nagatsu, T. 2001. Age-dependent and tissue-specific CAG repeat instability occurs in mouse knock-in for a mutant Huntington's disease gene. J. Neurosci. Res. 65:289–297.
80. Yu, Z.-X., Li, S.-H., Evans, J., Pillarisetti, A., Li, H., and Li, X.-J. 2003. Mutant huntingtin causes context-dependent neurodegeneration in mice with Huntington's disease. J. Neurosci. 23:2193–2202.
81. Browne, S. E., Wheeler, V., White, J. K., Fuller, S. W., MacDonald, M., and Beal, M. F. 1999. Dose-dependent alterations in local cerebral glucose use associated with the huntingtin mutation in Hdh CAG knock-in transgenic mice. Soc. Neurosci. Abstr. 25:218.11.
82. Gregorio, J., DiMauro, J.-P. P., Narr, S., Fuller, S. W., and Browne, S. E. 2002. Cerebral metabolism defects in HD: Glucose utilization abnormalities in multiple HD mouse models. Soc. Neurosci. Abstr. 28:195.10
83. Wheeler, V. C., Gutekunst, C. A., Vrbanac, V., Lebel, L. A., Schilling, G., Hersch, S., Friedlander, R. M., Gusella, J. F., Vonsattel, J. P., Borchelt, D. R., MacDonald, M. E. 2002. Early phenotypes that presage late-onset neurodegenerative disease allow testing of modifiers in Hdh CAG knock-in mice. Hum. Mol. Genet. 11:633–640.
84. Panov, A. V., Gutekunst, C. A., Lelavitt, B. R., Hayden, M. R., Burke, J. R., Strittmatter, W. J., and Greenamyre, J. T. 2002. Early mitochonrial calcium defects in Huntington's disease are a direct effect of polyglutamines. Nat. Neurosci. 5:731–736.
85. Tabrizi, S. J., Workman, J., Hart, P. E., Mangiarini, L., Mahal, A., Bates, G., Cooper, J. M., and Schapira, A. H. 2000. Mitochondrial dysfunction and free radical damage in the Huntington R6/2 transgenic mouse. Ann. Neurol. 47:80–86.
86. Panov, A. V., Burke, J. R., Strittmatter, W. J., and Greenamyre, J. T. 2003. In vitro effects of polyglutamine tracts on Ca^{2+}-dependent depolarization of rat and human mitochondria: Relevance to Huntington's disease. Arch. Biochem. Biophys. 410:1–6.
87. Bresolin, N., Bet, L., Binda, A., Moggio, M., Comi, G., Nador, F., Ferrante, C., Carenzi, A., and Searlato, G. 1988. Clinical and biochemical correlations in mitochondrial myopathies treated with coenzyme Q_{10}. Neurology 38:892–899.
88. Ihara, Y., Namba, R., Kuroda, S., Sato, T., and Shirabe, T. 1989. Mitochondrial encephalomyopathy (MELAS): Pathological study and successful therapy with coenzyme Q_{10} and idebenone. J. Neurol. Sci. 90:263–271.
89. Beal, M. F., Henshaw, D. R., Jenkins, B. G., Rosen, B. R., and Schulz, J. B. 1994. Coenzyme Q_{10} and nicotinamide block striatal lesions produced by the mitochondrial toxin malonate. Ann. Neurol. 36:882–888.
90. Schulz, J. B., Matthews, R. T., Henshaw, D. R., and Beal, M. F. 1996. Neuroprotective strategies for treatment of lesions produced by mitochondrial toxins: Implications for neurodegenerative diseases. Neurosci. 71:1043–1048.
91. Schilling, G., Coonfield, M. L., Ross, C. A., and Borchelt, D. R. 2001. Coenzyme Q10 and remacemide hydrochloride ameliorate motor deficits in a Huntington's disease transgenic mouse model. Neurosci. Lett. 315:149–153.
92. Ferrante, R. J., Andreassen, O. A., Dedeoglu, A., Ferrante, K. L., Jenkins, B. G., Hersch, S. M., and Beal, M. F. 2002. Therapeutic effects of coenzyme Q10 and remacemide in transgenic mouse models of Huntington's disease. J. Neurosci. 22:1592–1599.
93. Huntington Study Group. 2001. A randomized, placebo-controlled trial of coenzyme Q10 and remacemide in Huntington's disease. Neurology 57:375–376.
94. Wyss, M. and Schulze, A. 2002. Health implications of creatine: Can oral creatine supplementation protect against neurological and atherosclerotic disease? Neuroscience 112:243–260.

95. Tarnopolsky, M. A. and Beal, M. F. 2001. Potential for creatine and other therapies targeting cellular energy dysfunction in neurological disorders. Ann. Neurol. 49:561–574.
96. Ferrante, R. J., Andreassen, O. A., Dedeoglu, A., Kuemmerle, S., Kubilus, J. K., Kaddurah-Daouk, R., Hersch, S. M., and Beal, M. F. 2000. Neuroprotective effects of creatine in a transgenic mouse model of Huntington's disease. J. Neurosci. 20: 4389–4397.
97. Andreassen, O. A., Dedeoglu, A., Ferrante, R. J., Jenkins, B. J., Ferrante, K. L., Thomas, M., Friedlich, A., Browne, S. E., Schilling, G., Borchelt, D. R., Hersch, S. M., Ross, C. A., Beal, M. F. 2001. Creatine increase survival and delays motor symptoms in a transgenic animal model of Huntington's disease. Neurobiol. Dis. 8: 479–491.
98. Kaemmerer, W. F., Rodrigues, C. M., Steer, C. J., and Low, W. C. 2001. Creatine-supplemented diet extends Purkinje cell survival in spinocerebellar ataxia type 1 transgenic mice but does not prevent the ataxic phenotype. Neuroscience 103:713–724.
99. Andreassen, O. A., Ferrante, R. J., Huang, H. M., Dedeoglu, A., Park, L., Ferrante, K. L., Kwon, J., Borchelt, D. R., Ross, C. A., Gibson, G. E., and Beal, M. F. 2001. Dichloroacetate exerts therapeutic effects in transgenic mouse models of Huntington's disease. Ann. Neurol. 50:112–117.
100. Albin, R. L. and Greenamyre, J. T. 1992. Alternative excitotoxic hypotheses. Neurology 42:733–738.
101. Browne, S. E., Ferrante, R. J., and Beal, M. F. 1999. Oxidative stress in Huntington's disease. Brain Pathol. 9:147–163.
102. Novelli, A., Reilly, J. A., Lysko, P. G., and Henneberry, R. C. 1988. Glutamate becomes neurotoxic via the N-methyl-D-aspartate receptor when intracellular energy levels are reduced. Brain Res. 451: 205–212.
103. Henneberry, R. L., Novelli, A., Cox, J. A., and Lysko, P. G. 1989. Neurotoxicity at the N-methyl-D-aspartate receptor in energy-compromised neurons: An hypothesis for cell death in aging and disease. Ann. NY Acad. Sci. 568:225–233.
104. Zeevalk, G. D. and Nicklas, W. J. 1991. Mechanisms underlying initiation of excitotoxicity associated with metabolic inhibition. J. Pharm. Exp. Ther. 257:870–878.
105. Dure, L. S. 4th, Young A. B., and Penney, J. B. 1991. Excitatory amino acid binding sites in the caudate nucleus and frontal cortex of Huntington's disease. Ann. Neurol. 30:785–793.
106. Albin, R. L., Young, A. B., Penney, J. B., Handelin, B., Balfour, R., Anderson, K. D., Markel, D. S., Tourtellotte, W. W., and Reiner, A. 1990. Abnormalities of striatal projection neurons and N-methyl-D-aspartate receptors in presymptomatic Huntington's disease. N. Engl. J. Med. 322:1293–1298.
107. Ferrante, R. J., Kowall, N. W., Cipolloni, P. B., Storey, E., and Beal, M. F. 1993. Excitotoxin lesions in primates as a model for Huntington's disease: Histopathologic and neurochemical characterization. Exp. Neurol. 119:46–71.
108. Wullner, U., Young, A. B., Penney, J. B., and Beal, M. F. 1994. 3-Nitropropionic acid toxicity in the striatum. J. Neurochem. 63: 1772–1781.
109. Zeron, M. M., Hansson, O., Chen, N., Wellington, C. L., Leavitt, B. R., Brundin, P., Hayden, M. R., and Raymond, L. A. 2002. Increased sensitivity to N-methyl-D-aspartate receptor-mediated excitotoxicity in a mouse model of Huntington's disease. Neuron 33:849–860.
110. Petersen, A., Chase, K., Puschban, Z., DiFiglia, M., Brundin, P., and Aronin, N. 2002. Maintenance of susceptibility to neurodegeneration following intrastriatal injections of quinolinic acid in a new transgenic mouse model of Huntington's disease. Exp. Neurol. 175:297–300.
111. Hansson, O., Castilho, R. F., Korhonen, L., Lindholm, D., Bates, G. P., and Brundin, P. 2001. Partial resistance to malonate-induced striatal cell death in transgenic mouse models of Huntington's disease is dependent on age and CAG repeat length. J. Neurochem. 78:694–703.
112. Hickey, M. A. and Morton, A. J. 2000. Mice transgenic for the Huntington's disease mutation are resistant to chronic 3-nitopropionic acid-induced striatal toxicity. J. Neurochem. 75:2163–2171.
113. Petersen, A., Hansson, O., Puschban, Z., Sapp, E., Romero, N., Castilho, R. F., Sulzer, D., Rice, M., DiFiglia, M., Przedborski, S., and Brundin, P. 2001. Mice transgenic for exon 1 of the Huntington's disease gene display reduced striatal sensitivity to neurotoxicity induced by dopamine and 6-hydroxydopamine. Eur. J. Neurosci. 14:1425–1435.
114. Cepeda, C., Hurst, R. S., Calvert, C. R., Hernandez-Echeagaray, E., Nguyen, O. K., Jocoy, E., Christian, L. J., Ariano, M. A., and Levine, M. S. 2003. Transient and progressive electrophysiological alterations in the corticostriatal pathway in a mouse model of Huntington's disease. J. Neurosci. 23:961–996.
115. Schiefer, J., Landwehrmeyer, G. B., Luesse, H. G., Sprunken, A., Puls, C., Milkereit, A., Milkereit, E., and Kosinski, C. M. 2002. Riluzole prolongs survival time and alters nuclear inclusion formation in a transgenic mouse model of Huntington's disease. Mov. Disord. 17:748–757.
116. Polidori, M. C., Mecocci, P., Browne, S. E., Senin, U., and Beal, M. F. 1999. Oxidative damage to mitochondrial DNA in Huntington's disease parietal cortex. Neurosci. Lett. 272:53–56.
117. Bogdanov, M. B., Andreassen, O. A., Dedeoglu, A., Ferrante, R. J., Beal, M. F. 2001. Increased oxidative damage to DNA in a transgenic mouse model of Huntington's disease. J. Neurochem. 79:1246–1249.
118. Calabrese, V., Scapagnini, G., Giuffrida-Stella, A. M., Bates, T. E., and Clark, J. B. 2001. Mitochondrial involvement in brain function and dysfunction: Relevance to aging, neurodegenerative disorders and longevity. Neurochem. Res. 26:739–764.
119. Brown, G. C. and Borutaite, V. 2001. Nitric oxide, mitochondria, and cell death. IUBMB Life 52:189–195.
120. Lafon-Cazal, M., Culcasi, M., Gaven, F., Pietri, S., and Bockaert, J. 1993. Nitric oxide, superoxide and peroxynitrite: Putative mediators of NMDA-induced cell death in cerebellar granule cells. Neuropharmacology 32:1259–1266.
121. Dykens, J. A. 1994. Isolated cerebral and cerebellar mitochondria produce free radicals when exposed to elevated Ca^{2+} and Na^{+}: Implications for neurodegeneration. J. Neurochem. 63:584–591.
122. Bolanos, J. P., Heales, S. J. R., Land, J. M., and Clark, J. B. 1995. Effect of peroxynitrite on the mitochondrial respiratory chain: Differential susceptibility of neurones and astrocytes in primary culture. J. Neurochem. 64:1965–1972.
123. Schulz, J. B., Henshaw, D. R., MacGarvey, U., and Beal, M. F. 1996. Involvement of oxidative stress in 3-nitropropionic acid neurotoxicity. Neurochem. Intl. 29:167–171.
124. Schulz, J. B., Henshaw, D. R., Siweck, D., Jenkins, B. G., Ferrante, R. J., Cipolloni, P. B., Kowall, N. W., Rosen, B. R., Beal, M. F. 1995. Involvement of free radicals in excitotoxicity *in vivo*. J. Neurochem. 64:2239–2247.
125. Gines, S., Seong, I. S., Fossale, E., Ivanova, E., Trettel, F., Gusella, J. F., Wheeler, V. C., Persichetti, F., and MacDonald, M. E. 2003. Specific progressive cAMP reduction implicates energy deficit in presymptomatic Huntington's disease knock-in mice. Hum. Mol. Genet. 12:497–508.
126. Cramer, H., Warter, J. M., and Renaud, B. 1984. Analysis of neurotransmitter metabolites and adenosine 3′ 5′-monophosphate in the CSF of patients with extrapyramidal motor disorders. Adv. Neurol. 40:431–435.
127. Wyttenbach, A., Swartz, J., Kita, H., Thykjaer, T., Carmichael, J., Bradley, J., Brown, R., Maxwell, M., Schapira, A., Orntoft, T. F., et al. 2001. Polyglutamine expansions cause decreased CRE-mediated transcription and early gene expression changes prior to cell death in an inducible cell model of Huntington's disease. Hum. Mol. Genet. 10:1829–1845.
128. Ferrer, I., Goutan, E., Marin, C., Rey, M. J., and Ribalta, T. 2000. Brain-derived neurotrophic factor in Huntington disease. Brain Res. 866:257–261.

129. Zuccato, C., Ciammola, A., Rigamonti, D., Leavitt, B. R., Goffredo, D., Conti, L., MacDonald, M. E., Friedlander, R. M., Silani, V., Hayden, M. R. et al. 2001. Loss of huntingtin-mediated BDNF gene transcription in Huntington's disease. Science 293:493–498.
130. Luthi-Carter, R., Strand, A., Peters, N. L., Solano, S. M., Hollingsworth, Z. R., Menon, A. S., Frey, A. S., Spektor, B. S., Penney, E. B., Schilling, G., Ross, C. A., Borchelt, D. R., Tapscott, S. J., Young, A. B., Cha, J. H., Olson, J. M. 2000. Decreased expression of striatal signaling genes in a mouse model of Huntington's disease. Hum. Mol. Genet. 9:1259–1271.
131. Luthi-Carter, R., Hanson, S. A., Strand, A. D., Bergstrom, D. A., Chun, W., Peters, N. L., Woods, A. M., Chan, E. Y., Kooperberg, C., Krainc, D., Young A. B., Tapscott, S. J., and Olson, J. M. 2002. Dysregulation of gene expression in the R6/2 model of polyglutamine disease: Parallel changes in muscle and brain. Hum. Mol. Genet. 11:1911–1926.
132. Cheng, B. and Mattson, M. P. 1994. NT-3 and BDNF protect CNS neurons against metabolic excitotoxic insults. Brain Res. 640:56–67.
133. Duan, W. and Guo, Z. 2001. Brain-derived neurotrophic factor mediates an excitoprotective effect of dietary restriction in mice. J. Neurochem. 76:619–626.
134. Bemelmans, A. P., Horellou, P., Pradier, L., Brunet, I., Colin, P., and Mallet, J. 1999. Brain derived neurotrophic factor-mediated protection of striatal neurons in an excitotoxic rat model of Huntington's disease, as demonstrated by adenoviral gene transfer. Hum. Gene Ther. 10:2987–2997.
135. Perez-Navarro, E., Canudas, A. M., Akerund, P., Alberch, J., and Arenas, E. 2000. Brain-derived neurotrophic factor, neurotrophin-3 and neurotrophin-4/5 prevent the death of striatal projection neurons in a rodent model of Huntington's disease. J. Neurochem. 75:2190–2199.
136. Duan, W., Guo, Z., Jiang, H., Ware, M., Li, X. J., and Mattson, M. P. 2003. Dietary restriction normalizes glucose metabolism and BDNF levels, slows disease progression, and increases survival in huntingtin mutant mice. Proc. Natl. Acad. Sci. USA 100:2911–2916.
137. Luthi-Carter, R., Strand, A. D., Hanson, S. A., Kooperberg, C., Schilling, G., LaSpada, A. R., Merry, D. E., Young, A. B., Ross, C. A., Borchelt, D. R., Olson, J. M. 2002. Polyglutamine and transcription: Gene expression changes shared by DRPLA and Huntington's disease mouse models reveal context-independent effects. Hum. Mol. Genet. 11:1927–1937.
138. Chan, E. Y., Luthi-Carter, R., Strand, A., Solano, S. M., Hanson, S. A., DeJohn, M. M., Kooperberg, C., Chase, K. O., DiFigliia, M., Young, A. B., Leavitt, B. R., Cha, J. H., Aronin, N., Hayden, M. R., and Olson, J. M. 2002. Increased huntingtin protein length reduces the number of polyglutamine-induced gene expression changes in mouse models of Huntington's disease. Hum. Mol. Genet. 11:1939–1951.
139. Sipione, S., Rigamonti, D., Valenza, M., Zuccato, C., Conti, L., Pritchard, J., Kooperberg, C., Olson, J. M., and Cattaneo, E. 2002. Early transcriptional profiles in huntingtin-inducible striatal cells by microarray analyses. Hum. Mol. Genet. 11:1953–1965.
140. Ravikumar, B., Stewart, A., Kita, H., Kato, K., Duden, R., and Rubinsztein, D. C. 2003. Raised intracellular glucose concentrations reduce aggregation and cell death caused by mutant huntingtin exon 1 by decreasing mTOR phosphorylation and inducing autophagy. Hum. Mol. Genet. 12:985–994.
141. Ravikumar, B., Duden, R., and Rubinsztein, D. C. 2002. Aggregate-prone proteins with polyglutamine and polyalanine expansions are degraded by autophagy. Hum. Mol. Genet. 11:1107–1117.
142. Kita, H., Carmichael, J., Swartz, J., Muro, S., Wyttenbach, A., Matsubara, K., Rubinsztein, D. C., and Kato, K. 2002. Modulation of polyglutamine-induced cell death by genes identified by expression profiling. Hum. Mol. Genet. 11:2279–2287.

APPENDIX 3

Human Molecular Genetics, 2004, Vol. 13, No. 7 **703–714**
DOI: 10.1093/hmg/ddh083
Advance Access published on February 12, 2004

CHIP and Hsp70 regulate tau ubiquitination, degradation and aggregation

Leonard Petrucelli[1], Dennis Dickson[1], Kathryn Kehoe[1], Julie Taylor[1], Heather Snyder[2], Andrew Grover[1], Michael De Lucia[1], Eileen McGowan[1], Jada Lewis[1], Guy Prihar[1], Jungsu Kim[1], Wolfgang H. Dillmann[3], Susan E. Browne[4], Alexis Hall[5], Richard Voellmy[5], Yoshio Tsuboi[6], Ted M. Dawson[7,8,9], Benjamin Wolozin[2], John Hardy[10] and Mike Hutton[1,*]

[1]Mayo Clinic, Jacksonville, FL 32224, USA, [2]Loyola University School of Medicine, Department of Pharmacology, Maywood, IL 60153, USA, [3]University of California, Department of Medicine, La Jolla, CA, USA, [4]Weill Medical College of Cornell University, New York, NY 10021, USA, [5]University of Miami School of Medicine, Miami, FL 33136, USA, [6]Fukuoka University, Department of Internal Medicine, Japan, [7]Institute for Cell Engineering, [8]Department of Neurology, [9]Department of Neuroscience, Johns Hopkins University School of Medicine, Baltimore, MD 21205, USA and [10]National Institutes of Health, Department of Neurogenetics, Bethseda, MD 20892, USA

Received November 17, 2003; Revised and Accepted January 30, 2004

Molecular chaperones, ubiquitin ligases and proteasome impairment have been implicated in several neurodegenerative diseases, including Alzheimer's and Parkinson's disease, which are characterized by accumulation of abnormal protein aggregates (e.g. tau and α-synuclein respectively). Here we report that CHIP, an ubiquitin ligase that interacts directly with Hsp70/90, induces ubiquitination of the microtubule associated protein, tau. CHIP also increases tau aggregation. Consistent with this observation, diverse of tau lesions in human postmortem tissue were found to be immunopositive for CHIP. Conversely, induction of Hsp70 through treatment with either geldanamycin or heat shock factor 1 leads to a decrease in tau steady-state levels and a selective reduction in detergent insoluble tau. Furthermore, 30-month-old mice overexpressing inducible Hsp70 show a significant reduction in tau levels. Together these data demonstrate that the Hsp70/CHIP chaperone system plays an important role in the regulation of tau turnover and the selective elimination of abnormal tau species. Hsp70/CHIP may therefore play an important role in the pathogenesis of tauopathies and also represents a potential therapeutic target.

INTRODUCTION

Neurodegenerative diseases as diverse as Alzheimer's disease (AD) and Parkinson's disease (PD) share an obvious common feature—aggregation and accumulation of abnormal proteins. A large group of these diseases, known as the tauopathies, are characterized by filamentous lesions in neurons and sometimes in glia that are composed of aggregates of hyperphosphorylated microtubule-associated protein tau (tau).

Tau promotes microtubule (MT) assembly, reduces MT instability and plays a role in maintaining neuronal integrity and axonal transport (1,2). Human tau protein is encoded by a single gene on chromosome 17q21 that consists of 16 exons, and central nervous system isoforms are generated by alternative splicing involving 11 of these exons (3–7). Tau is a phosphoprotein, predominantly expressed in neurons, where it is largely localized in axons (8). During the development of tau pathology, tau becomes hyperphosphorylated, detaches from the axonal microtubules and aggregates. The abnormal tau eventually accumulates in filamentous inclusions within neuronal cell bodies and processes. The precise sequence of events and the mechanisms involved in this process are not fully understood, but it is clear that abnormal tau accumulation and aggregation are sufficient to cause neurodegeneration. This in turn leads progressively to the onset of clinical symptoms. The primary tauopathies include Pick's disease (PiD), corticobasal degeneration (CBD), progressive supranuclear palsy (PSP) and frontotemporal dementia and parkinsonism linked to chromosome 17 (FTDP-17). Tau also accumulates in AD, where where the tau neurofibrillary pathology (e.g. tangles and

*To whom correspondence should be addressed at: Department of Neuroscience, 4500 San Pablo Road, Jacksonville, FL 32224, USA. Email: hutton.michael@mayo.edu

neuropil threads) occurs with a second protein aggregate, the amyloid plaque. The identification of exonic and intronic tau gene mutations associated with FTDP-17 established that tau dysfunction can cause neurodegeneration (9–11).

Unfolded or misfolded protein generated under diverse conditions must be either refolded by molecular chaperones, for instance Hsc/Hsp70 and Hsp40, or eliminated by the ubiquitin proteasomal system (UPS) through an energy-dependent process and concerted action of a number of molecules, including specific ubiquitin ligases. CHIP (carboxyl terminus of the Hsc70-interacting protein) is a molecule with dual function: (i) a co-chaperone of Hsp70 linked through the tetratricopeptide repeat (TPR) domain of CHIP; and (ii) possessing intrinsic E3 ubiquitin ligase activity (U-box domain) which promotes ligation/chain elongation for substrates (12–16). It is structurally similar to RING finger motifs typical of E3 ligases, like parkin. CHIP interacts functionally and physically with the stress-responsive ubiquitin-conjugating (E2 conjugase) enzyme family UBCH5. Thus CHIP is a bona fide ubiquitin ligase which provides a direct link between the chaperone and UPS and has been suggested to contribute in regulating the cellular balance between folding and degradation (17).

Recently, Imai *et al.* (18,19) showed that CHIP, Hsp70, parkin and PAELR formed a complex *in vitro* and *in vivo*. Unfolded PAELR is a substrate of the E3 ubiquitin ligase parkin and accumulation of non-ubiquitinated PAELR in the endoplasmic reticulum (ER) of dopaminergic neurons induces ER stress, leading to neurodegeneration (19). CHIP promotes the dissociation of Hsp70 from parkin and PAELR, thus facilitating parkin-mediated PAELR ubiquitination. Moreover, CHIP enhances parkin-mediated *in vitro* ubiquitination of PAELR in the absence of Hsp70. CHIP also enhances the ability of parkin to inhibit cell death induced by PAELR (18).

The role of the chaperones Hsp70/90 in tau biology has previously been examined by Dou *et al.* (20), who found an inverse relationship between tau aggregation and chaperone levels. Specifically, transgenic mice harboring the V337M tau mutation, which develop hippocampal tau aggregates, had lower levels of Hsp90 than control mice, suggesting that Hsp90 might be degraded along with aggregated tau. In addition, a small number of neurons in the hippocampus that were devoid of aggregated tau were observed to have significantly higher levels of Hsp90. The same relationship between Hsp90 and Hsp70 and tau aggregates in post-mortem samples from a single human AD brain were also reported (20).

In cell cultures transfected with tau constructs increased levels of both Hsp70 and 90, induced by treatment with geldanamycin, led to an ~80% reduction in levels of aggregated, detergent-insoluble tau. This reduction, however, was not accompanied by a decrease in total tau levels, but rather by a redistribution of tau from the insoluble fraction to the soluble fraction. The increased levels of soluble tau were accompanied by an increase in microtubule-bound tau. Reduction of Hsp70 or Hsp90 by RNAi caused the levels of the microtubule-bound tau to decrease (20).

Overall, these studies suggest that abnormal tau accumulation might be associated with perturbation of the major components of the cellular protein quality control machinery—molecular chaperones and the UPS. Hsp70/90 and other chaperones identify proteins that require proper folding, whereas aberrant unfolded proteins are directed to the UPS. CHIP is a ubiquitin E3 ligase that is involved in ubiquitination of Hsp70-bound proteins; this generally results in their targeting to the proteasome. This is a tandem event (chaperone and UPS activity) such that perturbation in either of these systems might play a role in tau accumulation. Moreover, evidence suggests that the Hsp70/90 chaperones and ubiquitin ligases are neuroprotective and can suppress the toxicity associated with abnormal protein accumulation in *Drosophila* and mouse models of disease (21–24).

In the present study we examined the relationship between CHIP/Hsp70 and tau and the role of this chaperone system in tau degradation, ubiquitination and aggregation. We show that CHIP associates with tau through the microtubule-binding domain, is able to ubiquitinate tau and increases the level of insoluble aggregated tau. In addition, a diversity of neuronal and glial tau-related lesions in several neurodegenerative disorders have CHIP immunoreactivity. This suggests that CHIP may play a role in the formation of, or cellular response to, fibrillary tau lesions. Hsp70 also binds to tau, but has opposing effects. Hsp70 decreases tau steady-state levels and selectively reduces insoluble and hyperphosphorylated tau species. Together, these data suggest that the Hsp70–CHIP chaperone system plays an important role in tau biology and in the pathogenesis of tauopathies.

RESULTS

CHIP interacts with tau

Because Hsp70 is known to interact with tau, the major protein species in neurofibrillary pathology, we investigated whether the Hsp70 co-chaperone CHIP, an E3 ubiquitin ligase, was able to interact with and ubiquitinate tau. Although CHIP has several known substrates, none of these have been associated with neurodegenerative disease.

To determine if CHIP and tau interact we first conducted co-immunoprecipitation experiments. Myc-tagged CHIP, parkin and Hsp70 were separately co-transfected with V5-tagged tau into HEK293 cells and then immunoprecipitation was performed with the V5 antibody. Detection of co-immunoprecipitating species was performed by western blotting with the Myc-tag antibody. Tau was found to co-immunoprecipitate with CHIP and Hsp70 (Fig. 1A). Tau also co-immunoprecipitated with parkin, an E3 ligase associated with autosomal recessive juvenile parkinsonism (25). This was not surprising given that parkin has previously been shown to interact with CHIP and that there is considerable structural homology between these two E3 ligases. To determine whether CHIP and tau interact *in vivo*, we performed co-immunoprecipitation using an antibody against CHIP in brain homogenates from transgenic mice (JNPL3 line) expressing mutant (P301L) tau (26). Western blot analysis was then performed with an antibody against tau (Fig. 1B). Tau co-immunoprecipitated with CHIP (Fig. 1B). These data clearly support the physiological and potential pathological relevance of the observed CHIP–tau interaction.

Using co-immunoprecipitation and *in vitro* binding assays, we next examined which regions of CHIP are necessary for the

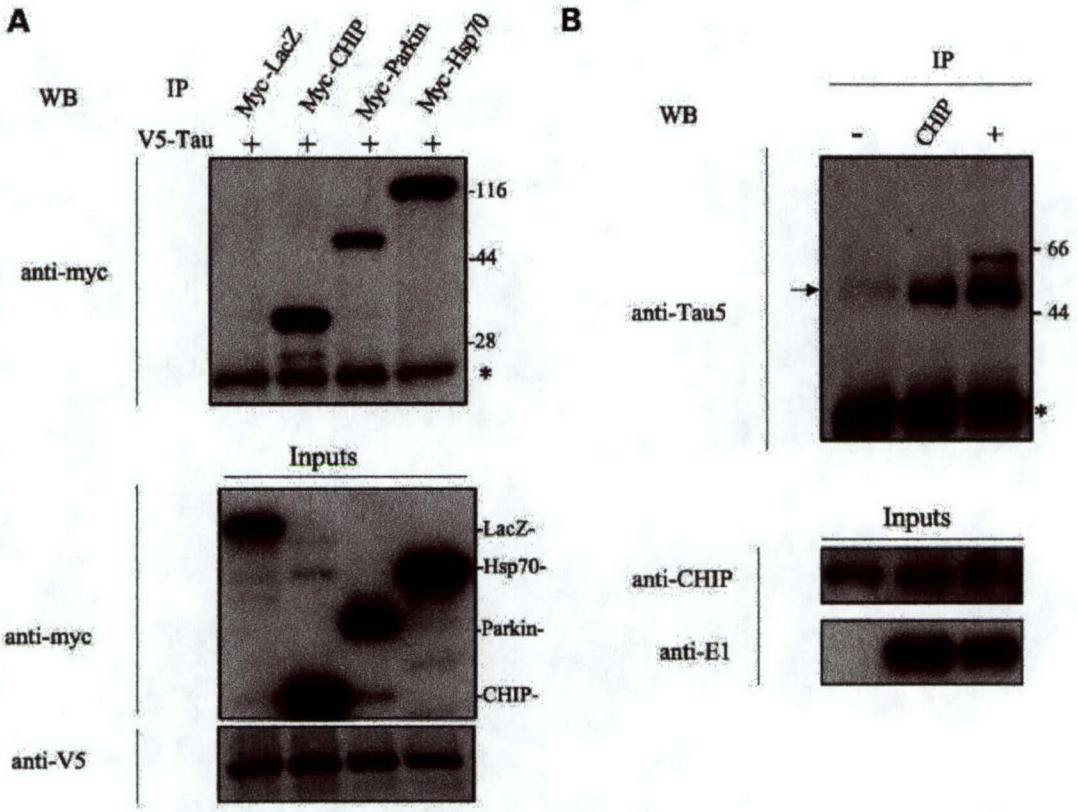

Figure 1. Tau associates with CHIP. (**A**) Interaction of Tau with CHIP, Hsp70 and parkin. Lysates from HEK293 cells transfected with an LacZ vector (Control), myc-tagged CHIP, myc-tagged Hsp70 or myc-tagged parkin and V5-tagged tau were immunoprecipitated with anti-V5 antibody. Immunoprecipitates (IP) and total soluble lysates (total lysate) were analyzed by western blotting (WB). (**B**) *In vivo* interaction of tau with CHIP in brain tissue. Mouse brain tissue from P301L transgenic mice (JNPL3) was homogenized as described in Experimental Procedures. The supernatant fractions were immunoprecipitated with anti-CHIP (CHIP), anti-E1 (+) or an irrelevant (−) polyclonal antibody. The co-precipitated tau was detected by western blotting using Tau5. An asterisk indicates the IgG light chain. The arrow indicates native tau species.

interaction with tau. CHIP contains two major structural motifs—a TPR motif and a U-box domain. The TPR motif is required for interaction with Hsc70 and Hsp90, while the U-box domain has ubiquitin ligase activity (Fig. 2A). To determine the site of interaction of CHIP with tau, we monitored the interaction of tau with these two domains of CHIP. The TPR mutant (C1; 1–189 amino acids) and U-box mutant (C2; 145-303 amino acids) both failed to bind to tau; in contrast, full-length CHIP bound strongly to tau (Fig. 2C). Although these results did not reveal a specific binding domain of CHIP with tau, it is conceivable that the interaction with tau requires both domains, as might be expected if complex formation with Hsp70 is required for the tau–CHIP interaction, or one of these domains and a third undefined region of CHIP. A series of truncated tau constructs were also generated to determine the domain of tau that interacted with CHIP (Fig. 2B). These experiments demonstrated that residues 187–311 contain the region of the tau protein necessary for interaction with CHIP. This includes the microtubule binding domains and the region immediately N-terminal (Fig. 2C).

CHIP ubiquitinates tau

To ascertain whether CHIP or parkin ubiquitinates tau, HEK293 cells were transfected with myc-tagged parkin or myc-tagged CHIP, V5-tagged tau and HA-tagged ubiquitin (Fig. 3A). Two days later, immunoprecipitation was performed with an antibody against V5 and probed with an antibody against HA to assess the degree of tau ubiquitination. Immunoprecipitated tau showed prominent anti-HA (ubiquitin) immunoreactivity in CHIP-transfected cells, with ubiquitin positive species appearing as mulitple higher molecular weight species, possibly representing oligomeric and multimeric ligations (Fig. 3A). To characterize the effect of Hsp70 on CHIP-mediated tau ubiquitination, cells were transfected as described above; however, they were also transfected with myc-tagged Hsp70 in the presence of CHIP. As shown in Figure 3B, Hsp70 attenuates CHIP activity, suggesting that Hsp70 antagonizes CHIP ubiquitination of tau. We further explored which ubiquitin lysine linkage (K48 or K68) was primarily responsible for ubiquitination of tau. Ubiquitin linkage through K48 is associated with proteasome targeting, while K68 ubiquitin linkage appears to be involved in cellular signaling/DNA repair (27). HEK293 cells were transfected with myc-tagged CHIP, V5-tagged tau and HA-tagged wild-type ubiquitin, K48 or K63 constructs. K48 and K63 refer to the particular lysine amino acid used to link the ubiquitins to each other. CHIP-mediated ubiquitination of tau did not discriminate between K48 or K63 type ubiquitin linkage suggesting that both types of linkage occur in tau (Fig. 3C). This has potential functional implications for the role of ubiquitination in tau biology. A further study showed that

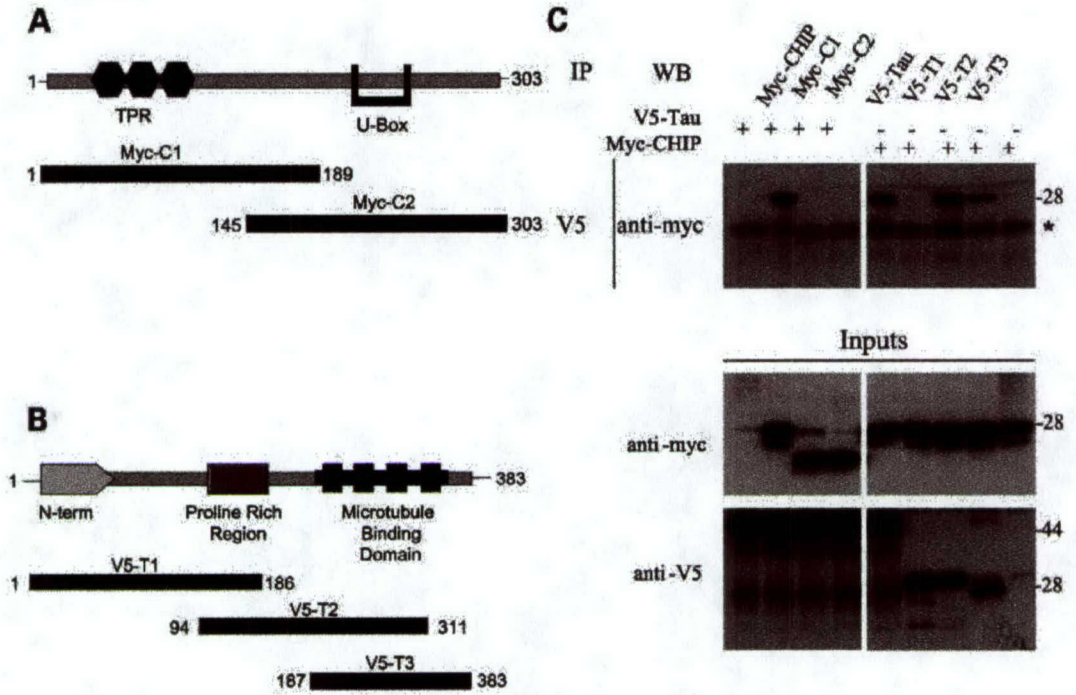

Figure 2. CHIP preferentially interacts with the microtubule-binding domain of tau and tau binding requires full-length CHIP. (**A**) Diagrammatically representation of full-length CHIP and the two structural domains (C1 and C2) used to determine the Tau binding. (**B**) Diagrammatically representation of tau and the three domains (T1, T2 and T3) used to determine the CHIP binding domain. (**C**) Lysates prepared from HEK293 cells transfected with V5-tagged tau and various myc-tagged CHIP domain constructs and various V5-tagged tau domains constructs and myc-CHIP and subjected to IP with anti-V5 followed by anti-myc immunoblotting. Lysates (inputs) were immunoblotted with either anti-V5 or anti-myc antibodies. The asterisk indicates IgG light chain. A representative result from three experiments is shown.

the amount of multimeric ubiquitinated tau (>200 kDa) increased dramatically after the cells were treated with the proteasome inhibitor MG-132, suggesting that a proportion of tau is degraded through the proteasome (Fig. 3D). In particular, it would appear that tau carrying long ubiquitin chains in the soluble fraction is degraded by the proteasome.

To verify the functional interaction between CHIP and tau, we reconstituted the ubiquitination reaction *in vitro*. In this experiment, immunoprecipitated CHIP or parkin and recombinant His-tagged tau were combined with other essential components for *in vitro* ubiquitination, including ATP and E2 conjugases. Again, immunoprecipitated CHIP, but not parkin, ubiquitinated tau (Fig. 4), demonstrating that tau is a substrate of CHIP. Further, when the western blot was re-probed with an antibody against the His-tag on tau, a ladder of species was observed, confirming that tau was directly ubiquitinated by CHIP. Finally, we observed that, in the absence of additional cellular components, Hsp70 had no impact on tau ubiquitination by CHIP; this is in contrast to the attenuation associated with increased Hsp70 activity observed in the *in vivo* ubiquitination studies. This suggests that *in vivo* an additional component of the complex or a particular Hsp70 conformation is required to down regulate tau ubiquitination by CHIP.

CHIP immunoreactivity in human neurodegenerative tauopathies

To evaluate the potential pathological significance of the interaction between tau and CHIP, we examined the immunolocalization of CHIP in postmortem brain sections of different human tauopathies, including AD, PSP, CBD, FTDP-17 and PiD, as well as JNPL3 transgenic mice that express mutant (P301L) tau. CHIP immunoreactivity was detected in a wide range of tau-positive lesions in both neurons and glia, including neurofibrillary tangles (NFTs; Fig. 5A) and dystrophic neurites in neuritic plaques (Fig. 5B) of AD, Pick bodies in PiD (Fig. 5C), globose NFTs (Fig. 5D) and tufted astrocytes (Fig. 5E) in PSP, and oligodendroglial coiled bodies and thread-like processes in CBD (Fig. 5F).

To confirm CHIP co-localization with tau lesions, serial sections from PiD, were immunostained with anti-phospho-tau (CP13; Fig. 5G) and with antibodies anti-CHIP (Fig. 5H), and to ubiquitin 3–39 (Fig. 5I).

The degree of CHIP immunoreactivity correlated to the predominant isoform of tau in the lesions, with 3R tauopathies showing more immunoreactivity than 3R+4R tauopathies or 4R tauopathies. Specifically, there was more robust CHIP immunoreactivity in Pick bodies (3R) than in NFTs in AD (3R+4R). Almost all Pick bodies were also ubiquitin-immunoreactive on adjacent sections stained for ubiquitin. In adjacent sections of AD stained for ubiquitin, most of the CHIP-positive NFTs were also ubiquitin-immunoreactive. The major exception was extracellular NFT, which had no CHIP-immunoreactivity yet variable ubiquitin immunoreactivity. Pre-tangles, neurons with non-fibrillar abnormal phospho-tau immunoreactivity, were negative for CHIP (data not shown). There were only a few NFTs stained in PSP, CBD and FTDP-17. These were all 4R tauopathies and neurofibrillary lesions in these disorders had

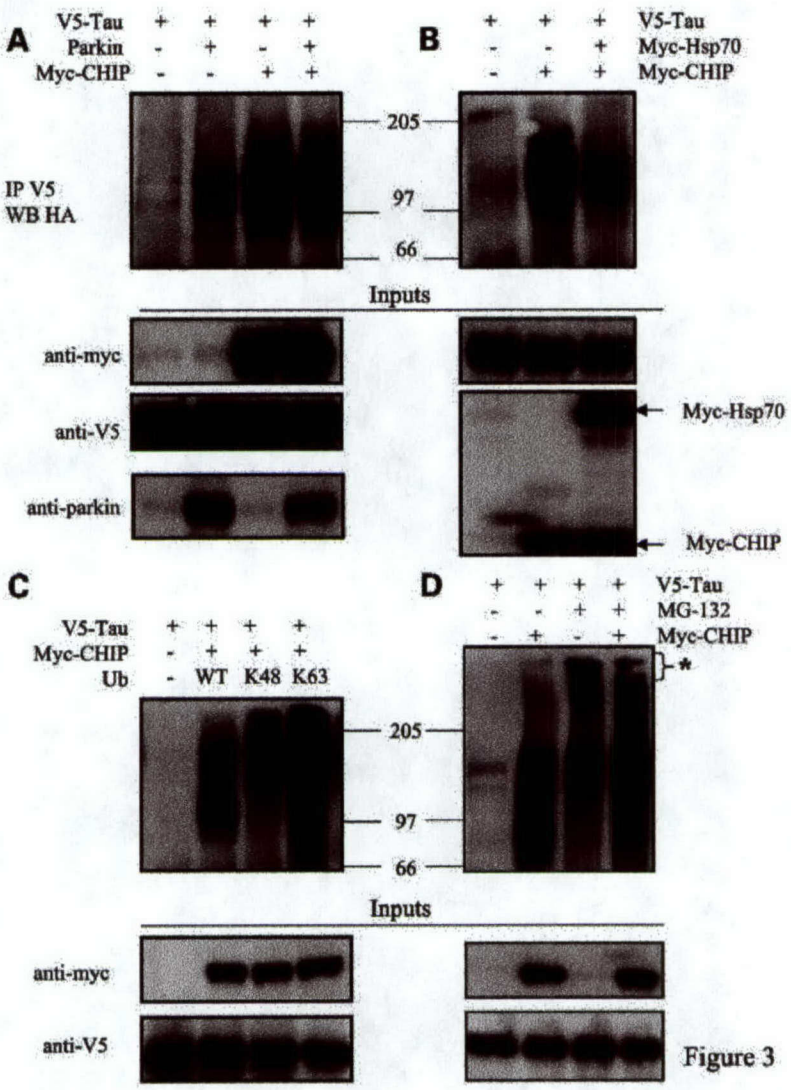

Figure 3. Tau tends to be ubiquitinated *in vivo*. (**A**) CHIP, not parkin, mediates tau ubiquitination. V5-tagged Tau cDNA combined with empty vector, untagged parkin or myc-tagged CHIP and HA-Ub construct were transfected into HEK293 cells. Immunoprecipitates with anti-V5 mAb (V5-IP) immunoblotted with HA mAb to assess the amount of ubiquitination. Total soluble lysates (inputs) were analyzed by western blotting using anti-myc, anti-V5 or anti-parkin. (**B**) Hsp70 attenuates CHIP activity. V5-tagged Tau cDNA combined with empty vector, myc-tagged CHIP and myc-tagged Hsp70 and HA-Ub construct were transfected into HEK293 cells. Immunoprecipitates with anti-V5 mAb immunoblotted with HA mAb to assess the amount of ubiquitination. Total soluble lysates (inputs) were analyzed by western blotting using anti-myc, anti-V5 or anti-parkin. (**C**) CHIP ubiquitinates tau through K48 and K63 ubiquitin linkages. V5-tagged Tau cDNA combined with myc-tagged CHIP (or vector as a control) and HA-tagged wild type or K48 or K63 ubiquitin mutants were transfected into HEK293 cells. Immunoprecipitates with anti-V5 mAb immunoblotted with HA mAb to assess the amount of ubiquitination. Total soluble lysates (inputs) were analyzed by western blotting using anti-myc or anti-V5. (**D**) Proteasome inhibition increases CHIP-mediated ubiquitination of tau. V5-tagged Tau cDNA combined with either empty vector or myc-tagged CHIP and HA-tagged ubiquitin were transfected into HEK293 cells. Thirty-six hours post-transfection cells were exposed to MG132 (5 μM, 12 h). Immunoprecipitates with anti-V5 and immunoblotted with HA mAb to access the amount of ubiquitination. Total soluble lysates (inputs) were analyzed by western blotting using anti-myc or anti-V5.

almost no ubiquitin immunoreactivity. Only a few glial lesions in the latter 4R tauopathies were CHIP-immunoreactive. Overall, the number of CHIP immunoreactive lesions was 50–70% for PiD, 5–10% for AD and 1–5% for both PSP and CBD. These data suggest a role for CHIP in pathologies involving tauopathies in humans. Similar to humans, neurofibrillary lesions in spinal cord sections of JNPL3 mice, which contain mutant 4R tau, were weakly immunoreactive for CHIP and ubiquitin, yet strongly positive for phospho-tau (data not shown).

Controls for specificity of CHIP included omission of primary antibody and absorption with CHIP synthetic peptide. These sections showed no immunoreactivity in Pick bodies (Fig. 5K) or NFTs (data not shown).

Effects of CHIP and Hsp70 on accumulation of detergent-insoluble tau

To examine the impact of CHIP-mediated ubiquitination on tau aggregation, COS-7 cells were transfected with a mutant

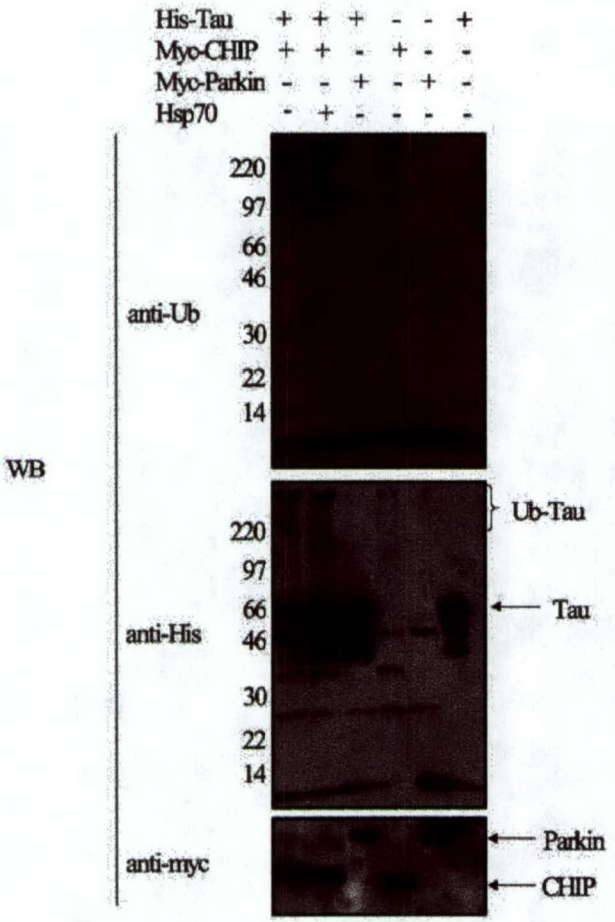

Figure 4. *In vitro* ubiquitination of tau by CHIP. The ubiquitination of Tau by CHIP (or parkin) was reconstituted by using immunoprecipitated myc-tagged parkin and myc-tagged CHIP from transfected HEK293 cells with the addition of purified UBCH7 or UBCH5b and the additional essential components for *in vitro* ubiquitination (see Materials and Methods). The reaction products were analyzed by western blot analysis with both anti-ubiquitin and anti-His antibodies. Inputs were immunoblotted with anti-myc antibodies. Brackets and molecular marker at 220 kDa indicate both Tau and ubiquitin-positive high molecular species. All experiments were replicated twice with similar results.

(P301L) tau expression construct in the absence or presence of either CHIP or Hsp70. Total tau was extracted and then fractionated into triton-soluble and insoluble pools. Transfection of CHIP dramatically increased the accumulation of high molecular weight aggregated tau species in the detergent (triton) insoluble fraction (Fig. 6), detected by western blot analysis with the Tau5 and E1 antibodies. The apparent molecular weight of these aggregated tau species ranged from ~90 kDa to large enough to be retained in the stacking gel. In contrast, expression of Hsp70 selectively reduced the amount of detergent insoluble tau to the point where little or no tau partitioned into the detergent-insoluble fraction. Although the level of insoluble tau was selectively reduced by Hsp70 transfection, there was no corresponding increase in detergent-soluble tau levels, which were also reduced relative to non-transfected cells (Fig. 6).

Induction of Hsp70 reduces tau levels *in vitro* and *in vivo*

To further explore the relationship between Hsp70 and tau steady-state levels *in vitro* we upregulated Hsp70 through geldanamycin (GA) treatment and activated heat shock factor 1 [(HSF-1 (+)] transfection (28). GA is a naturally occurring benzoquinone ansamycin that specifically binds to and interferes with the activity of the molecular chaperone Hsp90 (29), a negative regulator of heat-shock factor 1 (HSF-1), which regulates the transcription of several molecular chaperones, including Hsp70 (28,30). M17 human neuroblastoma cells, which express significant levels of endogenous tau, were either treated with GA or transfected with a mutant (constitutive active) form of HSF-1 (mHSF-1). As shown in Figure 7, treatment with GA reduced tau levels in a dose-dependent manner. Similar results were observed in cells transfected with mHSF-1. Both GA and mHSF-1 increased Hsp70 levels, with mHSF-1 causing the greater induction of the molecular chaperones (Fig. 7). HSF-1 (+), but not GA, also caused an increase in Hsp40 levels, suggesting that Hsp40 is unlikely to be necessary for the reduction of steady-state tau levels produced by these two treatments.

Based on the results described above, Hsp70 appears likely to be involved in regulating tau metabolism, especially the turnover of triton-insoluble species. To obtain additional evidence supporting this idea, we assessed the amount of endogenous tau in the brains of old mice overexpressing the inducible form of Hsp70 (31). There was no significant difference in age between transgenic and control littermates (30.6 ± 5.1 and 28.3 ± 2.1 months of age for non-transgenic and TgHsp70i mice, respectively). Whole brain homogenates from three non-transgenic and three tgHsp70 mice were homogenized and separated into 1% Triton X-100-soluble or -insoluble fractions. The fractions were then immunoblotted using Tau46, a polyclonal antibody to a carboxyl terminal epitope in tau that detects all forms of human and mouse tau (Fig. 8A). The amount of tau was normalized to β-actin levels in the brain of each mouse. Tau levels in TgHsp70 mice in both the soluble and insoluble fractions were significantly lower (~50% lower in both fractions) compared with NT mice (Fig. 8A and B). Moreover, high molecular weight triton-insoluble tau species present in the stacking gel that were observed in the very old NT mice were absent in the age-matched TgHsp70 mice (Fig. 8B). Tau levels were normalized to β-actin from the same gel from either the soluble or insoluble fractions with all the mice in the study. Statistical significance was estimated using Student's *t*-test for difference between NT and tgHsp70i mice in both fractions ($^{*}P < 0.01$, $^{**}P < 0.001$).

DISCUSSION

In the current study, we identified tau as a substrate for the ubiquitin ligase–chaperone protein CHIP. We concluded that tau is an authentic substrate of CHIP from the following evidence: first, CHIP interacts with tau and is specifically ubiquitinated by CHIP *in vivo* and *in vitro* in the presence of the E2 conjugase, UbcH5b. Second, proteasome inhibition augmented CHIP-mediated tau ubiquitination and promoted the insolubility of tau in triton-X-100 detergent. Finally, CHIP

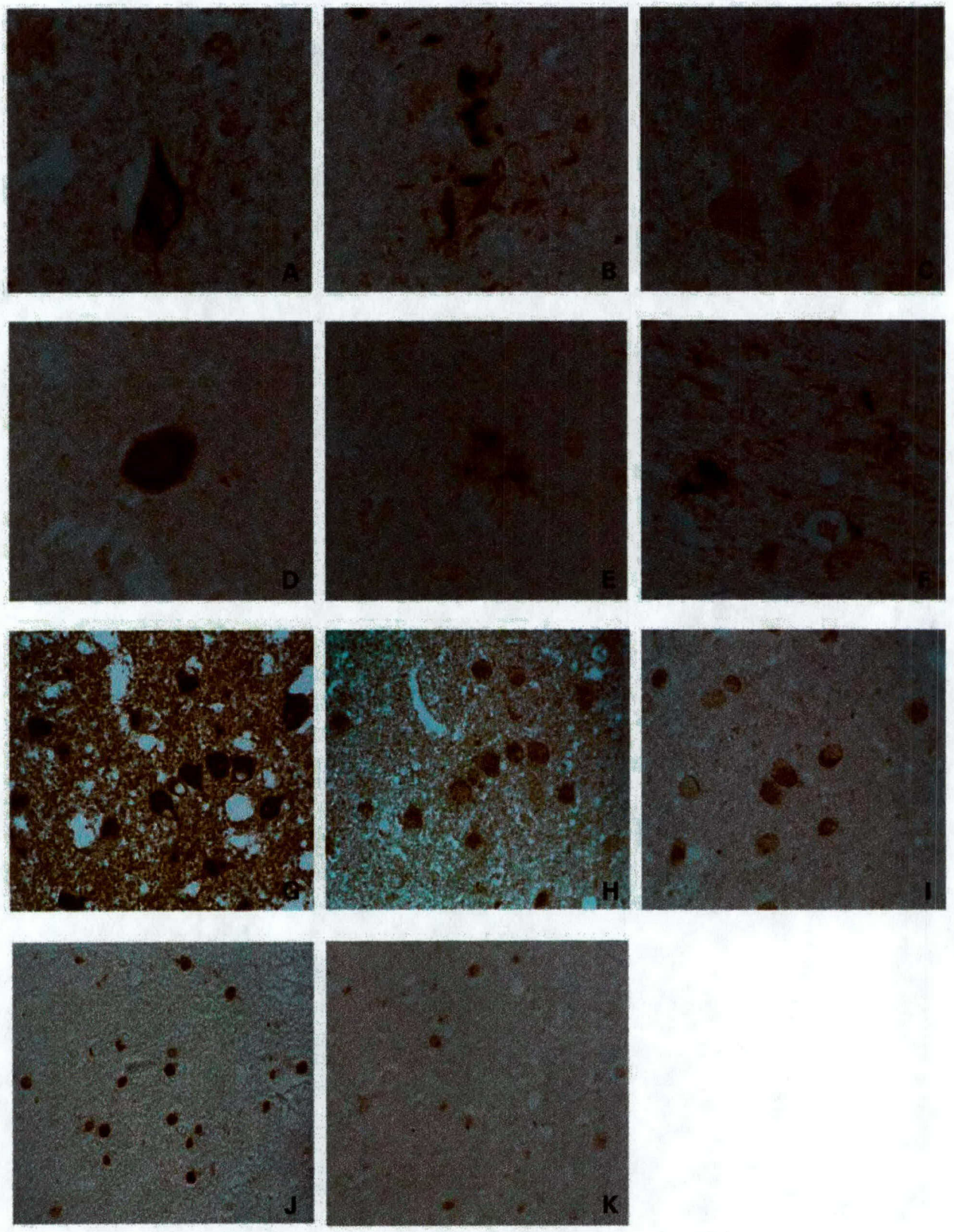

Figure 5. CHIP immunoreactivity is present in a diversity of neurodegenerative tauopathies. Immunostaining of CHIP in several tauopathies. (**A**) NFT in AD, (**B**) dystrophic neurites in senile plaques in AD, (**C**) Pick bodies in PiD, (**D**) globose NFT in PSP, (**E**) tufted astrocyte in PSP and (**F**) oligodendroglial coiled bodies and threads in CBD. CHIP co-localization with tau and ubiquitin was visualized using serial sections immunostained for phospho-tau with CP13 (**G**), CHIP (**H**) and anti-ubiquitin 3–39 (**I**). CHIP staining in PiD case (**J**) and preabsorption with CHIP synthetic peptide (**K**).

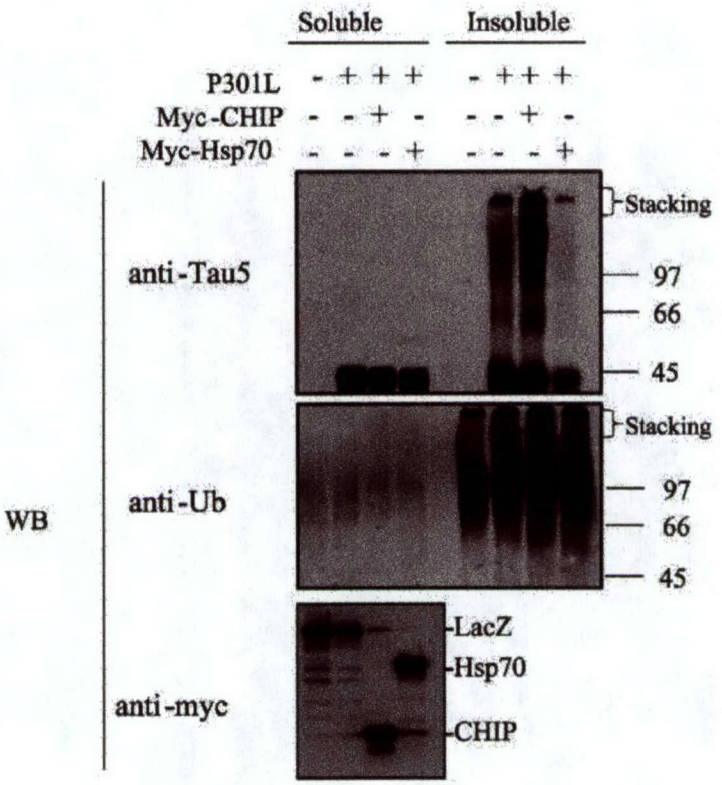

Figure 6. CHIP increases, Hsp70 suppresses tau aggregation. CHIP increases and Hsp70 decreases the accumulation of insoluble Tau in the COS7 cells. Cells transfected with vector plasmid (lacZ) or construct for mutant tau (P301L) combined with construct for mock (Control), myc-tagged CHIP or myc-Hsp70, were lysed and separated into 1% Triton X-100-soluble (S) or -insoluble (I) fractions, then immunoblotted with Tau5. Membrane was stripped and re-probed with anti-ubiquitin. Soluble fraction was used to demonstrate expression of respective constructs.

immunoreactivity was present in a range of tau lesions in several neurodegenerative tauopathies, especially those in which 3R tau is present in pathologic lesions, such as PiD and AD. The tauopathies with CHIP immunoreactivity were also those that have been shown in other studies to have ubiquitin-positive lesions (32). In contrast, disorders such as PSP or CBD in which lesions show almost no ubiquitin immunoreactivity were also negative for CHIP (35–38).

In this study, we found that CHIP mediated ubiquitination of tau. Moreover, both CHIP and Hsp70 interact with tau, suggesting that these two proteins act in concert to control tau metabolism. In fact, overexpression of Hsp70, in cells, attentuated the ubiquitination of tau induced by CHIP (Fig. 3B). These results suggest that Hsp70 and CHIP interact at the functional and/or cellular level. Interestingly the negative effect of Hsp70 on tau ubiquitination was not observed with *in vitro* assays, suggesting that additional chaperones that interact with the Hsp70/CHIP complex might play a role *in vivo*. Furthermore, it appears that a proportion of the tau ubiquitinated by CHIP via K48 ubiquitin linkage is consistent with the observed evidence of proteasome degradation of poly-ubiquitinated tau; however, tau was also ubiquitinated via K63 ubiquitin linkage, suggesting an alternative cellular fate for these species possibly including altered distribution and aggregation.

Although Dou *et al.* (20) reported that increased levels of Hsp70 reduce tau aggregation, which is in accord with results of the present study, they did not determine if this was a result of a reduction in tau levels (Figs 7 and 8), as our data indicate, rather than a redistribution of tau. Our data would further suggest that the CHIP and Hsp70 levels are critical to tau physiology such that excess CHIP would promote tau aggregation whereas Hsp70 would suppress it. In our model systems, insoluble tau aggregates represented a small fraction of total tau protein, which is a consistent observation in several tauopathies, including AD. Hsp/Hsc70 may protect against tau aggregation, neurofibrillary degeneration and neurotoxicity. Our data argue that Hsp70 (with CHIP) may be a critical determinant of normal tau degradation and may possibly be involved in the pathogenesis of human tauopathy. In this scheme, molecular chaperones would mediate tau degradation and directly or indirectly prevent tau aggregation and the toxicity associated with this protein. The balance between CHIP and Hsp70 levels may well be critical. Dai *et al.* (33) have recently shown that CHIP regulates activation of Hsp70 through induced trimerization and transcriptional activation of HSF-1. The activation of HSF-1 by CHIP emphasizes that a single protein (i.e. CHIP) within the complex can regulate major and often diametrically opposed chaperone activities (Hsp70) to alter the metabolism of substrate, in this case tau (33).

Although CHIP has been implicated in the ubiquitination of several substrates, including unfolded CFTR, glucocorticoid receptor and androgen receptor (14–16), tau is the first CHIP substrate that has been implicated in a number of

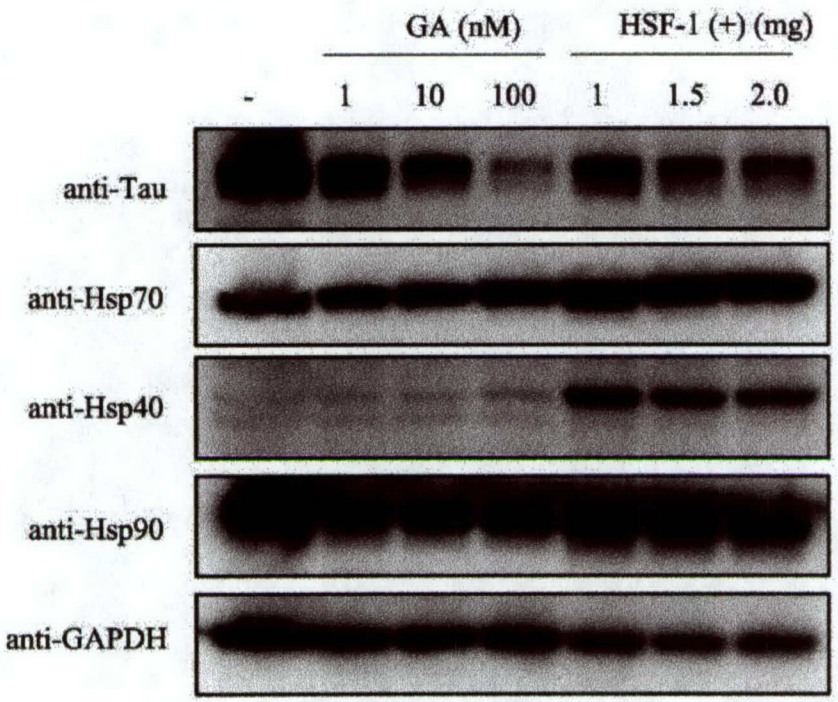

Figure 7. Induction of molecular chaperones decreases tau steady-state levels. M17 human neuroblastoma cell lines expressing endogenous tau were treated with geldanamycin (GA) at 1, 10 and 100 nM or transfected with activated heat shock factor 1 at 1, 1.5 and 2 μg DNA for 48 h. Cells were lysed and immunoblotted with Tau5 mAb. Membranes were stripped and sequentially re-probed with monoclonal antibodies to Hsp70, Hsp40, Hsp90 and GADPH (for protein loading).

neurodegenerative diseases. It is also clear that the another member of this chaperone complex, Hsp70, is involved in tau metabolism. Although many questions remain, the multiple effects of the Hsp70/CHIP chaperone system on tau biology make it of interest as a potential therapeutic target for the human tauopathies including AD.

MATERIALS AND METHODS

Expression vectors, cell culture and antibodies

cDNAs for parkin, tau (4R0N ± P301L), Hsp70 and CHIP were cloned into the mammalian expression vector pcDNA31.1 (Myc- or V5-tagged). Deletion constructs targeted for the respective domains were cloned into similar expression vectors. Ubiquitin constructs were obtained from Dr Ted Dawson (Johns Hopkins). A mutated cDNA sequence encoding an HSF1 lacking residues 203–315 was inserted into vector pcDNA3.1 to prepare expression construct HSF1(+). The integrity of all constructs was confirmed by automated sequencing.

COS-7 and HEK-293 cells were maintained in Optimem (Life Technologies) supplemented with 10% fetal bovine serum (Life Technologies), heat inactivated. Cells were transfected using Lipofectamine 2000 (Life Technologies) or FuGene6 (Roche) incubated for 48 h and treated as previously described. Human M17 Neuroblastoma cell lines stably overexpressing vector, wild-type tau (4R0N) and P301L cell lines were maintained in DMEM (Life Technologies) supplemented with 10% fetal bovine serum heat inactivated, glutamine, and 500 μg ml^{-1} G418.

CHIP polyclonal antibody was obtained from Abcam; HA and Myc antibodies was obtained from Roche; parkin antibody was obtained from Cell Signaling; Tau5 was generously provided by Dr Binder (Northwestern University); Hsp70 antibody was obtained from Stressgen abs; E1, human specific tau and Tau46 antibody were obtained from Dr Shu-Hui Yen (Mayo Clinic); CP13 (phospho-tau ser202) was obtained from Peter Davies (Albert Einstein College of Medicine) and ubiquitin 3–39 from Signet. HRP-coupled anti-mouse and anti-rabbit secondary antibodies were obtained from Jackson Immunoresearch. Ubiquitin polyclonal antibodies were obtained from Dako. His monoclonal antibody was obtained from Calbiochem. LB509 to α-synuclein (Zymed, San Francisco, CA, USA). Hsp40 and Hsp90 were obtained from BD Transduction laboratories. Hsp70 was obtained from Stressgen.

Ubiquitination assays

In vitro. Reactions were performed in 50 μl mixture containing 50 mM Tris–HCl, pH 7.5, 2.5 mM MgCl, 10 mM DTT, 4 mM ATP, 10 μg ubiquitin (Sigma), 500 ng of E1 (Calbiochem, San Diego, CA, USA), 200 ng of UbcH7 or UbcH5b (Affinti-Research, Exeter, UK), immunoprecipitated myc-tagged parkin or myc-tagged CHIP and 2 μg recombinant monomeric his-tagged tau (Dr Binder). Reactions were carried out for 2 h at 37°C before terminating with an equal volume of 2× SDS sample buffer. The reaction products were then subjected to western blot analysis with anti-ubiquitin (Dako, Carpinteria, CA, USA), Tau5 or anti-His antibodies.

In vivo. HEK293 cells were transfected with 4 μg of V5-tagged tau or 4 μg Myc-tagged parkin, Myc-tagged CHIP or Myc-tagged CHIP and Myc-tagged Hsp70 and 4 μg of

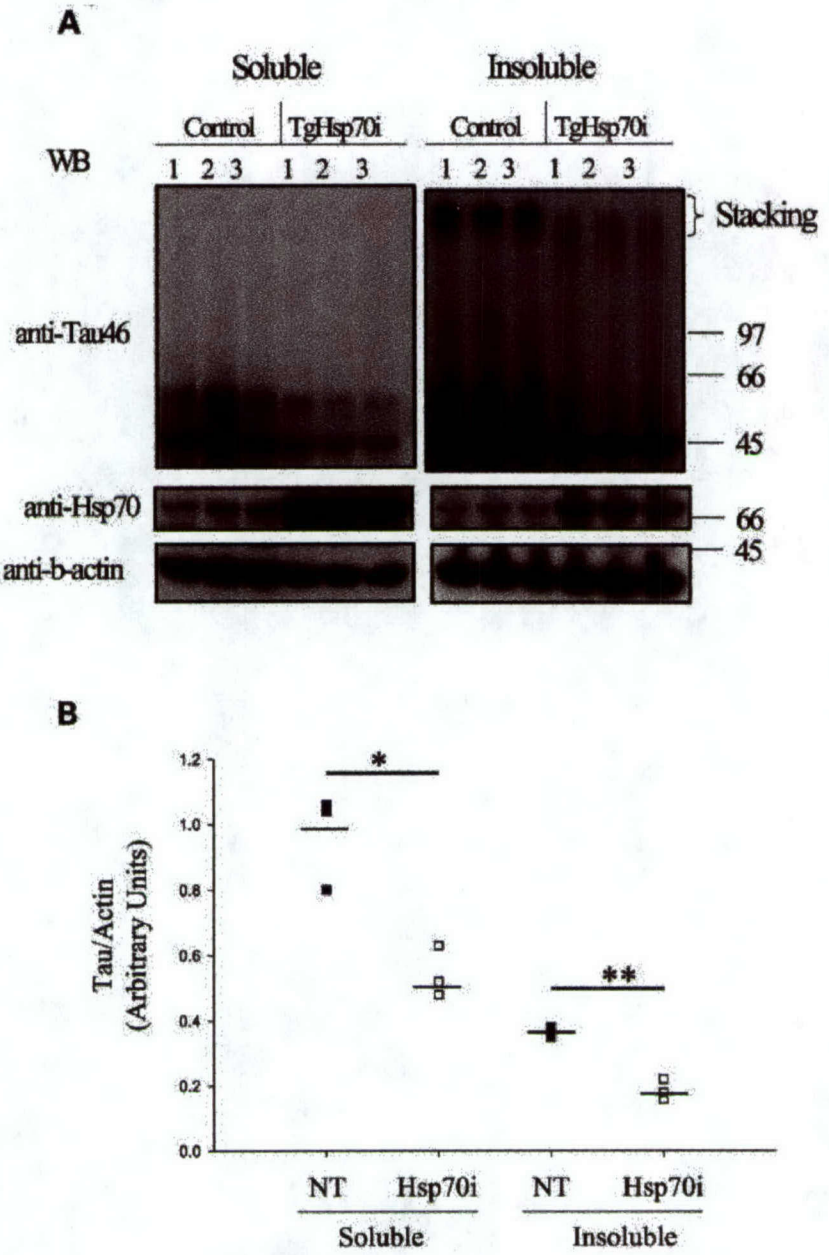

Figure 8. Tau levels in brains of mice overexpressing inducible form of Hsp70. (**A**, **B**) Whole brain tissues from 30-month-old normal (NT) or transgenic mice expressing the Hsp70 transgene were separated into 1% Triton X-100-soluble or -insoluble fractions, then immunoblotted with Tau46. Membrane was stripped and re-probed with anti-Hsp70 and anti-β-actin (control for protein loading). There was no significant difference between mice (30.6 ± 5.1 and 28.3 ± 2.1 months of age for NT and TgHsp70i, respectively). Tau normalized to β-actin from the same gel from either the soluble or insoluble fractions on all mice examined. Statistical significance was estimated using Student's *t*-test for difference between NT and tgHsp70i mice in both fractions. $*P < 0.01$; $**P < 0.001$.

pRK5–HA–wild-type ubiquitin, pRK5–HA–K48–ubiquitin, or pRK5–HA–K63–ubiquitin plasmids. After 48 h, immunoprecipitation was performed with an antibody against V5. The precipitates were submitted to western blotting with an antibody against HA.

Co-immunoprecipitation

For co-immunoprecipitation from cell cultures, HEK293 cells were transfected with 4 μg of each plasmid. After 48 h, cells were washed with cold PBS and harvested in immunoprecipitation buffer (0.1% Triton X-100, 2 μg/ml aprotinin, 100 μg/ml PMSF, 100 mM NaCl in 50 mM Tris–HCl, pH 7.2). The lysate was sonicated, pre-cleared for 1 h at 4°C with 25 μl of protein G (Pierce) and centrifuged at 14 000 rpm. The supernatants were incubated with 2 μg of an antibody against V5 (Life Technologies) and 60 μl of protein G and rocked at 4°C overnight. The protein G beads were pelleted and washed three times with immunoprecipitation buffer. The precipitates were resolved on SDS–PAGE gel and subjected to western blot

analysis. Bands were visualized with chemiluminescence (Pierce, Rockford, IL, USA).

For co-immunoprecipitation of proteins from mice, whole brains from adult mice expressing the P301L transgene brain (or non-transgenic mice as controls) were homogenized in 4 vols of ice-cold PBS containing 320 mM sucrose and 0.1% Triton X-100 with protease inhibitor cocktail (Sigma). The tissue homogenate was centrifuged at 37 000*g* at 4°C for 20 min. The supernatant was collected and 500 μg of protein was used for immunoprecipitation with one of the following antibodies: anti-CHIP, anti-E1 or anti-GFP (irrelevant antibody). The precipitates were subjected to western blot analysis and immunoblotted with Tau5.

M17 human neuroblastoma cells were either treated with GA (100 nM) or transfected with mHSF-1 (1, 1.5 and 2 μg DNA) for 48 h. Cells lysates were 1% Triton–PBS plus protease inhibitors. The precipitates were subjected to western blot analysis and immunoblotted with Tau5 and HSPs 70, 40 and 90.

Immunohistochemistry

Pre-absorption and specificity testing of polyclonal anti-CHIP antibody. CHIP peptide was re-suspended in 1% BSA in PBS to a concentration of 1 mg mL^{-1}. The peptide solution was added to diluted CHIP antibody in TBST to obtain a final dilution of 1 : 500. The mixture was rocked for 1 h at room temperature. The mixture was centrifuged at 13 500*g* for 2 min. The supernatant was separated from the pellet. Serial sections (5 μm thick) from a PiD case were deparaffinized and rehydrated in xylene and graded series of alcohol (100, 100, 95 and 70%). Antigen retrieval was performed in dH_2O in steam bath for 30 min. The sections were allowed to cool. The supernatant and diluted CHIP antibody (1 : 500 in TBST) were used for immunohistochemistry on the DAKO Autostainer (DakoCytomation, Carpinteria, CA, USA) using the DAKO EnVision HRP system on the serial sections. DAKO Liquid DAB Substrate–Chromogen system was the chromogen. The slides were then dehydrated and coverslipped.

Single antibody staining. Paraffin serial sections (5 μm thick) were used for immunohistochemistry from, diffuse Lewy body disease ($n = 6$), multiple system atrophy ($n = 2$) JNPL3 and littermate control mice (one each), AD ($n = 2$), PiD ($n = 4$), PSP ($n = 2$), CBD ($n = 2$), and FTDP_17 ($n = 2$). The sections were then processed the same as above. Primary antibodies used in the serial sections were: CHIP (1 : 250), CP13 (1 : 500) and 3–39 (1 : 200 000). In Lewy body disease and multiple system atrophy cases anti-synuclein (LB509, 1 : 100) replaced CP13. All antibodies were diluted in DAKO Antibody Diluent with background reducing components.

Fractionation experiments

For triton soluble/insoluble fractionation experiments, cells or tissue were lysed in a buffer containing PBS with 1% Triton X-100 and a cocktail of protease inhibitors. After sonication, cells were centrifuged at 100 000 *g* at 4°C for 30 min. Triton X-100 insoluble pellets were dissolved in a buffer containing 1% Triton X-100/1% SDS. The soluble and insoluble fractions were used in western blot analysis using the antibodies described in the figure legend.

ACKNOWLEDGEMENTS

This work was supported by NINDS grant RO1-NS41816-01.

NOTE ADDED IN PROOF

Very recently Shimura *et al.* (34) reported that tau binds to Hsc70 and phosphorylation is a requirement for ubiquitination by CHIP. In addition, CHIP was able to rescue phosphorylated tau-induced toxicity. Our data, while generally consistent with the findings of Shimura *et al.*, extends our understanding of the interaction between the Hsp70/CHIP chaperone system and tau by demonstrating the *in vivo* co-localization of CHIP with tau lesions in human patients with tauopathy and further by exploring the antagonistic action of Hsp70 and CHIP on tau ubiquitination and aggregation. In addition, while Shimura *et al.* report that CHIP ubiquitination is dramatically enhanced by GSK-3β driven phosphorylation of tau, our data show that GSK-3β phosphorylation is not absolutely required for CHIP to ubiquitinate tau.

REFERENCES

1. Ebneth, A., Godemann, R., Stamer, K., Illenberger, S., Trinczek, B. and Mandelkow, E. (1998) Overexpression of tau protein inhibits kinesin-dependent trafficking of vesicles, mitochondria, and endoplasmic reticulum: implications for Alzheimer's disease. *J. Cell Biol.*, **143**, 777–794.
2. Hirokawa, N. (1994) Microtubule organization and dynamics dependent on microtubule-associated proteins. *Curr. Opin. Cell. Biol.*, **6**, 74–81.
3. Andreadis, A., Brown, W.M. and Kosik, K.S. (1992) Structure and novel exons of the human tau gene. *Biochemistry*, **31**, 10626–10633.
4. Neve, R.L., Harris, P., Kosik, K.S., Kurnit, D.M. and Donlon, T.A. (1986) Identification of cDNA clones for the human microtubule-associated protein tau and chromosomal localization of the genes for tau and microtubule-associated protein 2. *Brain Res.*, **387**, 271–280.
5. Goedert, M., Wischik, C.M., Crowther, R.A., Walker, J.E. and Klug, A. (1988) Cloning and sequencing of the cDNA encoding a core protein of the paired helical filament of Alzheimer disease: identification as the microtubule-associated protein tau. *Proc. Natl Acad. Sci. USA*, **85**, 4051–4055.
6. Goedert, M., Spillantini, M.G., Potier, M.C., Ulrich, J. and Crowther, R.A. (1989) Cloning and sequencing of the cDNA encoding an isoform of microtubule-associated protein tau containing four tandem repeats: differential expression of tau protein mRNAs in human brain. *EMBO J.*, **8**, 393–399.
7. Goedert, M., Spillantini, M.G., Jakes, R., Rutherford, D. and Crowther, R.A. (1989) Multiple isoforms of human microtubule-associated protein tau: sequences and localization in neurofibrillary tangles of Alzheimer's disease. *Neuron*, **3**, 519–526.
8. Kanemaru, K., Takio, K., Miura, R., Titani, K. and Ihara, Y. (1992) Fetal-type phosphorylation of the tau in paired helical filaments. *J. Neurochem.*, **58**, 1667–1675.
9. Poorkaj, P., Bird, T.D., Wijsman, E., Nemens, E., Garruto, R.M., Anderson, L., Andreadis, A., Wiederholt, W.C., Raskind, M. and Schellenberg, G.D. (1998) Tau is a candidate gene for chromosome 17 frontotemporal dementia. *Ann. Neurol.*, **43**, 815–825.
10. Spillantini, M.G., Murrell, J.R., Goedert, M., Farlow, M.R., Klug, A. and Ghetti, B. (1998) Mutation in the tau gene in familial multiple system tauopathy with presenile dementia. *Proc. Natl Acad. Sci. USA*, **95**, 7737–7741.
11. Hutton, M., Lendon, C.L., Rizzu, P., Baker, M., Froelich, S., Houlden, H., Pickering-Brown, S., Chakraverty, S., Isaacs, A., Grover, A.*et al.* (1998) Association of missense and 5′-splice-site mutations in tau with the inherited dementia FTDP-17. *Nature*, **393**, 702–705.

12. Ballinger, C.A., Connell, P., Wu, Y., Hu, Z., Thompson, L.J., Yin, L.Y. and Patterson, C. (1999) Identification of CHIP, a novel tetratricopeptide repeat-containing protein that interacts with heat shock proteins and negatively regulates chaperone functions. *Mol. Cell. Biol.*, **19**, 4535–4545.
13. Jiang, J., Ballinger, C.A., Wu, Y., Dai, Q., Cyr, D.M., Hohfeld, J. and Patterson, C. (2001) CHIP is a U-box-dependent E3 ubiquitin ligase: identification of Hsc70 as a target for ubiquitylation. *J. Biol. Chem.*, **276**, 42938–42944.
14. Cardozo, C.P., Michaud, C., Ost, M.C., Fliss, A.E., Yang, E., Patterson, C., Hall, S.J. and Caplan, A.J. (2003) C-terminal Hsp-interacting protein slows androgen receptor synthesis and reduces its rate of degradation. *Arch. Biochem. Biophys.*, **410**, 134–140.
15. Connell, P., Ballinger, C.A., Jiang, J., Wu, Y., Thompson, L.J., Hohfeld, J. and Patterson, C. (2001) The co-chaperone CHIP regulates protein triage decisions mediated by heat-shock proteins. *Nat. Cell. Biol.*, **3**, 93–96.
16. Meacham, G.C., Patterson, C., Zhang, W., Younger, J.M. and Cyr, D.M. (2001) The Hsc70 co-chaperone CHIP targets immature CFTR for proteasomal degradation. *Nat. Cell. Biol.*, **3**, 100–105.
17. McClellan, A.J. and Frydman, J. (2001) Molecular chaperones and the art of recognizing a lost cause. *Nat. Cell. Biol.*, **3**, E51–53.
18. Imai, Y., Soda, M., Hatakeyama, S., Akagi, T., Hashikawa, T., Nakayama, K.I. and Takahashi, R. (2002) CHIP is associated with Parkin, a gene responsible for familial Parkinson's disease, and enhances its ubiquitin ligase activity. *Mol. Cell.*, **10**, 55–67.
19. Imai, Y., Soda, M. and Takahashi, R. (2000) Parkin suppresses unfolded protein stress-induced cell death through its E3 ubiquitin-protein ligase activity. *J. Biol. Chem.*, **275**, 35661–35664.
20. Dou, F., Netzer, W.J., Tanemura, K., Li, F., Hartl, F.U., Takashima, A., Gouras, G.K., Greengard, P. and Xu, H. (2003) Chaperones increase association of tau protein with microtubules. *Proc. Natl Acad. Sci. USA*, **100**, 721–726.
21. Cummings, C.J., Mancini, M.A., Antalffy, B., DeFranco, D.B., Orr, H.T. and Zoghbi, H.Y. (1998) Chaperone suppression of aggregation and altered subcellular proteasome localization imply protein misfolding in SCA1. *Nat. Genet.*, **19**, 148–154.
22. Auluck, P.K. and Bonini, N.M. (2002) Pharmacological prevention of Parkinson disease in Drosophila. *Nat. Med.*, **8**, 1185–1186.
23. Auluck, P.K., Chan, H.Y., Trojanowski, J.Q., Lee, V.M. and Bonini, N.M. (2002) Chaperone suppression of alpha-synuclein toxicity in a *Drosophila* model for Parkinson's disease. *Science*, **295**, 865–868.
24. Yang, Y., Nishimura, I., Imai, Y., Takahashi, R. and Lu, B. (2003) Parkin suppresses dopaminergic neuron-selective neurotoxicity induced by Pael-R in *Drosophila*. *Neuron*, **37**, 911–924.
25. Kitada, T., Asakawa, S., Hattori, N., Matsumine, H., Yamamura, Y., Minoshima, S., Yokochi, M., Mizuno, Y. and Shimizu, N. (1998) Mutations in the parkin gene cause autosomal recessive juvenile parkinsonism. *Nature*, **392**, 605–608.
26. Lewis, J., McGowan, E., Rockwood, J., Melrose, H., Nacharaju, P., Van Slegtenhorst, M., Gwinn-Hardy, K., Paul Murphy, M., Baker, M., Yu, X. *et al.* (2000) Neurofibrillary tangles, amyotrophy and progressive motor disturbance in mice expressing mutant (P301L) tau protein. *Nat. Genet.*, **25**, 402–405.
27. Marx, J. (2002) Cell biology. Ubiquitin lives up to its name. *Science*, **297**, 1792–1794.
28. Xia, W., Vilaboa, N., Martin, J.L., Mestril, R., Guo, Y. and Voellmy, R. (1999) Modulation of tolerance by mutant heat shock transcription factors. *Cell Stress Chaperones*, **4**, 8–18.
29. Whitesell, L., Mimnaugh, E.G., De Costa, B., Myers, C.E. and Neckers, L.M. (1994) Inhibition of heat shock protein HSP90-pp60v-src heteroprotein complex formation by benzoquinone ansamycins: essential role for stress proteins in oncogenic transformation. *Proc. Natl Acad. Sci. USA*, **91**, 8324–8328.
30. Zou, J., Guo, Y., Guettouche, T., Smith, D.F. and Voellmy, R. (1998) Repression of heat shock transcription factor HSF1 activation by HSP90 (HSP90 complex) that forms a stress-sensitive complex with HSF1. *Cell*, **94**, 471–480.
31. Marber, M.S., Mestril, R., Chi, S.H., Sayen, M.R., Yellon, D.M. and Dillmann, W.H. (1995) Overexpression of the rat inducible 70-kD heat stress protein in a transgenic mouse increases the resistance of the heart to ischemic injury. *J. Clin. Invest.*, **95**, 1446–1456.
32. Love, S., Saitoh, T., Quijada, S., Cole, G.M. and Terry, R.D. (1988) Alz-50, ubiquitin and tau immunoreactivity of neurofibrillary tangles, Pick bodies and Lewy bodies. *J. Neuropathol. Exp. Neurol.*, **47**, 393–405.
33. Dai, Q., Zhang, C., Wu, Y., McDonough, H., Whaley, R.A., Godfrey, V., Li, H.H., Madamanchi, N., Xu, W., Neckers, L.*et al.* (2003) CHIP activates HSF1 and confers protection against apoptosis and cellular stress. *EMBO J.*, **22**, 5446–5458.
34. Shimura, H., Schwartz, D., Gygi, S.P. and Kosik, K.S. (2004) CHIP-Hsc70 complex ubiquitinates phosphorylated Tau and enhances cell survival. *J. Biol. Chem.*, in press.
35. Wakabayashi, K., Oyanagi, K., Makifuchi, T., Ikuta, F., Homma, A., Homma, Y., Horikawa, Y. and Tokiguchi, S. (1994) Corticobasal degeneration: etiopathological significance of the cytoskeletal alterations. *Acta. Neuropathol. (Berl.)*, **87**, 545–553.
36. Yamada, T., McGeer, P.L. and McGeer, E.G. (1992) Appearance of paired nucleated, Tau-positive glia in patients with progressive supranuclear palsy brain tissue. *Neurosci. Lett.*, **135**, 99–102.
37. Verny, M., Duyckaerts, C., Delaere, P., He, Y. and Hauw, J.J. (1994) Cortical tangles in progressive supranuclear palsy. *J. Neural. Transm. Suppl.*, **42**, 179–188.
38. Yang, L. and Ksiezak-Reding, H. (1998) Ubiquitin immunoreactivity of paired helical filaments differs in Alzheimer's disease and corticobasal degeneration. *Acta. Neuropathol. (Berl.)*, **96**, 520–526.

Journal of Neurochemistry, 2004, **88**, 1352–1360 doi:10.1046/j.1471-4159.2003.02263.x

Mice deficient in dihydrolipoamide dehydrogenase show increased vulnerability to MPTP, malonate and 3-nitropropionic acid neurotoxicity

Peter Klivenyi,* Anatoly A. Starkov,* Noel Y. Calingasan,* Gabrielle Gardian,* Susan E. Browne,* Lichuan Yang,* Parvesh Bubber,*,† Gary E. Gibson,*,† Mulchand S. Patel‡ and M. Flint Beal*

**Department of Neurology and Neuroscience, Weill Medical College of Cornell University, New York Presbyterian Hospital, New York, New York, USA*

†Burke Medical Research Institute, White Plains, New York, USA

‡Department of Biochemistry, School of Medicine and Biomedical Sciences, State University of New York at Buffalo, Buffalo, New York, USA

Abstract

Altered energy metabolism, including reductions in activities of the key mitochondrial enzymes α-ketoglutarate dehydrogenase complex (KGDHC) and pyruvate dehydrogenase complex (PDHC), are characteristic of many neurodegenerative disorders including Alzheimer's Disease (AD), Parkinson's disease (PD) and Huntington's disease (HD). Dihydrolipoamide dehydrogenase is a critical subunit of KGDHC and PDHC. We tested whether mice that are deficient in dihydrolipoamide dehydrogenase ($Dld^{+/-}$) show increased vulnerability to 1-methyl-4-phenyl-1,2,3,6-tetrahydropyridine (MPTP), malonate and 3-nitropropionic acid (3-NP), which have been proposed for use in models of PD and HD. Administration of MPTP resulted in significantly greater depletion of tyrosine hydroxylase-positive neurons in the substantia nigra of $Dld^{+/-}$ mice than that seen in wild-type littermate controls. Striatal lesion volumes produced by malonate and 3-NP were significantly increased in $Dld^{+/-}$ mice. Studies of isolated brain mitochondria treated with 3-NP showed that both succinate-supported respiration and membrane potential were suppressed to a greater extent in $Dld^{+/-}$ mice. KGDHC activity was also found to be reduced in putamen from patients with HD. These findings provide further evidence that mitochondrial defects may contribute to the pathogenesis of neurodegenerative diseases.

Keywords: Alzheimer, Huntington, mitochondria, neurodegenerative diseases, Parkinson, oxidative damage.

J. Neurochem. (2004) **88**, 1352–1360.

There is accumulating evidence that the α-ketoglutarate dehydrogenase complex (KGDHC) is involved in neurodegenerative disorders. KGDHC activities are reduced in postmortem brain tissue of patients with Parkinson's disease (PD) (Mizuno *et al.* 1990; Gibson *et al.* 2003), and in both postmortem brain tissue and fibroblasts of patients with Alzheimer's disease (AD) (Gibson *et al.* 1988; Butterworth and Besnard 1990; Mizuno *et al.* 1990; Sheu *et al.* 1994; Kish *et al.* 1999). Interestingly, the KGDHC defect is found in postmortem brain tissue of patients with the Swedish amyloid precursor protein 670/671 mutation, which causes familial AD (Gibson *et al.* 1998). The enzyme is inactivated by oxidative stress induced by 4-hydroxynonenal, H_2O_2 and peroxynitrite (Chinopoulos *et al.* 1999; Park *et al.* 1999; Gibson *et al.* 2002).

Received October 6, 2003; revised manuscript received November 2, 2003; accepted November 5, 2003.

Address correspondence and reprint requests to M. Flint Beal, MD, Department of Neurology and Neuroscience, Weill Medical College of Cornell University, New York Presbyterian Hospital, 525 E 68th Street, New York, NY 10021, USA. E-mail: fbeal@med.cornell.edu

Abbreviations used: AD, Alzheimer's disease; BSA, bovine serum albumin; HD, Huntingdon's disease; KGDHC, α-ketoglutarate dehydrogenase complex; KPBS, potassium phosphate-buffered saline; MDA, malondialdehyde; MPP^+, 1-methyl-4-phenylpyridinium; MPTP, 1-methyl-4-phenyl-1,2,3,6-tetrahydropyridine; NeuN, neuron-specific nuclear protein; 3-NP, 3-nitropropionic acid; PBS, sodium phosphate-buffered saline; PD, Parkinson's disease; PDHC, pyruvate dehydrogenase complex; SDH, succinate dehydrogenase; TCA, tricarboxylic acid; TH, tyrosine hydroxylase.

KGDHC is a member of the α-ketoacid dehydrogenase complex family (Gibson *et al.* 2000a). This family also includes the pyruvate dehydrogenase complex (PDHC) and branched chain α-ketoacid dehydrogenase complex. Dihydrolipoamide dehydrogenase (EC 1.6.4.3) (encoded by *Dld* gene), which is also known as E3, is a critical subunit shared by all three dehydrogenases. It is a flavin-containing protein that transfers reducing equivalents from a dihydrolyl moiety to NAD^+, to form NADH and complete the catalytic process of the complex. The product of the *Dld* gene catalyzes the oxidation of dihydrolipoyl moities of four mitochondrial multienzyme complexes: PDHC, KGDHC, branched-chain α-ketoacid dehydrogenase and the glycine cleavage system.

Mice with a deficiency of dihydrolipoamide dehydrogenase have been developed (Johnson *et al.* 1997). Homozygous mice with disruption of the gene die *in utero* at a very early gastrulation stage. The heterozygous mice develop normally but have approximately half of wild-type activity for E3, for all affected multienzyme complexes, and the glycine cleavage system in liver and kidney (Johnson *et al.* 1997). In the present experiments we examined whether these mice show altered vulnerability to the dopaminergic neurotoxin 1-methyl-4-phenyl-1,2,3,6-tetrahydropyridine (MPTP), which has been used to model PD, and to malonate and 3-nitropropionic acid (3-NP), which have been used in models of Huntington's disease (HD) (Beal *et al.* 1993a, 1993b; Brouillet *et al.* 1995; Beal 2001).

Materials and methods

MPTP model

Heterozygous $Dld^{+/-}$ mice (C57BL/6), deficient in dihydrolipoamide dehydrogenase, were produced as described previously and genotyped using DNA extracted from the tail and a PCR assay (Johnson *et al.* 1997). We examined 12 $Dld^{+/-}$ and 12 littermate wild-type $Dld^{+/+}$ mice at 3–4 months of age. All experiments were carried out in accordance with the National Institute Health Guide for the Care and Use of Laboratory Animals and all procedures were approved by the local institutional animal care and use committee. Mice were housed in a room maintained at 20–22°C on a 12-h light–dark cycle with food and water available *ad libitum*. We administered MPTP to wild-type and $Dld^{+/-}$ mice at a dose of 20 mg/kg i.p. three times at 2-h intervals. Mice were killed 1 week later and the striata dissected.

1-Methyl-4-phenylpyridinium (MPP^+) levels

MPTP (20 mg/kg) was administered intraperitoneally three times at 2-h intervals. Mice were killed 90 min after the last injection. MPP^+ levels were quantified by HPLC with UV detection at 295 nm. Samples were sonicated in 0.1 M perchloric acid and an aliquot of supernatant was injected on to a Brownlee aquapore X 03–224 cation exchange column (Rainin, Woburn, MA, USA). Samples were eluted isocratically with 90% 0.1 mM acetic acid and 75 mM triethylamine HCl, pH 2.3, adjusted with formic acid and 10% acetonitrile.

Malondialdehyde (MDA) assay

MDA levels were measured by HPLC with fluorescence detection in striatal tissue at 18 h after administration of sodium phosphate-buffered saline (PBS) or MPTP (Ferrante *et al.* 1997). Malondialdehyde standard (98% purity) and other chemicals were purchased from Sigma (St Louis, MO, USA). Butylated hydroxytoluene solution was prepared in 95% ethanol to a final concentration of 0.05%. 2-Thiobarbituric acid was dissolved in water on a stirring hot-plate at 50–55°C to a concentration of 42 mM. The MDA standard was prepared with 40% ethanol solution. Standard curves were made with a series of MDA concentrations from 0.001 to 1.0 mM and a blank.

Brain tissues were homogenized in 40% ethanol. Sample derivatization was carried out in 2-mL plastic centrifuge tubes fitted with screw-on caps. To a 50 μL aliquot of sample homogenate or MDA standard, 50 μL butylated hydroxytoluene solution, 400 μL 0.44 M H_3PO_4 solution and 100 μL 2-thiobarbituric acid solution were added. Sample tubes were capped tightly, vortex mixed, then heated for 1 h on a 100°C dry-bath incubator. Following heat derivatization, samples were placed on an iced water bath (0°C) for 5 min to cool. Two hundred and fifty μL of *n*-butanol was subsequently added to each vial for extraction of the MDA–2-thiobarbituric acid complex. Tubes were vortex mixed for 5 min and then centrifuged for 3 min at 10 000 *g* to separate the two phases. Aliquots of 100 μL were removed from the *n*-butanol layer of each sample and placed in HPLC vials for analysis.

PDHC activity in brain tissue

Mice were decapitated and the heads were dropped into liquid N_2 immediately. The brains were removed under liquid nitrogen. The frozen brains were powdered in liquid N_2 and stored in liquid N_2-cooled cryo-vials (Corning Glass Works, Corning, NY, USA). Homogenates (2% by brain weight) were prepared for measurement of total and active forms of PDHC (Ksiezak-Reding *et al.* 1982; Huang *et al.* 1994). To measure the PDHC activity in the active form, the brain powders (2%) were homogenized in buffer without calcium and magnesium (50 mM Tris-HCl, pH 7.2, 1 mM dithiothreitol, 50 μM leupeptin, 0.4% Triton X-100). To measure total PDHC activity, the brain powder (2%) was incubated in the same buffer with the addition of 10 mM $MgCl_2$ and 1 mM $CaCl_2$ at 37°C for 30 min before assay. The total and active forms of PDHC for each brain were assayed in triplicate by monitoring the rate of acetyl-CoA formation as determined by its coupling to the acetylation of *p*-(*p*-aminophenylazo)-benzene sulfonic acid by arylamine *N*-acetyltransferase. PDHC activities were measured for 30 min at 37°C by following the decrease in the absorbence that occurs at 460 nm with the acetylation of *p*-(*p*-aminophenylazo)-benzene sulfonic acid on a spectrophotometric microtiter plate reader (Molecular Devices, Palo Alto, CA, USA). Protein was measured by the Bradford method with the Bio-Rad protein assay (Bio-Rad Laboratories, Hercules, CA, USA). Measurements were done at 595 nm on a spectrophotometric microtiter plate reader (Molecular Devices).

KGDHC activity assay

For assays of KGDHC activity, frozen pulverized tissue (as for PDHC) was prepared as 5% homogenates in 50 mM Tris-HCl pH 7.2, 1 mM dithiothreitol, 50 μM leupeptin 0.2 mM EGTA and 0.4% Triton X-100 (Gibson *et al.* 1988, 1998). KGDHC activity in

each sample was analyzed in triplicate in the presence of saturating concentrations of thiamine pyrophosphate, using a 96-well plate reader. Human postmortem control and brain tissue from patients with HD was obtained from the Harvard Brain Bank (McLean Hospital, Belmont, MA, USA).

Malonate lesions

We examined the effects of malonate-induced striatal lesions in 2.5-month-old $Dld^{+/-}$ mice. The mice were anesthetized with isoflurane and malonate (1.5 μmol in 1.0 μL, pH 7.4) was injected stereotaxically into the left striatum (anterior, 0.5 mm; lateral, 2 mm from bregma; ventral, 3.5 mm from dura). The injections were performed over 2 min using a 10-μL 26-gauge blunt-tipped Hamilton syringe. The needle was left in place for 5 min before being slowly withdrawn. Seven days after the striatal injections animals were killed.

3-NP lesions

Both $Dld^{+/-}$ mice and littermate controls aged 2.5 months were treated with 3-NP for 2 days at a dose of 50 mg/kg i.p. twice daily, followed by 60 mg/kg i.p. twice daily from day 3 to day 9. At 6 h after the last 3-NP injection, mice were killed.

Histological analysis

Mice were anesthetized with sodium pentobarbital and perfused transcardially with 0.1 M PBS, pH 7.4, followed by 4% paraformaldehyde in 0.1 M phosphate buffer (pH 7.4). Brains were removed, postfixed for 2 h in the same fixative, and then placed in 30% sucrose overnight at 4°C. For MPTP-lesioned brains, serial coronal sections (50 μm) were cut through the substantia nigra. Two sets, consisting of eight sections each 100 μm apart, were prepared. One set of sections was used for Nissl staining (cresyl violet). Another set was processed for tyrosine hydroxylase (TH) immunohistochemistry using the avidin–biotin peroxidase technique. Briefly, free-floating sections were pretreated with 3% H_2O_2 in PBS for 30 min. The sections were incubated sequentially in (1) 1% bovine serum albumin (BSA)/0.2% Triton X-100 for 30 min; (2) rabbit anti-TH affinity-purified antibody (Chemicon, Temecula, CA, USA; 1 : 2000 in PBS/0.5% BSA) for 18 h; (3) biotinylated anti-rabbit IgG (Vector Laboratories, Burlingame, CA, USA; 1 : 500 in PBS/0.5% BSA) for 1 h; and (4) avidin–biotin–peroxidase complex (Vector; 1 : 500 in PBS) for 1 h. The immunoreaction was visualized using 3,3′-diaminobenzidine tetrahydrochloride dihydrate with nickel intensification (Vector) as the chromogen. All incubations and rinses were performed with agitation using an orbital shaker at room temperature (37°C). The sections were mounted on to gelatin-coated slides, dehydrated, cleared in xylene and coverslipped. The numbers of Nissl-stained or TH-immunoreactive cells in the substantia nigra pars compacta were counted using the optical fractionator method in the Stereo Investigator (version 4.35) software program (Microbrightfield, Burlington, VT, USA).

Sections from 3-NP- and malonate-lesioned brains were immunostained using an anitibody against the neuronal marker neuron-specific nuclear protein (NeuN). Briefly, sections were pretreated with 0.05 M potassium phosphate-buffered saline (KPBS) containing 1% NaOH and 3% H_2O_2 for 30 min. After rinsing in KPBS three times for 10 min each, the sections were treated with 0.4% Triton X-100 and 1% BSA in KPBS for 30 min. The sections were incubated in NeuN antibody (Chemicon; 1 : 1000 in KPBS/1% BSA/0.4% Triton) for 18 h. After rinsing in KPBS containing 0.25% BSA and 0.02% Triton X-100, the sections were incubated in biotinylated anti-mouse IgG (1 : 200 in KBPS/0.25% BSA/0.02% Triton) for 1 h followed by the avidin–biotin–peroxidase complex (1 : 200) in KPBS for 1 h. The sections were rinsed in 0.05 M KPBS, and the reaction was developed in 0.05% 3,3′-diaminobenzidine tetrahydrochloride dihydrate containing 0.003% H_2O_2 in KBPS. Stereological analysis of lesion volumes was performed using the Cavalieri method in the Stereo Investigator (version 4.35) software program (Microbrightfield). Every other NeuN-stained section was examined.

Mitochondrial respiration

Mouse forebrain mitochondria were isolated according to the method of Rosenthal *et al.* (1987), except that Nagarse protease treatment was omitted and the amount of digitonin was adjusted to the smaller tissue sample (Starkov & Fiskum, 2003). Respiration of isolated mitochondria was measured at 37°C with a commercial Clark-type oxygen electrode (Hansatech Instruments, Kings Lynn, Norfolk, UK). The incubation medium was composed of 125 mM KCl, 10 mM HEPES, pH 7.2, 2 mM $MgCl_2$, 0.4 mg/ml BSA (fatty acid free), 0.8 mM ADP, and a respiratory substrate as indicated in figure legends. Mitochondria were added at 0.5 mg/ml. Membrane potentials of isolated mitochondria were estimated using the fluorescence of safranine O (3 μM), with excitation and emission wavelengths of 495 nm and 586 nm respectively. The incubation medium was as described above. KDGHC activity in mitochondria was measured fluorimetrically. The reaction medium was composed of 50 mM KCl, 10 mM HEPES, pH 7.4, 20 μg/mL alamethicin, 0.3 mM thiamine, 0.01 mM $CaCl_2$, 0.2 mM $MgCl_2$, 5 mM α-ketoglutarate, 1 μM rotenone and 0.2 mM NAD^+. The reaction was started by adding 0.14 mM Coenzyme A (CoASH) to permeabilized mitochondria (0.1–0.25 mg/mL). Reduction of NAD^+ was followed at 460 nm emission after excitation at 346 nm. The scale was calibrated by adding known amounts of freshly prepared NADH.

Succinate dehydrogenase (SDH) activity

SDH (EC 1.3.99.1) was measured spectrophotometrically as described previously (Arrigon and Singer 1962). The reaction medium was composed of 50 mM KCl, 10 mM HEPES, pH 7.4, 20 μg/mL alamethicin, 10 mM succinate, 2 mM KCN, 1 μM rotenone, 50 μM 2,3-dimethoxy-5-methyl-6-decyl-1,4-benzoquinone, 50 μM 2,6-dichlorophenol indophenol and 20 μM EDTA. The reaction was monitored at 600 nm, and the activity was calculated, employing $E_{mM} = 21\ cm^{-1}$ for 2,6-dichlorophenol indophenol.

Statistical analysis

Data are expressed as mean ± SEM. Statistical analysis was performed using one-way ANOVA followed by Newman–Keuls post-hoc test. The Mann–Whitney *U*-test and Student's *t*-test were used to analyze differences in lesion volumes.

Results

We measured KDGHC, total PDHC and active PDHC in cerebral cortex of wild-type and $Dld^{+/-}$ mice ($n = 9$).

KDGHC activity was significantly reduced from 14.0 ± 0.43 mU per mg protein in wild-type mice to 10.11 ± 0.34 mU per mg protein in $Dld^{+/-}$ mice ($p < 0.001$). Similarly, total PDHC activity was significantly reduced from 37.96 ± 1.16 to 30.95 ± 2.61 mU per mg protein in the $Dld^{+/-}$ mice ($p < 0.05$). There was a reduction in active PDHC from 32.3 ± 1.3 to 27.6 ± 2.4 mU per mg protein, but this was not statistically significant ($p = 0.12$). A preliminary study in the putamen of brains from three controls and seven patients with HD showed that KDGHC activity was significantly reduced from 11.5 ± 24 mU per mg protein in controls to 1.6 ± 0.6 mU mg protein in HD postmortem brain tissue ($p < 0.04$).

We carried out studies of MPTP neurotoxicity in $Dld^{+/-}$ mice. We administered MPTP at a dose of 20 mg/kg i.p. three times at 2-h intervals to littermate controls and heterozygous $Dld^{+/-}$ mice. MPTP produced a significantly greater depletion of TH- and Nissl-stained neurons in the $Dld^{+/-}$ mice than in littermate controls (Figs 1 and 2). We

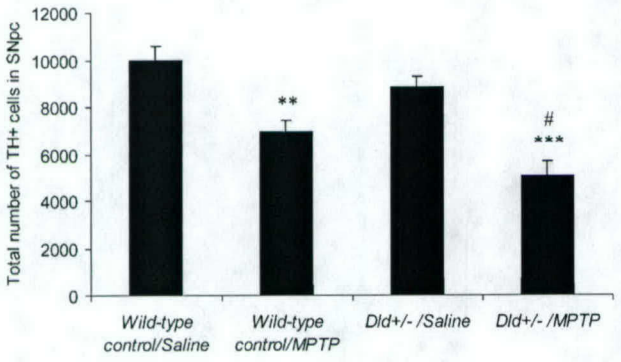

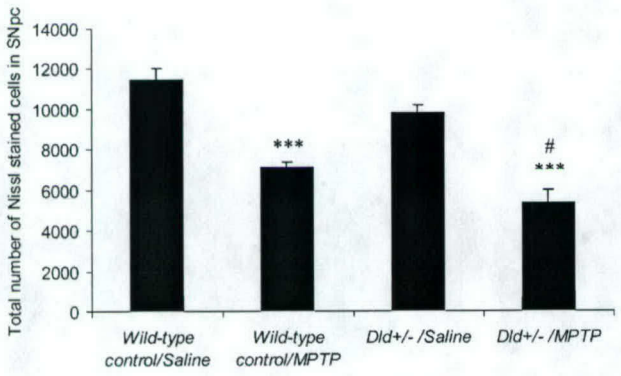

Fig. 1 Stereological (optical fractionator) counts of TH-positive (top) and Nissl-stained neurons (bottom) in the substantia nigra pars compacta (SNpc) of 2-month-old wild-type and $Dld^{+/-}$ mice. MPTP produced a significantly greater depletion of TH-positive and Nissl-stained neurons in the $Dld^{+/-}$ knockout mice than in the wild-type controls. Values are mean ± SEM. $^{**}p < 0.01$ versus wild-type control/saline, $^{***}p < 0.001$ versus respective $Dld^{+/-}$/saline, $\#p < 0.05$ versus wild-type control/MPTP by ANOVA.

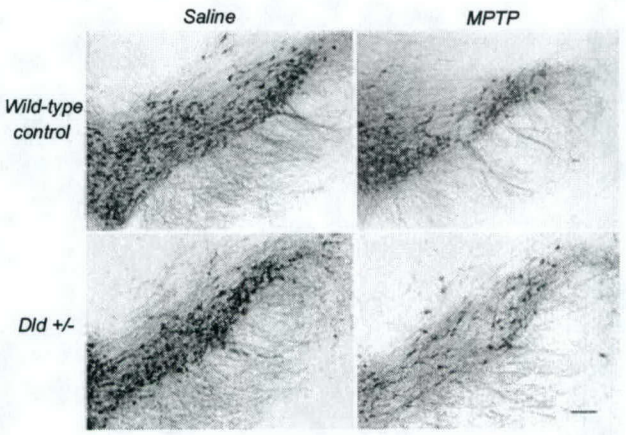

Fig. 2 Photomicrographs of TH-immunoreactive neurons in the substantia nigra pars compacta showing more severe MPTP-induced dopaminergic neuronal loss in $Dld^{+/-}$ mice than in wild-type controls. Scale bar 50 μm.

examined MDA in 6-month-old $Dld^{+/-}$ mice and littermate controls. MDA levels were significantly increased in the striatum of $Dld^{+/-}$ mice and increased further following MPTP administration (Fig. 3). MPP^+ levels were similar in control and $Dld^{+/-}$ mice: 49.7 ± 3.3 ng per mg protein ($n = 12$) versus 49.4 ± 2.7 ng per mg protein ($n = 10$) respectively.

We examined the effects of malonate-induced striatal lesions in $Dld^{+/-}$ mice. Malonate lesion volumes were approximately three-fold larger in the $Dld^{+/-}$ mice than controls (1.9 ± 0.5 vs. 0.7 ± 0.2 mm^3 respectively; $p < 0.05$) (Figs 4 and 5). We also examined 3-NP-induced lesions in the $Dld^{+/-}$ mice and littermate controls (Figs 6 and 7). There were bilateral areas of NeuN-positive cell loss in the striatum of wild-type and $Dld^{+/-}$ mice. The lesion volume in the $Dld^{+/-}$ mice was 3.5 ± 0.6 mm^3 whereas that

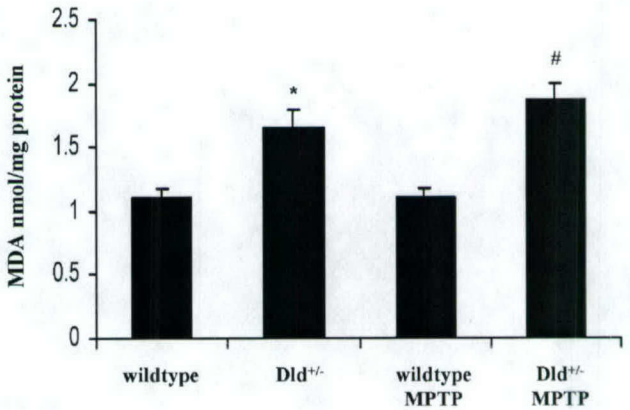

Fig. 3 Striatal MDA levels in $Dld^{+/-}$ mice and littermate controls at 6 months of age at baseline and following administration of MPTP. Values are mean ± SEM. $^{*}p < 0.05$ versus wild-type control, $\#p < 0.001$ versus wild-type control/MPTP by ANOVA.

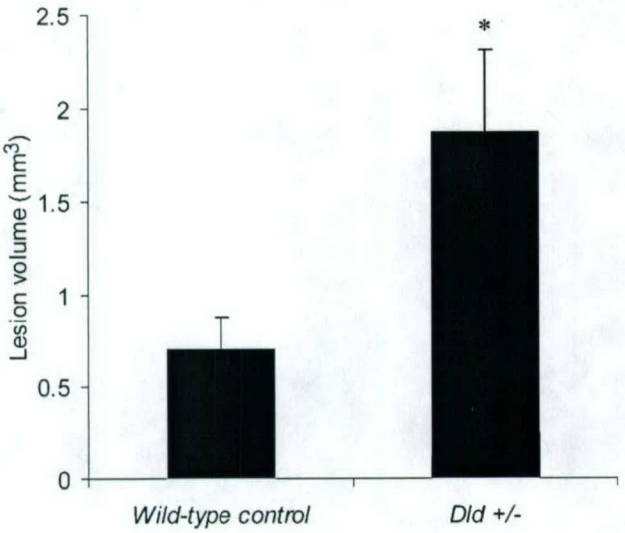

Fig. 4 Lesion volumes (Cavalieri method) in 2.5-month-old wild-type and *Dld*$^{+/-}$ mice after unilateral striatal malonate injection showing significantly larger lesions in the *Dld*$^{+/-}$ mice. Values are mean ± SEM. *$p < 0.05$ versus wild-type control by Mann–Whitney *U*-test.

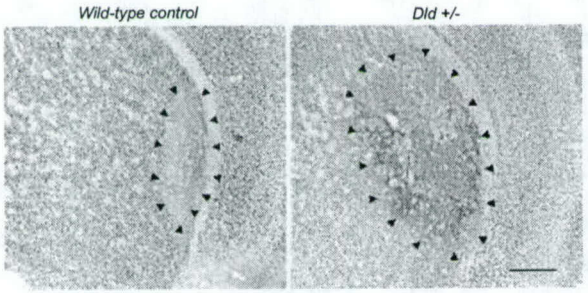

Fig. 5 Photomicrographs of NeuN-immunostained sections through the caudate–putamen of wild-type and *Dld*$^{+/-}$ mice showing malonate lesions. The lesion in the caudate–putamen (outlined by arrowheads) is larger in the *Dld*$^{+/-}$ mouse than that in the wild-type mouse. The dark staining at the lesion sites, which is more extensive in the *Dld*$^{+/-}$ mouse, represents IgG extravasation as detected by anti-mouse IgG, the secondary antibody used for NeuN immunohistochemistry. Scale bar 0.5 mm.

in wild-type mice was 0.9 ± 0.5 mm^3 ($p < 0.05$; $n = 17$ per group).

We examined the effects of 3-NP treatment on bioenergetics of isolated brain mitochondria (Figs 8 and 9). As expected, 3-NP treatment resulted in severe inhibition of SDH (Fig. 8a). However, succinate-supported respiration (Fig. 8c) and the membrane potential (Fig. 8b) were suppressed to a greater extent in mitochondria from *Dld*$^{+/-}$ mice. Figure 8(b) shows that the membrane potential was lower in *Dld*$^{+/-}$ mitochondria both in State 3 and following the induction of State 4 by carboxyatractylate, an inhibitor of the ATP/ADP antiporter. The addition of pyruvate to mitochondria oxidizing succinate resulted in an increase in the membrane potentials to almost

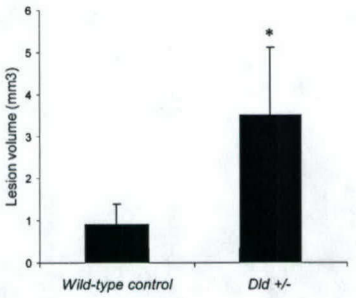

Fig. 6 Lesion volumes (Cavalieri method) of 2.5-month-old wild-type and *Dld*$^{+/-}$ mice after 3-NP injection, showing significantly larger lesions in the *Dld*$^{+/-}$ mice. Values are mean ± SEM. *$p < 0.05$ versus wild-type control by Mann–Whitney *U*-test.

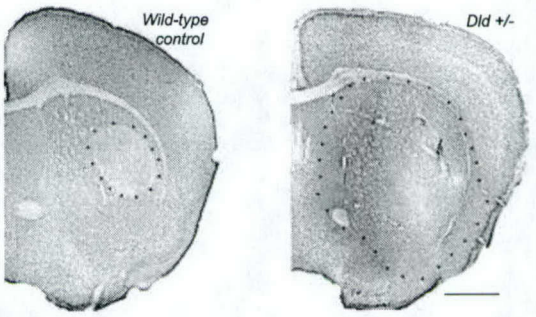

Fig. 7 Photomicrographs of NeuN-immunostained sections through the caudate–putamen of 3-NP treated wild-type and *Dld*$^{+/-}$ mice. The lesion in the caudate–putamen (outlined by arrowheads) is larger in the *Dld*$^{+/-}$ mouse than that in the wild-type mouse. The dark staining at the lesion site in the *Dld*$^{+/-}$ mouse represents IgG extravasation as detected by anti-mouse IgG, the secondary antibody used for NeuN immunohistochemistry. Scale bar 1 mm.

equal levels in *Dld*$^{+/-}$ and *Dld*$^{+/+}$ mitochondria. This increase was sensitive to the complex I inhibitor rotenone. Therefore, the membrane potential was most probably lower in *Dld*$^{+/-}$ mitochondria because of the lower SDH activity *per se* which was limiting the flux of electrons through the respiratory chain. In accordance with this interpretation, SDH activity in *Dld*$^{+/-}$ mitochondria was about 50% of that in *Dld*$^{+/+}$ mitochondria (Fig. 8c).

Figure 9(a) shows that 3-NP treatment also resulted in approximately 30% inhibition of phosphorylating respiration of mitochondria oxidizing pyruvate and malate. However, there were no differences in State 3 respiration rates between mitochondria from *Dld*$^{+/-}$ mice and their littermates with normal KGDHC activity. State 4 respiration rates were not affected by 3-NP treatment (data not shown). The reasons for inhibition of pyruvate and malate oxidation by 3-NP treatment are not clear. As mentioned above, 3-NP is a selective inhibitor of SDH and fumarase (EC 4.2.1.2), and neither of these enzymes is known to control the rate of State

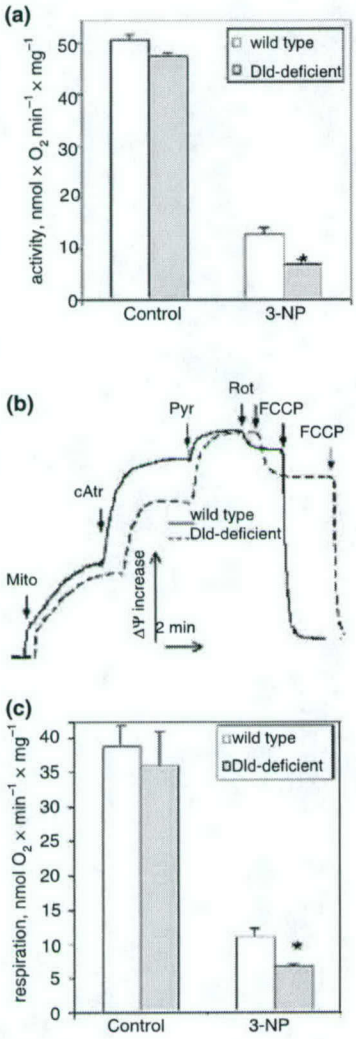

Fig. 8 Effect of *in vivo* 3-NP treatment, State 3 respiration, membrane potential and SDH activity in $Dld^{+/+}$ and $Dld^{+/-}$ mitochondria. (a) SDH activity. (b) Membrane potentials of mitochondria isolated from 3-NP-treated animals. The membrane potential was estimated from fluorescence of safranine O. The incubation medium was supplemented with 10 mM succinate, and 3 μM safranine O was included. Additions: Mito, 0.5 mg/mL mitochondria; cAtr, 4 μM carboxyatractylate; Pyr, 7 mM pyruvate; Rot, 1 μM rotenone; FCCP, 50 nM FCCP. (c) State 3 respiration of mitochondria. Incubation medium (see Materials and methods) was supplemented with 10 mM succinate and 1 μM rotenone. Control, mitochondria from mice not treated with 3-NP ($n = 6$); 3-NP, mitochondria from 3-NP-treated mice ($n = 4$). Values in (a) and (c) are mean ± SEM. There were no differences in State 3 rates (c) and SDH activities (a) between control groups. *$p < 0.05$ versus 3-NP-treated wild-type mice.

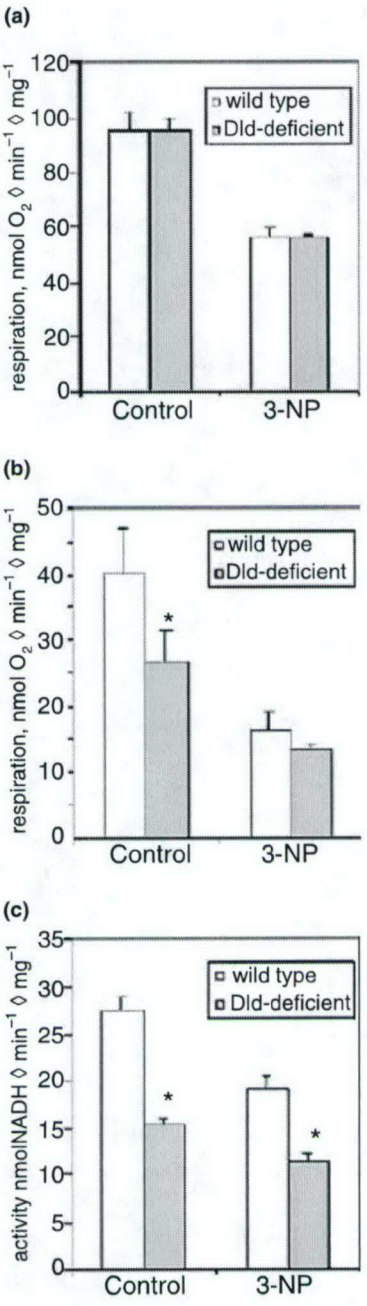

Fig. 9 Inhibition of mitochondrial phosphorylating respiration and KGDHC activity by *in vivo* 3-NP treatment. (a, b) State 3 respiration. Incubation medium and other conditions were as in Fig. 8(c), except that succinate and rotenone were replaced with 7 mM pyruvate and 0.8 mM malate (a) or with 10 mM α-ketoglutarate (b). (c) KGDHC activity. Control, mitochondria from control mice ($n = 7$); 3-NP, mitochondria from 3-NP-treated mice ($n = 4$). Values are mean ± SEM. *Statistically significant difference $p < 0.05$ compared with wild-type controls.

3 respiration supported by pyruvate and malate oxidation. Unexpectedly, 3-NP treatment significantly reduced KGDHC activity. State 3 respiration supported by α-ketoglutarate was suppressed by ~ 60% in wild-type mitochondria and by ~ 48% in $Dld^{+/-}$ mitochondria (Fig. 9b). In accordance with the respiration data, the activity of KGDHC in mitochondria was also inhibited (Fig. 9c).

Discussion

There is substantial evidence that alterations in α-ketoacid dehydrogenases may play a role in the pathogenesis of neurodegenerative diseases. Strong evidence has accumulated implicating KGDHC deficiency in AD (Gibson *et al.* 1988, 1998; Butterworth *et al.* 1990; Sheu *et al.* 1994). The clinical dementia rating scale is highly correlated with postmortem brain KGDHC activity (Gibson *et al.* 2000). There is also evidence for decreases in KGDHC in the substantia nigra of patients with PD (Mizuno *et al.* 1990, 1995; Gibson *et al.* 2003). Immunostaining for KGDHC declines in many melanized neurons and this reduction correlates with the severity of the degeneration (Mizuno *et al.* 1994). KGDHC is more vulnerable to degeneration than complex II, III and IV as shown by immunostaining. There is evidence for reduced PDHC activity in both AD and HD (Sorbi *et al.* 1983; Butterworth *et al.* 1985).

Although previous studies showed reduced PDHC activity in HD postmortem brain tissue, there have been no reports on measurement of KDGHC activity. We found that KDGHC activity was reduced in the putamen. This may also be a consequence of oxidative damage as we and others found increased oxidative damage in both HD postmortem brain tissue and a transgenic mouse model of HD (Bodganov *et al.* 2001; Browne *et al.* 1999; Perez-Severiano *et al.* 2000; Tabrizi *et al.* 2000). This finding shows that KDGHC activity is reduced in three of the most common neurodegenerative diseases, AD, PD and HD.

Genetic studies also implicate KGDHC in PD and AD. In PD a polymorphism occurs in exon 9 of the *DLST E2* gene of KGDHC (Kobayashi *et al.* 1998). A single nucleotide substitution between G (in allele 1) and A exon 9 (in allele 2) occurs, but it does not change the amino acid code. Frequencies of the genotype that carry the A allele are significantly higher in patients with PD than in controls. These results suggest that a genetic variant of the *E2* gene itself, or in close proximity to the gene, constitutes a risk factor for PD. Polymorphisms in the $Dld^{+/-}$ gene also appear to be a risk factor for AD in caucasians (Sheu *et al.* 1999).

Previous studies showed that MPTP and isoquinoline derivative neurotoxicity was associated with reduced activity of KGDHC (McNaught *et al.* 1995; Joffe *et al.* 1998). The MPTP metabolite MPP^+ inhibits KGDHC (Mizuno *et al.* 1988). It is possible that these effects may be mediated by oxidative stress. Previous work showed that KGDHC is sensitive to a number of oxidants including hydroxynonenal, H_2O_2 and peroxynitrite (Chinopoulos *et al.* 1999; Park *et al.* 1999; Gibson *et al.* 2002). The inactivation by peroxynitrite (Park *et al.* 1999) is particularly interesting as peroxynitrite-mediated neurotoxicity has been strongly implicated in MPTP neurotoxicity (Schulz *et al.* 1995a; Hantraye *et al.* 1996; Przedborski *et al.* 1996). Peroxynitrite may also be involved in PD as shown by increases in 3-nitrotyrosine staining of Lewy bodies in the substantia nigra of patients with PD (Good *et al.* 1998; Giasson *et al.* 2000). KDGHC is also inhibited by oxidized derivatives of dopamine (Shen *et al.* 2000). Exposure of Chinese hamster ovary cells to hyperoxia results in cell death and complete inactivation of KDGHC, whereas KDGHC activity is preserved in cells that are resistant to hyperoxia (Schooner *et al.* 1990, 1991).

In the present experiments we examined whether $Dld^{+/-}$ mice show increased vulnerability to MPTP neurotoxicity. We found that both KGDHC and total PDHC activities were significantly reduced in the cerebral cortex of $Dld^{+/-}$ mice. If a deficiency in KGDHC contributes to PD pathogenesis one would expect these mice to show increased vulnerability to the toxin, which is known to impair mitochondrial function. We found that the $Dld^{+/-}$ mice showed greater loss of TH-stained neurons in the substantia nigra pars compacta. There were no alterations in MPP^+ levels to suggest altered processing or metabolism of MPTP in these mice.

We also examined the effects of malonate lesions in the $Dld^{+/-}$ mice. Malonate is a reversible inhibitor of SDH. We and others showed that intrastriatal injections of malonate produce lesions that in many respects resemble the neuropathology of HD (Beal *et al.* 1993b; Greene *et al.* 1993). The lesions occur by an indirect excitotoxic mechanism as they are blocked by excitatory amino acid antagonists (Beal *et al.* 1993b; Greene *et al.* 1993). The lesions are associated with increases in markers of free radical damage and are attenuated by free radical scavengers (Schulz *et al.* 1995b). This might lead to further inactivation of KGDHC. In the present experiments, we found that striatal lesions produced by malonate were markedly exacerbated in $Dld^{+/-}$ mice. Lesion volumes were approximately three-fold greater than those seen in littermate controls. This is consistent with the possibility that inhibition of the tricarboxylic acid (TCA) cycle at multiple sites may greatly exacerbate bioenergetic defects.

We also examined the effects of 3-NP in $Dld^{+/-}$ mice. 3-NP is a suicide inhibitor of the mitochondrial TCA enzyme SDH (Alston *et al.* 1977; Coles *et al.* 1979) and a reversible inhibitor *in vitro* of fumarase, another TCA enzyme (Porter and Bright 1980). Systemic administration of 3-NP inhibits SDH in the whole brain as well as in the liver and heart (Gould and Gustine 1982; Gould *et al.* 1985), and results in abnormal succinate build-up and inhibition of the mitochondrial TCA cycle (Hassel and Sonnewald 1995).

Systemic administration of 3-NP produces selective lesions in the striatum, which closely mimic the neuropathologic features of HD, as it produces relative sparing of NADPH-diaphorase neurons, a characteristic feature of HD neuropathology (Beal *et al.* 1993a). In baboons, it produces a choreiform movement disorder as well as dystonia (Brouillet *et al.* 1995; Palfi *et al.* 1996). The lesions are attenuated in mice overexpressing Cu/Zn superoxide dismutase (Beal *et al.* 1995). We therefore examined the effects of 3-NP in

$Dld^{+/-}$ mice. $Dld^{+/-}$ mice were significantly more vulnerable to the neurotoxic effects of 3-NP. The lesion volumes in the deficient mice were three- to four-fold larger than those seen in controls.

The *in vivo* treatment with 3-NP induced more pronounced inhibition of SDH activity in brain mitochondria isolated from $Dld^{+/-}$ mice than in mitochondria from $Dld^{+/+}$ mice. Interestingly, KGDHC activity was also severely inhibited. To our knowledge, there are no published reports on inhibition of the purified KGDHC enzyme complex by 3-NP or that 3-NP treatment can inhibit mitochondrial KGDHC activity *in situ* or *in vivo*. Therefore, the mechanism of the inhibition is not clear, although it might be secondary to oxidative damage. However, the KGDHC inhibition may explain the observed decrease in State 3 respiration rates supported by oxidation of pyruvate and malate (Fig. 9), provided that KGDHC exerted significant control over the flux of reducing equivalents in the TCA cycle under our experimental conditions. The data indicate that there may be a direct interaction between SDH and KGDHC *in vivo*, in such a way that an impairment of one of these enzymes results in an increased vulnerability of the other enzyme, consistent with an oxidative stress mechanism. Another interesting possibility relates to the *DLST* gene, which encodes the dihydrolipoamide succinyltansferase component subunit of KGDHC, and was recently shown to possess another important function in regulating mitochondrial energy production. In addition to its full-length product (E2 subunit of KGDHC), this gene encodes truncated mRNA for another protein designated MIRTD, that localizes to mitochondria where it somehow regulates the biogenesis of mitochondrial respiratory chain (Kanamori *et al.* 2003).

In summary, we found that $Dld^{+/-}$ mice show increased vulnerability to MPTP, malonate and 3-NP. These findings provide further evidence that reductions in KGDHC may contribute to the pathogenesis of neurodegenerative diseases.

Acknowledgements

Sharon Melanson, Greta Strong and Connie Boyd are thanked for secretarial assistance. This work was supported by grants from the Department of Defense, National Institute on Aging (NIA) grant AG 14930 and the Parkinson's Disease Foundation.

References

Alston T. A., Mela L. and Bright H. J. (1977) 3-Nitropropionate, the toxic substance of Indigo/era, is a suicide inactivator of succinate dehydrogenase. *Proc. Natl Acad. Sci. USA* **74**, 3767–3771.

Arrigon O. and Singer T. (1962) Limitations of the phenazine methosulfate assay for succinic and related dehydrogenases. *Nature* **193**, 1256–1258.

Beal M. F. (2001) Experimental models of Parkinson's disease. *Nat. Rev. Neurosci.* **2**, 325–334.

Beal M. F., Brouillet E., Jenkins B. G., Ferrante R. J., Kowall N. W., Miller J. M., Storey E., Srivastava R., Rosen B. R. and Hyman B. T. (1993a) Neurochemical and histological characterization of striatal excitotoxic lesions produced by the mitochondrial toxin 3-nitropropionic acid. *J. Neurosci.* **13**, 4181–4192.

Beal M. F., Brouillet E., Jenkins B., Henshaw R., Rosen B. and Hyman B. T. (1993b) Age-dependent striatal excitotoxic lesions produced by the endogenous mitochondrial inhibitor malonate. *J. Neurochem.* **61**, 1147–1150.

Beal M. D., Ferrante R. J., Henshaw R., Matthews R. T., Chan P. H., Kowall N. W., Epstein C. J. and Schulz J. B. (1995) 3-Nitroproprionic acid neurotoxicity is attenuated in copper/zinc superoxide dismutase transgenic mice. *J. Neurochem.* **65**, 919–922.

Bodganov M. B., Andreassen O. A., Dedeoglu A., Ferrante R. J. and Beal M. F. (2001) Increased oxidatve damage to DNA in transgenic mouse model of Huntington's disease. *J. Neurochem.* **79**, 1246–1249.

Brouillet E., Hantraye P., Ferrante R. J., Dolan R., Leroy-Willig A., Kowall N. W. and Beal M. F. (1995) Chronic mitochondrial energy impairment produces selective striatal degeneration and abnormal choreiform movements in primates. *Proc. Natl Acad. Sci. USA* **92**, 7105–7109.

Browne S. E., Ferrante R. J. and Beal M. F. (1999) Oxidative stress in Huntington's disease. *Brain Pathol.* **9**, 147–163.

Butterworth J., Yates C. M. and Reynolds G. P. (1985) Distribution of phosphate-activated glutaminase, succinic dehydrogenase, pyruvate dehydrogenase and gamma-glutamyl transpeptidase in post-mortem brain from Huntington's disease and agonal cases. *J. Neurol. Sci.* **67**, 161–171.

Butterworth R. F. and Besnard A. M. (1990) Thiamine-dependent enzyme changes in temporal cortex of patients with Alzheimer's disease. *Metab. Brain Dis.* **5**, 179–184.

Chinopoulos C., Tretter L. and. Adam-Vizi V. (1999) Depolarization of *in situ* mitochondria due to hydrogen peroxide-induced oxidative stress in nerve terminals: inhibition of alpha-ketoglutarate dehydrogenase. *J. Neurochem.* **73**, 220–228.

Coles C. J., Edmondson D. E. and Singer T. P. (1979) Inactivation of succinate dehydrogenase by 3-nitropropionate. *J. Biol. Chem.* **254**, 5161–5167.

Ferrante R. J., Shinobu L. A., Schult Z. J. B., Matthews R. T., Thomas C. E., Kowall N. W., Gurney M. E. and Beal M. F. (1997) Increased 3-nitrotyrosine and oxidative damage in mice with a human copper/zinc superoxide dismutase mutation. *Ann. Neurol.* **42**, 326–334.

Giasson B. I., Duda J. E., Murray I. V., Chen Q., Souza J. M., Hurtig H. I., Ischiropoulos H., Trojanowski J. Q. and Lee V. M. (2000) Oxidative damage linked to neurodegeneration by selective alpha-synuclein nitration in synucleinopathy lesions. *Science* **290**, 985–989.

Gibson G. E., Sheu R. K. F., Blass J. P., Baker A., Carlson K. C. and Harding B. and. Perrino P. (1988) Reduced activities of thiamine-dependent enzymes in the brains and peripheral tissues of patients with Alzheimer's disease. *Arch. Neurol.* **45**, 836–840.

Gibson G. E., Zhang H., Sheu K. F.-R., Bogdanovich N., Lindsay J. G., Lannfelt L., Vestling M. and Cowburn R. F. (1998) Alpha-ketoglutarate dehydrogenease in Alzheimer brain bearing the APP670/671 mutation. *Ann. Neurol.* **44**, 671–681.

Gibson G. E., Park L. C., Sheu K. F., Blass J. P. and Calingasan N. Y. (2000) The alpha-ketoglutarate dehydrogenase complex in neurodegeneration. *Neurochem. Int.* **36**, 97–112.

Gibson G. E., Zhang H., Xu H., Park L. C. and Jeitner T. M. (2002) Oxidative stress increases internal calcium stores and reduces a key mitochondrial enzyme. *Biochim. Biophys. Acta* **1586**, 177–189.

Gibson G. E., Kingsbury A. E., Xu H., Lindsay J. G., Daniel S., Foster O. J. F., Lees A. J. and Blass J. P. (2003) Deficits in a Krebs cycle

enzyme in brains from patients with Parkinson's disease. *Neurochem. Int.* **43**, 129–135.

Good P. F., Hsu A., Werner P., Perl D. P. and Olanow C. W. (1998) Protein nitration in Parkinson's disease. *J. Neuropathol. Exp. Neurol.* **57**, 338–339.

Gould D. H. and Gustine D. L. (1982) Basal ganglia degeneration, myelin alterations, and enzyme inhibition in mice induced by the plant toxin 3-nitropropionic acid. *Neuropathol. Appl. Neurobiol.* **8**, 377–393.

Gould D. H., Wilson M. P. and Hamar D. W. (1985) Brain enzyme and clinical alterations induced in rats and mice by nitroaliphatic toxicants. *Toxicol. Lett.* **27**, 83–89.

Greene J. G., Porter R. H., Eller R. V. and Greenamyre J. T. (1993) Inhibition of succinate dehydrogenase by malonic acid produces an 'excitotoxic' lesion in rat striatum. *J. Neurochem.* **61**, 1151–1154.

Hantraye P., Brouillet E., Ferrante R., Palfi S., Dolan R., Matthews R. T. and Beal M. F. (1996) Inhibition of neuronal nitric oxide synthase prevents MPTP-induced parkinsonism in baboons. *Nat. Med.* **2**, 1017–1021.

Hassel B. and Sonnewald U. (1995) Selective inhibition of the tricarboxylic acid cycle of GABAergic neurons with 3-nitropropionic acid In vivo. *J. Neurochem.* **65**, 1184–1191.

Huang H. M., Toral-Barza L., Sheu K. F. R. and Gibson G. E. (1994) The role of calcium in the regulation of pyruvate dehydrogenase in synaotosomes. *Neurochem. Res.* **19**, 89–95.

Joffe G. T. P., Parks J. K. and Parker W. D. Jr (1998) Secondary inhibition of 2-ketoglutarate dehydrogenase complex by MPTP. *Neuroreport* **9**, 2781–2783.

Johnson M. T., Yang H.-S., Magnuson T. and Patel M. S. (1997) Targeted disruption of the murine dihydrolipoamide dehydrogenase gene (*Dld*) results in perigastrulation lethality. *Proc. Natl Acad. Sci. USA* **94**, 14512–14517.

Kanamori T., Nishimaki K., Asoh S. *et al.* (2003) Truncated product of the bifunctional DLST gene involved in biogenesis of the respiratory chain. *EMBO J.* **22**, 2913–2923.

Kish S. J., Mastrogiacomo F., Guttman M., Furukawa Y., Taanman J. W., Dozic S., Pandolfo M., Lamarche J., DiStefano L. and Chang L. J. (1999) Decreased brain protein levels of cytochrome oxidase subunits in Alzheimer's disease an in hereditary spinocerebellar ataxia disorders: a nonspecific change? *J. Neurochem.* **72**, 700–707.

Kobayashi T., Matsumine H., Matuda S. and Mizuno Y. (1998) Association between the gene encoding the E2 subunit α-ketoglutarate dehydrogenase complex and Parkinson's disease. *Ann. Neurol.* **43**, 120–123.

Ksiezak-Reding H., Blass J. P. and Gibson G. E. (1982) Studies on the pyruvate dehydrogenase complex in brain with the arylamine acetyl-transferase-coupled assay. *J. Neurochem.* **38**, 1627–1636.

McNaught K. S., Altomare C., Cellamare S., Carotti A., Thull U., Carrupt P. A., Testa B., Jenner P. and Marsden C. D. (1995) Inhibition of alpha-ketoglutarate dehydrogenase by isoquinoline derivatives structurally related to 1-methyl-4-phenyl-1,2,3,6-tetrahydropyridine (MPTP). *Neuroreport* **6**, 1105–1108.

Mizuno Y., Sone N., Suzuki K. and Saitoh T. (1988) Studies on the toxicity of 1-methyl-4-phenylpyridinium ion (MPP+) against mitochondria of mouse brain. *J. Neurol. Sci.* **86**, 97–110.

Mizuno Y., Suzuki K. and Ohta S. (1990) Postmortem changes in mitochondrial respiratory enzymes in brain and a preliminary observation in Parkinson's disease. *J. Neurol. Sci.* **96**, 49–57.

Mizuno Y., Matuda S., Yoshino H., Mori H., Hattori N. and Ikebe S.-I. (1994) An immunohistochemical study on α-ketoglutarate dehydrogenase complex in Parkinson's disease. *Ann. Neurol.* **35**, 204–210.

Mizuno Y., Ikebe S., Hattori N., Nakagawa-Hattori Y., Mochizuki H., Tanaka M. and Ozawa T. (1995) Role of mitochondria in the etiology and pathogenesis of Parkinson's disease. *Biochim. Biophys. Acta* **1271**, 265–274.

Palfi S., Ferrante R. J., Brouillet E., Beal M. F., Dolan R., Guyot M. C., Peschanski M. and Hantraye P. (1996) Chronic 3-nitropropionic acid treatment in baboons replicates the cognitive and motor deficits of Huntington's Disease. *J. Neurosci.* **16**, 3019–3025.

Park L. C., Zhang H., Sheu K. F., Calingasan N. Y., Kristal B. S., Lindsay J. G. and Gibson G. E. (1999) Metabolic impairment induces oxidative stress, compromises inflammatory responses, and inactivates a key mitochondrial enzyme in microglia. *J. Neurochem.* **72**, 1948–1958.

Perez-Severiano F., Rios C. and Segovia J. (2000) Striatal oxidative damage parallels the expression of a neurological phenotype in mice transgenic for the mutation of Huntington's disease. *Brain Res.* **862**, 234–237.

Porter D. J. T. and Bright H. J. (1980) 3-Carbanionic substrate analogues bind very tightly to fumarase and aspartase. *J. Biol. Chem.* **255**, 4772–4780.

Przedborski S., Jackon-Lewis V., Yokoyama R., Shibata T., Dawson V. L. and Dawson T. M. (1996) Role of neuronal nitric oxide in 1-methyl-4-phenyl-1,2,3,6-tetrahydropyridine (MPTP)-induced dopaminergic neurotoxicity. *Proc. Natl Acad. Sci. USA* **93**, 4565–4571.

Rosenthal R. E., Hamud F., Fiskum G., Varghese P. J. and Sharpe S. (1987) Cerebral ischemia and reperfusion: prevention of brain mitochondria injury by lidoflazine. *J. Cereb. Blood Flow Metab.* **7**, 752–758.

Schooner W. G., Wanamarta A. H., van der Klei-van Moorsel J. M., Jakobs C. and Joenje H. (1990) Respiratory failure and stimulation of glycolysis in Chinese hamster ovary cells exposed to normobaric hyperoxia. *J. Biol. Chem.* **265**, 1118–1124.

Schooner W. G., Wanamarta A. H., van der Kleivan Moorsel J. M., Jakobs C. and Joenje H. (1991) Characterization of oxygen-resistant Chinese hamster ovary cells. III. Relative resistance of succinate and alpha-ketoglutarate dehydrogenase to hyperoxic inactivation. *Free Radic. Biol. Med.* **10**, 111–118.

Schulz J. B., Henshaw D. R., Matthews R. T. and Beal M. F. (1995a) Coenzyme Q_{10} and nicotinamide and a free radical spin trap protect against MPTP neurotoxicity. *Exp. Neurol.* **132**, 279–283.

Schulz J. B., Henshaw D. R., Siwek D., Jenkins B. G., Ferrante R. J., Cipolloni P. B., Kowall N. W., Rosen B. R. and Beal M. F. (1995b) Involvement of free radicals in excitotoxicity *in vivo*. *J. Neurochem.* **64**, 2239–2247.

Shen X. M., Li H. and Dryhurst G. (2000) Oxidative metabolites of 5-*S*-cysteinyldopamine inhibit the alpha-ketoglutarate dehydrogenase complex: possible relevance to the pathogenesis of Parkinson's disease. *J. Neural Transm.* **107**, 959–978.

Sheu K. F., Brown A. M., Kristal B. S., Kalaria R. N., Lilius L., Lannfelt L. and Blass J. P. (1999) A *DLST* gene associated with reduced risk for Alzheimer's disease. *Neurology* **52**, 1505–1507.

Sheu R.-K. F., Cooper A. J., Koike K., Koike M., Lindsay J. G. and Blass J. P. (1994) Abnormality of the alpha-ketoglutarate dehydrogenase complex in fibroblasts from familial Alzheimer's disease. *Ann. Neurol.* **35**, 312–318.

Sorbi S., Bird E. D. and Blass J. P. (1983) Decreased pyruvate dehydrogenase complex activity in Huntington and Alzheimer brain. *Ann. Neurol.* **13**, 72–78.

Starkov A. A. and Fiskum G. (2003) Regulation of brain mitochondrial H_20_2 production by membrane potential and NAD(P)H redox state. *J. Neurochem.* **86**, 1101–1107.

Tabrizi S. J., Workman J., Hart P. E., Mangiarini L., Mahal A., Bates G., Cooper J. M. and Schapira A. H. (2000) Mitochondrial dysfunction and free radical damage in the Huntington R6/2 transgenic mouse. *Ann. Neurol.* **47**, 80–86.

Journal of Neuroscience Research 74:278–285 (2003)

APPENDIX 5

Minocycline Enhances MPTP Toxicity to Dopaminergic Neurons

Lichuan Yang,[1] Shuei Sugama,[2] Jason W. Chirichigno,[1] Jason Gregorio,[1] Stefan Lorenzl,[1] Dong H. Shin,[2] Susan E. Browne,[1] Yoshinori Shimizu,[2] Tong H. Joh,[2] M. Flint Beal,[1] and David S. Albers[1]

[1]Neurochemistry and Neurodegenerative Disease Laboratory, Weill Medical College at Cornell University, New York, New York

[2]Burke Medical Research Institute, Department of Neurology and Neuroscience, Weill Medical College at Cornell University, New York, New York

Minocycline has been shown previously to have beneficial effects against ischemia in rats as well as neuroprotective properties against excitotoxic damage in vitro, nigral cell loss via 6-hydroxydopamine, and to prolong the life-span of transgenic mouse models of Huntington's disease (HD) and amyotrophic lateral sclerosis (ALS). We investigated whether minocycline would protect against toxic effects of 1-methyl-4-phenyl-1,2,3,6-tetrahydropyridine (MPTP), a toxin that selectively destroys nigrostriatal dopaminergic (DA) neurons and produces a clinical state similar to Parkinson's disease (PD) in rodents and primates. We found that although minocycline inhibited microglial activation, it significantly exacerbated MPTP-induced damage to DA neurons. We present evidence suggesting that this effect may be due to inhibition of DA and 1-methyl-4-phenylpridium (MPP^+) uptake into striatal vesicles.

Key words: inflammation; Parkinson's disease; vesicles; tetracycline; doxycycline

Parkinson's disease (PD) is a neurodegenerative disorder of unknown etiology characterized by the loss of dopaminergic neurons (DA) in the substantia nigra pars compacta (SNpc). The clinical features of PD include a resting tremor, bradykinesia, stooped posture, shuffling gait, difficulty swallowing, and rigidity in the extremities accompanied by a loss in control of fine movements. A pivotal event in PD research was the demonstration of the toxicity of 1-methyl-4-phenyl-1,2,3,6-tetrahydropyridine (MPTP) to DA neurons. Systemic administration of MPTP produces DA cell loss and a clinical state similar to idiopathic PD in both humans and experimental animals (Langston et al., 1983; Heikkila et al., 1984). MPTP is converted to its toxic metabolite 1-methyl-4-phenylpyridium (MPP^+) by monoamine oxidase B (Chiba et al., 1984). MPP^+ is accumulated actively in DA neurons by the high-affinity DA transporter (Javitch et al., 1985) and exerts its toxic effects by inhibiting complex I of the mitochondrial electron transport chain (Nicklas et al., 1985) leading to many deleterious consequences, including increased free radical production, resulting ultimately in cell death.

There is accumulating evidence that suggests the involvement of specific immune reactions in pathogenesis of several neurodegenerative disorders, including PD (McGeer et al., 1993). These include studies demonstrating the presence of microglia, T-lymphocytes, and inducible nitric oxide synthase (iNOS) in PD SNpc as well as increased expression of inflammatory cytokines in the striatum from parkinsonian brains (for review, see Nagatsu et al., 2000). Further, microglial and astrocytic proliferation have been described in damaged regions after MPTP administration (Kurkowska-Jastrzebska et al., 1999). These results, coupled with the observation that tyrosine-hydroxylase (TH)-immunoreactive SNpc cell bodies in mice lacking the iNOS gene are relatively resistant to MPTP toxicity (Liberatore et al., 1999), suggest that glial activation and the subsequent release of nitric oxide (NO) may contribute to MPTP toxicity.

Minocycline, a second-generation tetracycline, has anti-inflammatory properties independent of its antimicrobial effects. Minocycline has been reported to have beneficial effects against both focal and global ischemia in rats (Yrjanheikki et al., 1998, 1999) as well as neuroprotective properties against excitotoxic damage in vitro and nigral cell loss via 6-hydroxydopamine in mice (He et al., 2001; Tikka et al., 2001). It has been reported to delay disease progression and prolong the life-span of transgenic

Contract grant sponsor: USAMRC; Contract grant sponsor: The Parkinson's Disease Foundation; Contract grant sponsor: National Institute of Neurological Disorders and Stroke (NINDS).

*Corresponding author: M. Flint Beal, MD, Department of Neurology and Neuroscience, Weill Medical College at Cornell University, Room F 610, 525 East 68th Street, New York, NY 10021.
E-mail: fbeal@med.cornell.edu

Received 22 April 2003; Revised 16 May 2003; Accepted 20 May 2003

Published online 26 August 2003 in Wiley InterScience (www.interscience.wiley.com). DOI: 10.1002/jnr.10709

mouse models of Huntington's disease (HD) and amyotrophic lateral sclerosis (ALS) (Chen et al., 2000; Zhu et al., 2002). Several mechanisms have been suggested to explain these neuroprotective properties of minocycline, including inhibition of caspase-1, caspase-3, inducible nitric oxide synthase (iNOS) expression, and the mitochondrial permeability transition (Amin et al., 1996; Yrjanheikki et al., 1998, 1999; Chen et al., 2000; Du et al., 2001; He et al., 2001; Tikka et al., 2001; Zhu et al., 2002). We investigated whether minocycline would protect against toxic effects of MPTP. A recent report showed that minocycline blocked MPTP-induced microglial activation and toxicity to DA neurons (Wu et al., 2002). Using a different dosing regimen, we found that minocycline blocked MPTP-induced microglial activation, but in contrast we found that MPTP toxicity to DA neurons was exacerbated.

MATERIALS AND METHODS

MPTP, tetracycline, doxycycline, minocycline, amphetamine, and creatine were obtained from Sigma (St. Louis, MO). Minocycline (0.005%), creatine (2%), and the combined minocycline (0.005%)/creatine (2%) test diets were manufactured by Purina Test Diet, Inc. (Richmond, IN). All drugs were dissolved in phosphate-buffered saline (PBS; pH 7.4).

Animals and Drug Administration

All experiments were conducted in either young (2–3 month) or old (8 month) male C57BL mice (Jackson Labs, Bar Harbor, ME) in accordance with the NIH Guide for the Care and Use of Laboratory Animals, and all procedures were approved by a local Animal Care and Use Committee. Mice were group-housed at 20–22°C and maintained on a 12-hr light-dark cycle with food and water available ad lib.

Mice received four intraperitoneal (i.p.) injections of MPTP (5, 10, 15, or 20 mg/kg) or PBS vehicle at 2-hr intervals, as described previously (Sonsalla et al., 1992). Mice were pretreated 1 day before MPTP administration with minocycline, doxycycline, tetracycline (2× 45 mg/kg or 60 mg/kg i.p.), or PBS vehicle at 12-hr intervals. Mice were again treated with PBS or minocycline, doxycycline, or tetracycline (2× 45mg/kg or 60 mg/kg at 12-hr intervals) on the day of MPTP administration and post-treated for 1 day with a reduced dose (2× 22.5 mg/kg or 30 mg/kg at 12-hr intervals). We also tested effects on MPTP toxicity of minocycline administered orally, either by gavage or in the diet. Mice were pretreated 2 days before MPTP administration with PBS or minocycline (1× 90 or 120 mg/kg/day, orally by gavage) and for 7 days after MPTP treatment. In another experimental group, mice were fed for 2 weeks before and during MPTP administration (4× 10 mg/kg at 2-hr intervals) with diets containing minocycline (0.005%), creatine (2%), or combined minocycline (0.005%)/creatine (2%). Control animals were fed unsupplemented diet. In these studies, animals were fed the special diets throughout the study period until the day of sacrifice. In all MPTP experiments, mice were sacrificed 7 days after MPTP treatment. Both neostriata were dissected, frozen rapidly and stored at −80°C until assayed.

Neurochemical Measurements

Striatal levels of DA and its metabolites were measured by high-pressure liquid chromatography (HPLC) with electrochemical detection, and TH activity by a radioenzymatic technique as described previously (Albers et al., 1996; Yang et al., 1998). Striatal MPP^+ levels were measured by HPLC with UV detection as described previously (Matthews et al., 1999). All samples were normalized for protein content, which was determined spectrophotometrically using the Bio-Rad protein assay kit (Bio-Rad, Hercules, CA).

HPLC Assay for Minocycline and Tetracycline

For HPLC determinations of minocycline and tetracycline levels, 4 animals were examined from each group (minocycline or tetracycline alone and minocycline or tetracycline with co-injection of MPTP). Minocycline or tetracycline were administered at 45 mg/kg i.p. twice per day, starting 12 hr before administration of MPTP, which was administered at 10 mg/kg i.p. every 2 hr, for 4 doses. At 2 hr after the last MPTP dose and 1 hr after the last minocycline or tetracycline dose, animals were perfused intracardially with PBS to wash out blood from the brain, and perfused brain tissues were taken for HPLC assay.

Dissected striata were sonicated and centrifuged (14,000 × *g*, 2× 10 min) in chilled 0.05 M perchloric acid, and 50 μl of supernatant was isocratically eluted through a 250 × 4.6 mm × 5 μm C18 column (Tosoh Biosep, Japan) with a mobile phase containing 200 mM NaH_2PO_4, 1 mM 1-octanesulfonic acid, and 25% (v/v) acetonitrile, and detected at 354 nm wavelength by a Waters 490 UV detector (Sharon, MA). Concentrations of minocycline and tetracycline are expressed as pg/mg protein. Protein concentration was determined by using the Bio-Rad method and Perkin Elmer Bio Assay Reader (Norwalk, CT).

Vesicle Preparation

Vesicles were prepared as described previously (Staal and Sonsalla, 2000). Striata from mice (total of 120–150 mg wet weight tissue) were homogenized in 0.32 M sucrose and subjected to a number of centrifugation steps. At the end of the last centrifugation, the pellet was resuspended in vesicle assay buffer (VAB, pH 7.4): 25 mM HEPES, 100 mM potassium tartrate, 0.5 mM EDTA, 0.05 mM EGTA, 2 mM ATP-Mg^{2+}, 1.7 mM ascorbic acid and 4 mM KCl, pH 7.4). The final vesicle suspension was used for [^{3}H]-DA and [^{3}H]-MPP^+ uptake and protein determination.

Vesicular [^{3}H]-DA and [^{3}H]-MPP^+ Uptake

Vesicle suspensions (5 μg protein) were incubated with buffers containing [^{3}H]-DA and cold DA or [^{3}H]-MPP^+ and cold MPP for 2 min at 37°C and uptake terminated by the addition of ice-cold VAB (no ascorbate or ATP-Mg^{2+}) as described previously (Del Zompo et al., 1993; Staal et al., 2000). Vesicles were collected on Whatman F filters washed with 0.5% polyethylenenine to prevent MPP^+ sticking to glass filters, washed with ice-cold VAB, and immersed in ethanol to extract the [^{3}H]-DA or [^{3}H]-MPP^+. Radioactivity was determined by scintillation spectroscopy. Nonspecific uptake was determined as

TABLE I. Neurochemical Effects of MPTP and Minocycline in Young and Old C57BL Mice†

Treatment	*n*	DA (ng/mg protein)	DOPAC (ng/mg protein)	DOPAC/DA ratio	HVA (ng/mg protein)	TH activity (nmol/g/hr)
Young mice (2–3 months old)						
PBS	26	124 ± 7.7	10.4 ± 0.8	0.10 ± 0.01	14.4 ± 0.5	519 ± 26
Minocycline (2 × 45 mg/kg, ip)	22	130 ± 9.2	12.4 ± 1.2	0.12 ± 0.02	16.3 ± 0.7	588 ± 64
MPTP (4 × 10 mg/kg)	33	66 ± 3.8*	7.9 ± 1.0*	0.10 ± 0.01	10.4 ± 0.4*	260 ± 27*
+ Minocycline (2 × 45 mg/kg, ip)	20	36 ± 3.6**	7.2 ± 1.2*	0.18 ± 0.02**	8.2 ± 0.4**	130 ± 18**
+ Minocycline (2 × 60 mg/kg, ip)	10	43 ± 4.2**	13.5 ± 1.0**	0.18 ± 0.01**	9.2 ± 0.4**	ND
+ Minocycline (1 × 90 mg/kg, po)	9	49 ± 5.2**	16.6 ± 1.3**	0.20 ± 0.01**	9.8 ± 0.4*	ND
+ Minocycline (1 × 120 mg/kg, po)	11	53 ± 4.6**	16.3 ± 1.2**	0.18 ± 0.01**	10.1 ± 0.3*	ND
MPTP (4 × 15 mg/kg)	32	36 ± 3.3*	2.6 ± 0.2*	0.09 ± 0.002	6.5 ± 0.3*	ND
+ Minocycline (2 × 45 mg/kg, ip)	31	19 ± 1.8**	1.7 ± 0.1**	0.12 ± 0.04**	5.3 ± 0.2**	ND
MPTP (4 × 20 mg/kg)	10	24 ± 2.4*	2.3 ± 0.2*	0.10 ± 0.01	5.7 ± 0.4*	ND
+ Minocycline (2 × 45 mg/kg, ip)	10	16 ± 3.9**	1.5 ± 0.2**	0.14 ± 0.01**	4.4 ± 0.4**	ND
Old mice (8 months old)						
PBS	7	80 ± 4.7	14.7 ± 3.3	0.19 ± 0.05	9.4 ± 0.4	340 ± 34
Minocycline (2 × 45 mg/kg, ip)	8	82 ± 1.6	16.0 ± 3.0	0.20 ± 0.03	10.5 ± 0.4	370 ± 22
MPTP (4 × 5 mg/kg)	10	33 ± 6.4*	12 ± 1.9	0.38 ± 0.03*	6.7 ± 0.6*	222 ± 38*
MPTP + minocycline	9	16 ± 3.9**	7.6 ± 1.3**	0.52 ± 0.05**	5.4 ± 0.5*	104 ± 16**

†Data expressed as mean ± SEM. ND, not determined. DA, dopamine; DOPAC, 3,4-dihydroxyphenylacetic acid; HVA, homovanillic acid; TH, tyrosine hydroxlase.
*Significantly different from PBS-treated controls ($P < 0.05$).
**Significantly different from MPTP-treated mice ($P < 0.05$).

TABLE II. TH-Immunopositive and Cresyl Violet-Stained Cell Counts in SNpc 7 days After Minocycline and MPTP Treatment†

Treatment	*n*	TH-immunopositive neurons	Cresyl violet-stained neurons
PBS	4	10,320 ± 303	13,016 ± 494
Minocycline alone (2 × 45 mg/kg, ip)	4	10,658 ± 160	13,160 ± 450
MPTP alone (4 × 10 mg/kg, ip)	4	9,286 ± 186*	11,416 ± 284*
Minocycline + MPTP	4	3,720 ± 792**	4,816 ± 304**

†Data expressed as mean ± SEM. TH, tyrosine hydroxylase.
*Statistically different from PBS alone ($P < 0.05$).
**Statistically different from MPTP alone ($P < 0.05$).

[^{3}H]-DA or [^{3}H]-MPP$^+$ uptake in samples incubated on ice, and by the effects of amphetamine.

Immunostaining for Tyrosine Hydroxylase and Microglia

Hindbrains from mice were fixed in 4% paraformaldehyde for 24 hr and cryoprotected in 30% sucrose overnight. Sections (40 μm) were washed for 30 min in PBS, incubated with 1% bovine serum albumin (BSA) and 0.2% Triton X-100 in 0.1 M PBS for 1 hr, washed in PBS containing 0.5% BSA for 30 min, then incubated overnight in blocking solution containing antibodies to either TH (1:25,000; Weiser et al., 1993) or CD11b (1:1,000: Serotec, UK). CD11b reacts with the mouse complement type 3 receptor (CR3). Sections were washed in PBS-BSA, incubated for 1 hr with biotinylated secondary anti-rabbit or anti-rat antibodies (Vector Laboratories, Burlingame, CA) and visualized by reaction with 3,3′-diaminobenzidine-tetrahydrochloride (DAB; 0.05%) as a chromagen and hydrogen peroxide (0.003%) for 5 min. Sections were mounted on gelatin-coated slides, dehydrated through graded ethanols, and cleared in xylene before being coverslipped with Permount.

Cresyl Violet Staining

Midbrain sections containing SNpc were stained with cresyl violet. Sections were then mounted on gelatinized slides, left to dry overnight, dehydrated in increasing alcohol concentrations, and coverslipped with Permount.

Cell Counting

The total number of TH-immunoreactive cell bodies and cresyl violet-stained SNpc neurons were counted in 4 mice per group using the optical dissector technique, as published previously (Coggeshall, 1992; Gundersen, 1992; DeGiorgio et al., 1998; Volpe et al., 1998) with minor modifications. In brief, serial midbrain sections containing SNpc were stained for TH and cresyl violet. Digital images of TH-immunoreactive SNpc neurons were acquired at 30× magnifications on a Zeiss Axiophot microscope fitted with an Axiocam video camera. A counting frame (100 μm × 100 μm) created by KS 400 image analysis software (Zeiss, Thornwood, NY) was systematically passed over the outlined SNpc by a motorized stage. Neurons were counted under 100× oil magnification as they appeared within the counting frame (50 μm × 50 μm). This procedure

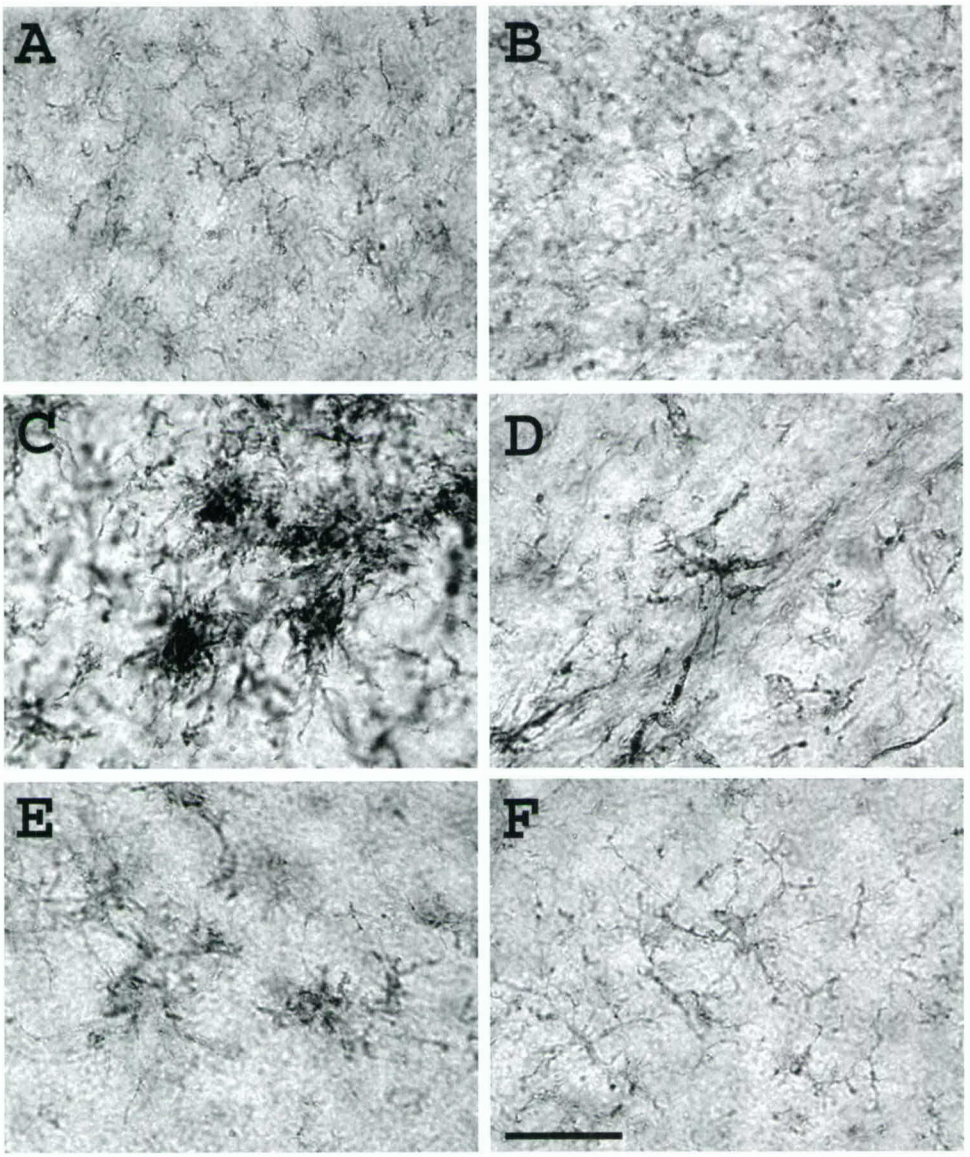

Fig. 1. Microglial staining in SNpc (**A,C,E**) and SNpr (**B,D,F**) in 8-month-old mice treated with PBS (A,B), MPTP alone (C,D), and MPTP+ minocycline. (E,F). As expected, there is robust microglial activation after MPTP treatment in the SNpc and SNpr (C,D), which is blocked by concurrent administration of minocycline (E,F). Scale bar = 20 μm.

was carried out on four sections at a periodicity of 160 μm in the SNpc. All TH- or cresyl violet-stained neurons were counted. An average neuron density was obtained by summing the number of neuron profiles divided by the calculated volume. The total number of neurons was calculated as the product of the neuron density and the volume of SNpc as described previously (Volpe et al., 1995; DeGiorgio et al., 1998).

Statistical Analysis

Values of neurochemical measurements are expressed as the mean ± SEM. Results were analyzed by non-parametric Mann-Whitney *U*-test or one-way analysis of variance (ANOVA) followed by Newman-Keuls test (Instat, San Diego, CA). Differences were considered significant at $P < 0.05$.

RESULTS AND DISCUSSION

The MPTP dosing regimens employed in these studies have been characterized previously (Sonsalla et al., 1992) and shown to result in moderate DA depletion within the adult mouse striatum. Seven days after MPTP treatment, striatal DA, its metabolites 3,4-dihydroxyphenylacetic acid (DOPAC) and homovanillic acid (HVA), as well as tyrosine hydroxylase (TH) activity were decreased in a dose-dependent manner (Table I). Using an

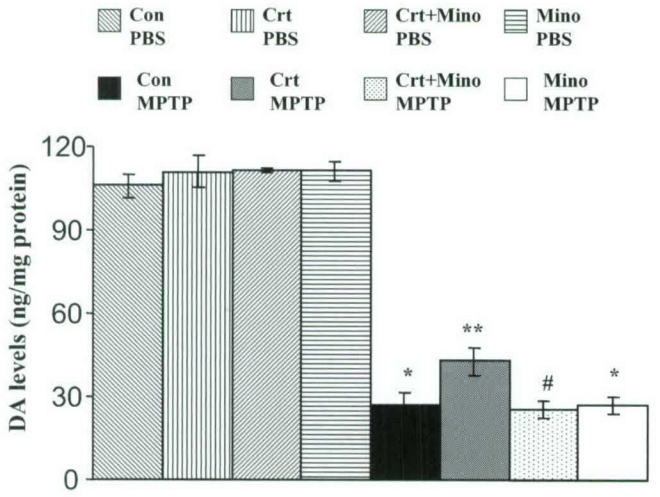

Fig. 2. Effects of 0.005% minocycline supplementation on MPTP toxicity. Mice were fed control, minocycline (mino)-containing, 2% creatine (crt)-containing, or minocycline and creatine (crt+mino)-containing mouse feed for 2 weeks before MPTP administration. Data are expressed as the mean ± SEM of 10 mice per group. Minocycline supplementation did not have any effect whereas creatine supplementation reversed the effects of MPTP toxicity as compared to MPTP-treated mice on control diet. The mixed diet produced the same level of DA depletion as MPTP-treated mice on control diet, suggesting minocycline reversed the creatine effect. *Significantly different from PBS-treated animals, $P < 0.05$; **Significantly different from MPTP-treated animals, $P < 0.05$; #Significantly different from CRT + MPTP-treated animals, $P < 0.05$.

intraperitoneal dosing paradigm for minocycline shown previously to be neuroprotective (Yrjanheikki et al., 1998, 1999), we observed a significant reduction ($P < 0.05$) in striatal DA levels and TH activities in young (2–3 month) mice treated with MPTP and minocycline, as compared to mice treated with MPTP alone, for all doses of MPTP tested (Table I). Minocycline alone did not have any effect on striatal DA levels or TH activity 7 days after administration.

Striatal MPP^+ levels measured 2 hr after the last MPTP injection (4× 10 mg/kg) in young mice were not different in animals treated with MPTP alone, or MPTP and minocycline (686 ± 149 and 675 ± 111 ng/mg protein, respectively; $P > 0.05$). Of note, a significant reduction in body weight (from 25.7 ± 0.1 to 24.3 ± 0.1 g; $P < 0.001$) was observed in minocycline-treated mice after pretreatment; this reduction was not observed in PBS-injected control mice in this same period. After MPTP injections, both minocycline-injected mice and PBS-treated controls showed similar weight losses (24.3 ± 0.1 to 23.0 ± 0.2 g, $P < 0.01$; and 25.8 ± 0.2 to 24.5 ± 0.3 g, $P < 0.01$, respectively). Further, there was an accompanying 10% loss of TH-immunopositive cell bodies in the substantia nigra pars compacta (SNpc) in MPTP-treated mice (4× 10 mg/kg; Table II). This loss of TH-immunopositive neurons was exacerbated significantly (−65%) in mice co-treated with minocycline (Table II). We stained serial sections with cresyl violet to determine whether this loss of immunostaining was due to loss of TH-positive neurons, or a downregulation of TH. The reductions in cresyl violet-stained cells were similar to those found via TH immunohistochemistry, confirming the loss of TH-immunopositive cells (Table II). It is noteworthy that the mean number of SNpc neurons in our analysis is comparable to previously published reports (German and Manaye, 1993; Volpe et al., 1995).

It has been suggested that neuroprotective effects of minocycline are due to inhibition of microglial activation (Yrjanheikki et al., 1998, 1999; Chen et al., 2000; Du et al., 2001; He et al., 2001; Tikka et al., 2001; Wu et al., 2002). To examine effects of minocycline treatment on microglial activation in our dosing paradigm, we conducted studies in older mice (8 months), where a robust MPTP-induced microglial activation can been observed as early as 12 hrs post-MPTP and remains elevated for up to 14 days (Kurkowska-Jastrzebska et al., 1999). A lower dose of MPTP (4× 5 mg/kg, i.p.) was administered due to the age-dependency of MPTP toxicity in older mice (Sonsalla et al., 1992). In agreement with our studies in young animals, a significant exacerbation in striatal DA depletion and decreased TH activity was measured in minocycline-treated MPTP mice (see Table I). The MPTP treatment induced robust microglial activation in the SNpc and substantia nigra pars reticulata (SNpr) of these animals, whereas the microglial staining pattern was less much intense in mice treated with minocycline and MPTP (Fig. 1), consistent with previous reports showing inhibition of microglial activation via minocycline (Yrjanheikki et al., 1998, 1999; Chen et al., 2000; He et al., 2001; Tikka et al., 2001; Wu et al., 2002).

It is clear from our studies that minocycline is not neuroprotective with the present dosing regimens of MPTP. Indeed, a range of doses of minocycline, as well as different routes of administration, all produced a consistent potentiation of MPTP-induced striatal damage. It is important to note that neither systemic minocycline alone nor minocycline via oral administration had any effect on basal striatal DA levels (Table I). In MPTP-treated mice (4× 10 mg/kg) fed mouse chow containing 0.005% minocycline, striatal DA levels were similar to MPTP-treated mice fed control diet (Fig. 2). Further, no apparent weight reduction was observed in the minocycline-fed mice (data not shown). Given the marked exacerbation of MPTP toxicity after intraperitoneal minocycline administration, these results suggest that the minocycline dose in the diet may be too low to exacerbate MPTP toxicity. Dietary supplementation of 0.005% minocycline, however, reversed the neuroprotective effects of 2% creatine (Matthews et al., 1999), suggesting that this dose of minocycline had a deleterious effect (Fig. 2).

We also examined the effects of tetracycline and doxycycline against MPTP toxicity in young mice. Consistent with our findings with minocycline, combined treatments of doxycycline with MPTP or tetracycline with MPTP produced greater reductions in striatal DA levels (Table III) as compared to mice treated with MPTP alone (4× 10 mg/kg). The results with tetracycline were unex-

TABLE III. Minocycline, Doxycycline, and Tetracycline in the Presence and Absence of MPTP in Two- to Three-Month-Old C57BL Mice†

Treatment	*n*	Striatal DA (ng/mg protein)	Striatal TH activity (nmol/g/hr)
PBS	9	123 ± 5.5	534 ± 31
Minocycline alone (2 × 45 mg/kg, ip)	5	132 ± 3.3	588 ± 68
Doxycycline alone (2 × 45 mg/kg, ip)	5	131 ± 11	590 ± 20
Tetracycline alone (2 × 45 mg/kg, ip)	5	140 ± 5.6	634 ± 38
MPTP alone (4 × 10 mg/kg)	20	73 ± 8.1★	268 ± 17★
Minocycline + MPTP	11	38 ± 7.2★★	130 ± 18★★
Doxycycline + MPTP	10	32 ± 4.8★★	194 ± 15★★
Tetracycline + MPTP	11	43 ± 8.7★★	135 ± 20★★

†Data expressed as mean ± SEM. DA, dopamine; TH, tyrosine hydroxylase.
★Significantly different from PBS-treated controls ($P < 0.05$).
★★Significantly different from MPTP-treated mice ($P < 0.05$).

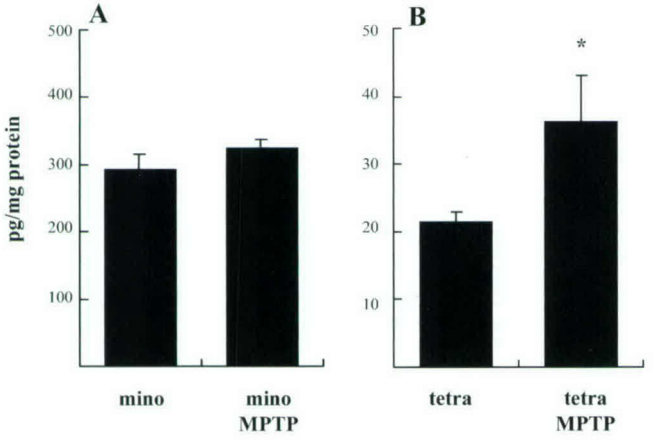

Fig. 3. Minocycline and tetracycline brain levels before and after MPTP administration. Data are mean ± SEM. ★Significantly different from tetracycline alone ($P < 0.05$).

pected due to its low brain penetration. We therefore measured brain minocycline and tetracycline levels after administration of the compounds both alone and with MPTP (15 mg/kg × 4 doses). We found that brain concentrations of minocycline were approximately 10-fold greater than those of tetracycline; however, tetracycline did accumulate in brain, and levels were almost doubled after MPTP administration (Fig. 3).

The exacerbation of MPTP-induced damage by minocycline is strikingly similar to the neurochemical deficits observed by two independent groups in MPTP-treated VMAT2 knockout mice (Takahashi et al., 1997; Gainetdinov et al., 1998). Furthermore, pharmacologic inhibition of VMAT2 exacerbates MPTP toxicity (German et al., 2000). Thus, we investigated whether minocycline had a direct effect on VMAT2 function, in particular reducing the sequestration of DA into vesicles. In vesicular preparations from C57BL/6 mouse striata, we observed V_{max} values for [^{3}H]-DA uptake consistent with those reported previously (Del Zompo et al., 1993; Staal and Sonsalla, 2000). Moreover, [^{3}H]-DA uptake was blocked by amphetamine (1 and 10 μM) by 44 and 80%, respectively (data not shown), consistent with a previous study (Del Zompo et al., 1993), which demonstrates the integrity of our vesicular preparations. In these preparations, the addition of minocycline (0.1, 1, and 10 μM) decreased V_{max} values for [^{3}H]-DA uptake (Fig. 4) by 23, 30, and 40% (1 and 10 μM were significant; $P < 0.05$), respectively, compared to vehicle-treated controls. We also found that minocycline significantly inhibited vesicular uptake of MPP^+. As shown in Table I, the DOPAC/DA ratio was increased consistently in mice treated with minocycline and MPTP, consistent with an effect on VMAT2, because this increases dopamine in the cytoplasm, allowing more to be metabolized to DOPAC.

Our studies therefore demonstrate that minocycline exacerbates MPTP-induced damage to DA neurons by interfering acutely with VMAT2 function (i.e., sequestration of MPP^+, DA, or both). It is well established that vesicular uptake of MPP^+ reduces its toxicity (Liu et al., 1992; Staal and Sonsalla, 2000). This seems to account for the resistance of rats to MPTP (Staal et al., 2000). Thus, perturbation in intracellular sequestration of MPP^+, via pharmacologic or genetic manipulation, results in increased concentrations of free MPP^+, resulting in increased mitochondrial accumulation and more extensive damage to DA neurons. Further, compromised VMAT2 function can lead to increased free DA within the presynaptic nerve terminal, which in turn can lead to the formation DA metabolites (increased DOPAC/DA ratios; Table I) as we observed. DA quinones and reactive oxygen species can modify protein function directly by oxidative modifications (Berman and Hastings, 1999; Kristal et al., 2001). The present data coupled with a recent report describing the destruction of synaptic vesicles by protofibrillar α-synuclein (Volles et al., 2001), highlights the vulnerability of DA neurons to pharmacologic, environmental, or genetic insults that affect specific vesicular properties. Furthermore, DA neurons are selectively vulnerable to toxic effects of overexpression of α-synuclein in vitro (Xu et al., 2002).

Previous studies have suggested the suppression of microglial activation by minocycline accounts for the ob-

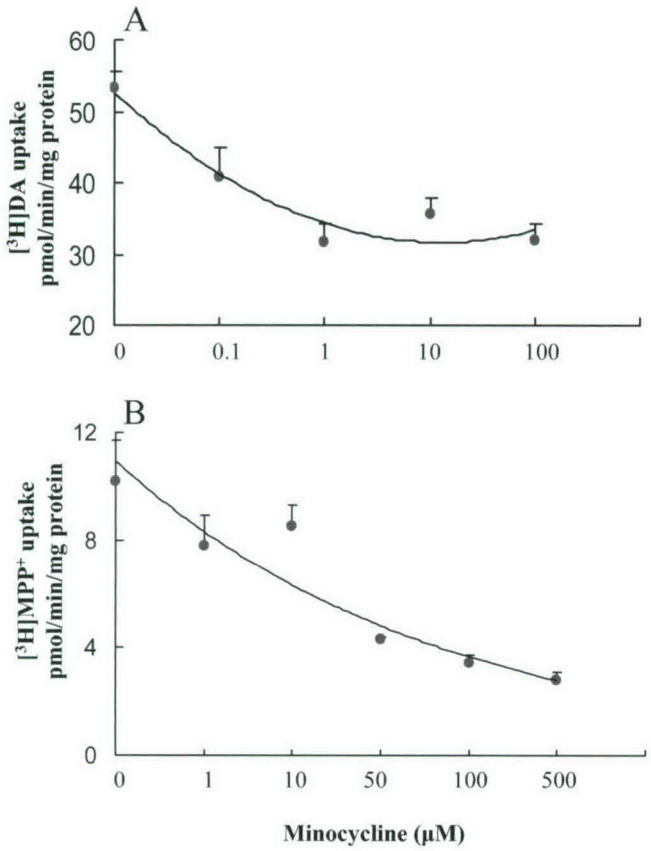

Fig. 4. Effects of minocycline on [^{3}H]-DA or [^{3}H]-MPP$^+$ uptake into vesicular preparations. Uptake of [^{3}H]-DA into vesicles isolated from C57BL/6 mouse striata was inhibited by the addition minocycline (0.1–10 μM) in a dose-dependent manner as compared to vehicle controls. Data are expressed as mean ± SEM of four separate experiments. *Significantly different from vehicle-containing controls.($P < 0.05$).

served neuroprotection (Amin et al., 1996; Yrjanheikki et al., 1998, 1999; Chen et al., 2000; Du et al., 2001; He et al., 2001; Tikka et al., 2001; Wu et al., 2002), although the mechanisms by which microglia become activated remain unknown. One consequence of a microglial response is the recruitment of other components of an immune response such as cytokines including IL-1β, IL-6, TNF-α, and IFN-γ, which may be part of a repair and protect response. Thus, it is tempting to speculate that another mechanism to explain the effect of minocycline on MPTP-induced toxicity is that minocycline suppresses the ability of microglia to supply these cytokines needed for neuronal survival; however, microglia also produce proinflammatory cytokines and oxygen-derived reactive species, namely nitric oxide (NO) from iNOS, which have been demonstrated to play a role in MPTP-mediated neuronal injury (Liberatore et al., 1999). Inhibiting inflammation may not always be beneficial, because recent work showed MPTP-induced dopamine depletion was exacerbated in IL-6-deficient mice as well as mice deficient in TNFα receptors (Bolin et al., 2002; Rousselet et al., 2002).

A recent study by Du et al. (2001) reported neuroprotective effects of minocycline in the MPTP-treated mouse model. In their study, the observed neuroprotection by minocycline was associated with its ability to suppress the MPTP-induced increases in iNOS and caspase-1 expression in the midbrain. They administered minocycline by gavage in sucrose. Similarly, the recent study of Wu et al. (2002) showed neuroprotective effects of minocycline against MPTP-induced damage to TH neurons, which was attributed to inhibition of microglia. In this study, protection was seen with MPTP administered 4 times at 16 mg/kg but not at 18 mg/kg. This dosing regimen differed from ours. We administered minocycline every 12 hr for 3 days starting 1 day before the first MPTP dose, whereas they administered minocycline i.p. starting 30 min. after the first MPTP dose and then for an additional 4 days. Another group reported that minocycline blocked the microglial response in the nigra and did not affect striatal DA depletion induced by MPTP (Ghulam et al., 2001).

We observed robust nigral microglial activation after MPTP administration that was reversed by minocycline, consistent with previous reports. Nevertheless, relative to levels in vehicle-treated mice, there was increased striatal DA depletion in mice treated with minocycline and MPTP, as compared to MPTP-treated mice. These studies clearly demonstrate the ability of minocycline to block inflammatory responses resulting from MPTP treatment, yet it is perplexing that the results on dopaminergic markers vary between laboratories. It is possible that differences in routes of administration, dosing intervals, or drug concentrations could account for such differences. The present data show that minocycline significantly exacerbates MPTP-induced damage to DA neurons and inhibits VMAT2 function of striatal vesicles, which is a novel mechanism of action. The results suggest that although minocycline is a promising neuroprotective agent for the treatment of neurodegenerative disease, some caution in its administration may be warranted.

REFERENCES

Albers DS, Zeevalk GD, Sonsalla PK. 1996. Damage to dopaminergic nerve terminals in mice by combined treatment of intrastriatal malonate with systemic methamphetamine or MPTP. Brain Res 718:217–220.

Amin AR, Thakker GD, Patel PD, Vyas PR, Patel RN, Patel IR, Abramson SB. 1996. A novel mechanism of action of tetracyclines: effects on nitric oxide synthases. Proc Natl Acad Sci USA 93:14014–14019.

Berman SB, Hastings TG. 1999. Dopamine oxidation alters mitochondrial respiration and induces permeability transition in brain mitochondria: implications for Parkinson's disease. J Neurochem 73:1127–1137.

Bolin LM, Strycharska-Orczyk I, Murray R, Langston JW, DiMonte D. 2002. Increased vulnerability of dopaminergic neurons in MPTP-lesioned interleukin-6 deficient mice. J Neurochem 83:167–175.

Chen MO, Li M, Ferrante RJ, Fink KB, Zhu S, Bian J, Guo L, Farrell LA, Hersch SM, Hobbs W, Vonsattel JP, Cha JH, Friedlander RM. 2000. Minocycline inhibits caspase-1 and caspase-3 expression and delays mortality in a transgenic mouse model of Huntington disease. Nat Med 6:797–801.

Chiba K, Trevor A, Castagnoli N Jr. 1984. Metabolism of the neurotoxic tertiary amine, MPTP, by brain monoamine oxidase. Biochem Biophys Res Commun 120:574–578.

Coggeshall R. 1992. A consideration of neural counting methods. Trends Neurosci 15:9–12.

DeGiorgio LA, Dibinis C, Milner TA, Saji M, Volpe BT. 1998. Histological and temporal characteristics of nigral transneuronal degeneration after striatal injury. Brain Res 795:1–9.

Del Zompo M, Piccardi MP, Ruiu S, Quartu M, Gessa GL, Vaccari A. 1993. Selective MPP+ uptake into synaptic dopamine vesicles: possible involvement in MPTP neurotoxicity. Br J Pharmacol 109:411–414.

Du Y, Ma Z, Lin S, Dodel RC, Gao F, Bales KR, Triarhou LC, Chernet E, Perry KW, Nelson DL, Luecke S, Phebus LA, Bymaster FP, Paul SM. 2001. Minocycline prevents nigrostriatal dopaminergic neurodegeneration in the MPTP model of Parkinson's Disease. Proc Natl Acad Sci USA 98:14669–14674.

Gainetdinov RR, Fumagalli F, Wang YM, Jones SR, Levey AI, Miller GW, Caron MG. 1998. Increased MPTP neurotoxicity in vesicular monoamine transporter 2 heterozygote knockout mice. J Neurochem 70:1973–1978.

German DC, Liang CL, Manaye KF, Lane K, Sonsalla PK. 2000. Pharmacological inactivation of the vesicular monoamine transporter can enhance 1-methyl-4-phenyl-1,2,3,6-tetrahydropyridine-induced neurodegeneration of midbrain dopaminergic neurons, but not locus coeruleus noradrenergic neurons. Neuroscience 101:1063–1069.

German DC, Manaye KE. 1993. Midbrain dopaminergic neurons (Nuclei A9 and A10). J Comp Neurol 331:297–309.

Ghulam N, Sager T, Laursen H, Vaudano E. 2001. Minocycline reduces microglia activation in the chronic MPTP mouse model of Parkinson's Disease. Soc Neurosci 27:887–888.

Gundersen HJ. 1992. Stereology: the fast lane between neuroanatomy and brain function—or still only a tightrope? Acta Neurol Scand 137:8–13.

He Y, Appel S, Le W. 2001. Minocycline inhibits microglial activation and protects nigral cells after 6-hydroxydopamine injection into mouse striatum. Brain Res 909:187–193.

Heikkila RE, Hess A, Duvoisin RC. 1984. Dopaminergic neurotoxicity of 1-methyl-4-phenyl-1,2,3,6-tetrahydropyridine mice. Science 224:1451–1453.

Javitch JA, D'Amato RJ, Strittmatter SM, Snyder SH. 1985. Parkinsonism-induced neurotoxin, N-methyl-4-phenyl-1,2,3,6-tetrahydropyridine: uptake of the metabolite N-methyl-4-phenylpyridinium by dopamine neurons explains selective toxicity. Proc Natl Acad Sci USA 82:2173–2177.

Kristal BS, Conway AD, Brown AM, Jain JC, Ulluci PA, Li SW, Burke WJ. 2001. Selective dopaminergic vulnerability: 3,4-dihydroxy-phenylacetaldehyde targets mitochondria. Free Rad Biol Med 30:924–931.

Kurkowska-Jastrzebska I, Wronska A, Kohutnicka M, Czlonkowska A, Czlonkowska A. 1999. The inflammatory reaction following 1-methyl-4-phenyl-1,2,3,6-tetrahydropyridine intoxication in mouse. Exp Neurol 156:50–61.

Langston JW, Ballard P, Tetrud JW, Irwin I. 1983. Chronic parkinsonism in humans due to a product of meperidine-analog synthesis. Science 219:979–980.

Liberatore GT, Vukosavic S, Mandir AS, Vila M, McAuliffe WG, Dawson VL, Dawson TM, Przedborski S. 1999. Inducible nitric oxide synthase stimulates dopaminergic neurodegeneration in the MPTP model of Parkinson's disease. Nat Med 5:1403–1409.

Liu Y, Peter D, Roghani A, Schuldiner S, Prive GG, Eisenberg D, Brecha N, Edwards RH. 1992. A cDNA that suppresses MPP+ toxicity encodes a vesicular amine transporter. Cell 70:539–551.

Matthews RT, Klivenyi P, Yang L, Klein AM, Mueller G, Kaddurah-Daouk R, Beal MF. 1999. Creatine and cyclocreatine attenuate MPTP neurotoxicity. Exp Neurol 157:142–149.

McGeer PL, Kawamata T, Walker DG, Akiyama H, Tooyama I, McGeer EG. 1993. Microglia in degenerative neurological disease. Glia 7:84–92.

Nagatsu T, Mogi M, Ichinose H, Togari A. 2000. Changes in cytokines and neurotrophins in Parkinson's disease .J Neural Transm Suppl 60:277–920.

Nicklas WJ, Vyas I, Heikkila RE. 1985. Inhibition of NADH-linked oxidation by brain mitochondria by 1-methyl-4-phenylpyridine, a metabolite of the neurotoxin, 1-methyl-4-phenyl-1,2,3,6-tetrahydropyridine. Life Sci 36:2503–2508.

Rousselet E, Callebert J, Parain K, Joubert C, Hunot S, Hartmann A, Jacque C, Perez-Diaz F, Cohen-Salmon C, Launay J-M, Hirsch EC. 2002. Role of TNFalpha receptors in mice intoxicated with the parkinsonian toxin MPTP. Exp Neurol 17:183–192.

Sonsalla PK, Giovanni A, Sieber BA, Donne KD, Manzino L. 1992. Characteristics of dopaminergic neurotoxicity produced by MPTP and methamphetamine. Ann N Y Acad Sci 648:229–238.

Staal RG, Hogan KA, Liang C-L, German DC, Sonsalla PK. 2000. In vitro studies of striatal vesicles containing the vesicular monoamine transporter (VMAT2): Rat versus mouse differences in sequestration of 1-methyl-4-phenylpyridinium. J Pharmacol Exp Ther 293:329–335.

Staal RG, Sonsalla PK. 2000. Inhibition of brain vesicular monoamine transporter (VMAT2) enhances 1-methyl-4-phenylpyridium in vivo in rat striata. J Pharmacol Exp Ther 293:336–342.

Takahashi N, Miner LL, Sora I, Ujike H, Revay RS, Kostic V, Jackson-Lewis V, Przedborski S, Uhl GR. 1997. VMAT2 knockout mice: heterozygotes display reduced amphetamine-conditioned reward, enhanced amphetamine locomotion, and enhanced MPTP toxicity. Proc Natl Acad Sci USA 94:9938–9943.

Tikka T, Fiebich BL, Goldsteins G, Keinanen R, Koistinaho J. 2001. Minocycline, a tetracycline derivative, is neuroprotective against excitotoxicity by inhibiting activation and proliferation of microglia. J Neurosci 21:2580–2588.

Volles MJ, Lee SJ, Rochet JC, Shtilerman MD, Ding TT, Kessler JC, Lansbury PT Jr. 2001. Vesicle permeabilization by protofibrillar alpha-synuclein: implications for the pathogenesis and treatment of Parkinson's disease. Biochemistry 40:7812–7819.

Volpe BT, Blau AD, Wessel TC, Saji M. 1995. Delayed histopathological neuronal damage in the substantia nigra compacta (nucleus A9) after transient forebrain ischaemia. Neurobiol Dis 2:119–127.

Volpe BT, Wildmann J, Altar CA. 1998. Brain-derived neurotrophic factor prevents the loss of nigral neurons induced by excitotoxic striatal-pallidal lesions. Neuroscience 83:741–748.

Weiser M, Baker H, Wessel TC, Joh TH. 1993. Differential spatial and temporal gene expression in response to axotomy and deafferentation following transection of the medial forebrain bundle. J Neurosci 13:3472–3484.

Wu DC, Jackson-Lewis V, Vila M, Tieu K, Teismann P, Vadseth C, Choi D-K, Ischiropoulos H, Przedborski S. 2002. Blockade of microglial activation is neuroprotective in the 1-methyl-4-phenyl-1,2,3,6-tetrahydropyridine mouse model of Parkinson's disease. J Neurosci 22:1763–1771.

Xu J, Kao SY, Lee FJ, Song W, Jin LW, Yankner BA. 2002. Dopamine-dependent neurotoxicity of alpha-synuclein: a mechanism for selective neurodegeneration in Parkinson disease. Nat Med 8:600–606.

Yang L, Schulz JB, Klockgether T, Liao AW, Martinou JC, Penney JB Jr, Hyman BT, Beal MF. 1998. 1-Methyl-4-phenyl-1,2,3,6-tetrahydropyridine neurotoxicity is attenuated in mice overexpressing Bcl-2. J Neurosci 18:8145–8152.

Yrjanheikki J, Keinanen R, Goldsteins G, Chan PH, Koistinaho J. 1999. A tetracycline derivative, minocycline, reduces inflammation and protects against focal cerebral ischemia with a wide therapeutic window. Proc Natl Acad Sci USA 96:13496–13500.

Yrjanheikki J, Pellikka M, Hokfelt T, Koistinaho J. 1998. Tetracyclines inhibit microglial activation and are neuroprotective in global brain ischemia. Proc Natl Acad Sci USA 95:15769–15774.

Zhu S, Stavrovskaya IG, Drozda M, Kim BY, Ona V, Li M, Sarang S, Liu AS, Hartley DM, Wu du C, Gullans S, Ferrante RJ, Przedborski S, Kristal BS, Friedlander RM. 2002. Minocycline inhibits cytochrome c release and delays progression of amyotrophic lateral sclerosis in mice. Nature 417:74–78.

Journal of Neurochemistry, 2003, **86**, 267–272

APPENDIX 6

doi:10.1046/j.1471-4159.2003.01868.x

Increased survival and neuroprotective effects of BN82451 in a transgenic mouse model of Huntington's disease

Peter Klivenyi,* Robert J. Ferrante,† Gabrielle Gardian,* Susan Browne,* Pierre-Etienne Chabrier‡ and M. Flint Beal*

**Department of Neurology and Neuroscience, Weill Medical College of Cornell University, New York-Presbyterian Hospital, New York*

†*Geriatric Research Education and Clinical Center, Bedford VA Medical Center, Bedford, MA and Neurology, Pathology and Psychiatry Departments, Boston University School of Medicine, Boston, Massachusetts, USA*

‡*Department of Biochemical Pharmacology, Institute Henri Beaufour, Les Ulis, France*

Abstract

There is substantial evidence that excitotoxicity and oxidative damage may contribute to Huntington's disease (HD) pathogenesis. We examined whether the novel anti-oxidant compound BN82451 exerts neuroprotective effects in the R6/2 transgenic mouse model of HD. Oral administration of BN82451 significantly improved motor performance and improved survival by 15%. Oral administration of BN82451 significantly reduced gross brain atrophy, neuronal atrophy and the number of neuronal intranuclear inclusions at 90 days of age. These findings provide evidence that novel anti-oxidants such as BN82451 may be useful for treating HD.

Keywords: experimental therapeutics, huntington, inflammation, neurodegeneration, oxidative damage, transgenic mice.

J. Neurochem. (2003) **86,** 267–272.

Huntington's disease (HD) is an autosomal dominant progressive neurodegenerative disease that starts in mid life and eventually leads to death. The mean survival after onset is 15–20 years and at present there is no known effective treatment for HD. The mutation that causes the illness is an expanded CAG/polyglutamine repeat stretch that has been postulated to confer its toxic effects by a gain of function. There is accumulating evidence that the polyglutamine expansion causes effects on gene transcription (Cha 2000; Luthi-Carter *et al.* 2000; Wyttenbach *et al.* 2002). These effects may be secondarily linked to energy dysfunction, oxidative damage and excitotoxicity, which are implicated in the pathogenesis of HD. Alternatively, N-terminal fragments of huntingtin may directly impair mitochondrial function (Panov *et al.* 2002).

A breakthrough in HD research was the development of transgenic mouse models. Transgenic mice with exon 1 of the human HD gene with an expanded CAG repeat develop a progressive neurological disorder (Mangiarini *et al.* 1996). These mice (line R6/2) have CAG repeat lengths of 141–157 under the control the human HD promotor. At approximately 6 weeks of age, the R6/2 mice show loss of body weight, and at 9–11 weeks they develop an irregular gait, stuttering stereotypic movements, resting tremors and epileptic seizures. The mice develop progressive weight loss and brain atrophy. Neuronal intranuclear inclusions that are immunopositive for huntingtin and ubiquitin are detected in the striatum at 4.5 weeks.

We and others found that that there is evidence of increased oxidative damage in the R6/2 transgenic mouse model of HD. It was shown that there is increased immunostaining for 3-nitrotyrosine, increased lipid peroxidation and increases in oxidative damage to DNA (Bogdanov *et al.* 2000; Perez-Severiano *et al.* 2000; Tabrizi *et al.* 2000). There is also some evidence that inflammatory mechanisms may contribute to disease pathogenesis (Ona *et al.* 1999; Luthi-Carter *et al.* 2000). In the present studies, we therefore examined whether a novel compound which has both

Received January 27, 2003; revised manuscript received April 14, 2003; accepted April 14, 2003.

Address correspondence and reprint requests to M. Flint Beal, MD, Chairman, Neurology Department, New York Presbyterian Hospital-Weill Medical College of Cornell University, 525 East 68th Street, New York, NY 10021, USA. E-mail: fbeal@med.cornell.edu

Abbreviations used: CBP, CREB binding protein; HD, Huntington's disease.

anti-oxidant and anti-inflammatory properties, BN82451, exerts beneficial effects on survival as well as motor performance and weight loss in the R6/2 transgenic mouse model of HD.

Materials and methods

Animals

Male transgenic HD mice of the R6/2 strain were obtained from Jackson Laboratories (Bar Harbor, ME, USA). Male R6/2 mice were bred locally with females from their background strain (B6CBAFI/J). The offspring were genotyped with a PCR assay on tail DNA. Nine to 10 mice in each group were examined for survival with equal numbers of males and females in each group. All animal experiments were carried out in accordance with the NIH *Guide for the Care and Use of Laboratory animals* and were approved by the local animal care committee.

Treatment

At 30 days of age the mice were fed lab chow diets supplemented with BN82451 at 0.015%, or a standard unsupplemented diet. Assuming an intake of 5 g of lab chow daily, this results in a dose of 30 mg/kg/day.

Behavior and weight assessment

Motor performance was assessed from 30 days of age in the R6/2 experiments ($n = 9$–10 mice per group) using the rotarod apparatus (Columbus Instruments, Columbus, OH, USA). Mice were tested at 12 r.p.m. Mice were given two trials and better result was recorded. They were weighed at the same time, once a week.

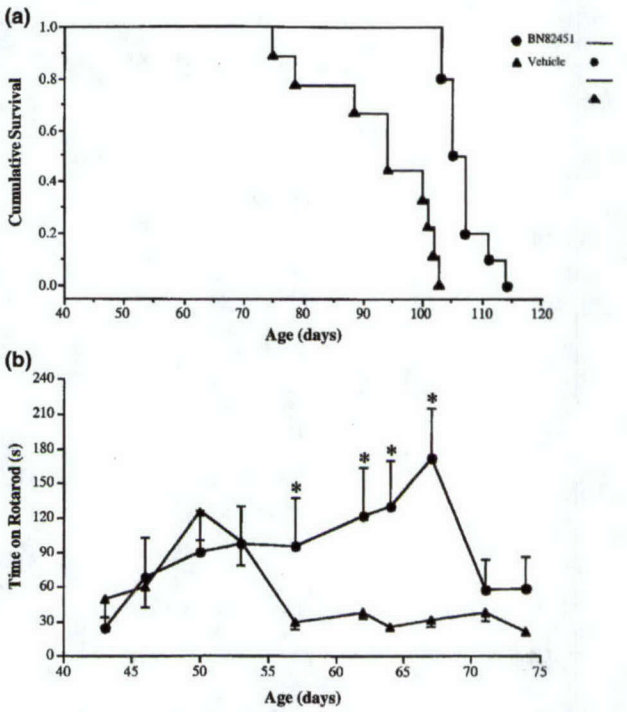

Fig. 1 (a) Cumulative probability of BN82451 on survival in R6/2 transgenic mice, $p < 0.001$ compared with controls. (b) Effects of BN82451 on rotorod performance in R6/2 transgenic mice. The treatment significantly improved motor performance on day 57, 60, 64 and 67 ($^*p < 0.05$).

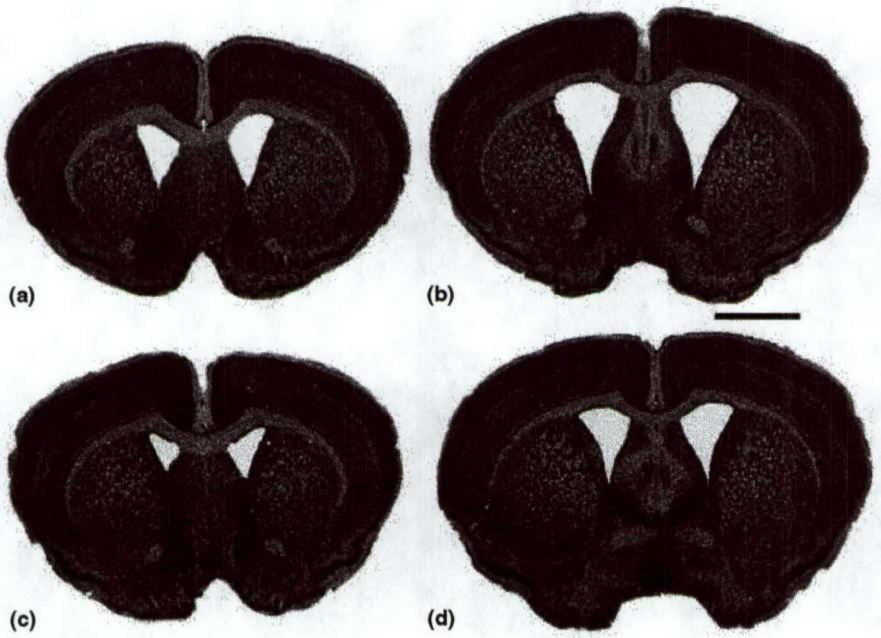

Fig. 2 Effects of BN8541 treatment on gross atrophy and ventricular enlargement in R6/2 mice at 10 weeks of age. Coronal step-sections through the rostral levels of the anterior commissure in untreated R6/2 (b and d) and BN8541-treated R6/2 mice (a and c). There is marked gross atrophy in the untreated R6/2 mouse tissues section with enlarged lateral ventricles. These findings are not as severe in the BN8541-treated mouse. Scale bar (shown in b): 2 mm.

Survival

Mice were observed every morning and late afternoon. The criteria for killing was the point in time at which mice were unable to initiate movement after being gently prodded for 2 min.

Stereology/quantitation

Serial-cut coronal tissue-sections from the rostral segment of the neostriatum at the level of the anterior commissure (interaural 5.34 mm/bregma 1.54 mm to interaural 3.7 mm/bregma −0.10 mm), were used for aggregate analysis. Unbiased stereologic counts of ubiquitin-positive aggregates (≥ 1.0 μm) were obtained from the neostriatum in 10 mice, each from BN82451-treated and unsupplemented diet R6/2 mice at 90 days using Neurolucida Stereo Investigator software (Microbrightfield, Colchester, VT, USA). The total areas of the neostriatum were defined in serial sections in which counting frames were randomly sampled. The dissector counting method was employed in which ubiquitin-positive aggregates were counted in an unbiased selection of serial sections in a defined volume of the neostriatum. Striatal neuron areas were analyzed by microscopic videocapture using a Windows-based image analysis system for area measurement (Optimas, Bioscan Incorporated, Edmonds, WA, USA). The software automatically identifies and measures profiles. Identified cell profiles were manually verified as neurons and exported to Microsoft Excel. Cross-sectional areas were analyzed using Statview.

Statistics

Data are expressed as the mean ± standard error of the mean (SEM). Rotarod and weight data were compared by analysis of variance (ANOVA). Survival data were analyzed by the Kaplan–Meier test.

Results

Oral administration of BN82451 in the diet resulted in significant improvements in the survival of R6/2 mice compared with the survival of mice fed unsupplemented diet (Fig. 1a). The controls deteriorated at 57 days and the treated mice at 72 days of age consistent with a delay in disease onset. The mean survival increased from 92.6 ± 3.5 days to 106.8 ± 1.1 days with BN82451 ($p < 0.001$). Survival was extended by 14 days (15.3%). The treated mice had significantly better motor performance from 57 to 67 days of age than mice fed unsupplemented diets (Fig. 1b). This finding was replicated in another group of control and BN82451-treated mice. The compound did not delay the weight loss, as there were no differences in body weight between the groups (data are not shown). Oral administration of BN82451 attenuated the development of gross atrophy and ventricular enlargement at 10 weeks of age (Fig. 2). At 90 days, striatal volumes: BN82451-treated R6/2 mice: 702 ± 41 mm^3; unsupplemented R6/2 mice: 576 ± 63 mm^3 0.76, $p < 0.01$. At 90 days, ventricular volumes: BN82451-treated R6/2 mice: 212 ± 27 mm^3; unsupplemented R6/2 mice: 120 ± 18 mm^3 0.76, $p < 0.01$. Oral administration of BN82451 also attenuated the development of neuronal atrophy (Fig. 3). Measurements of striatal neuron area at

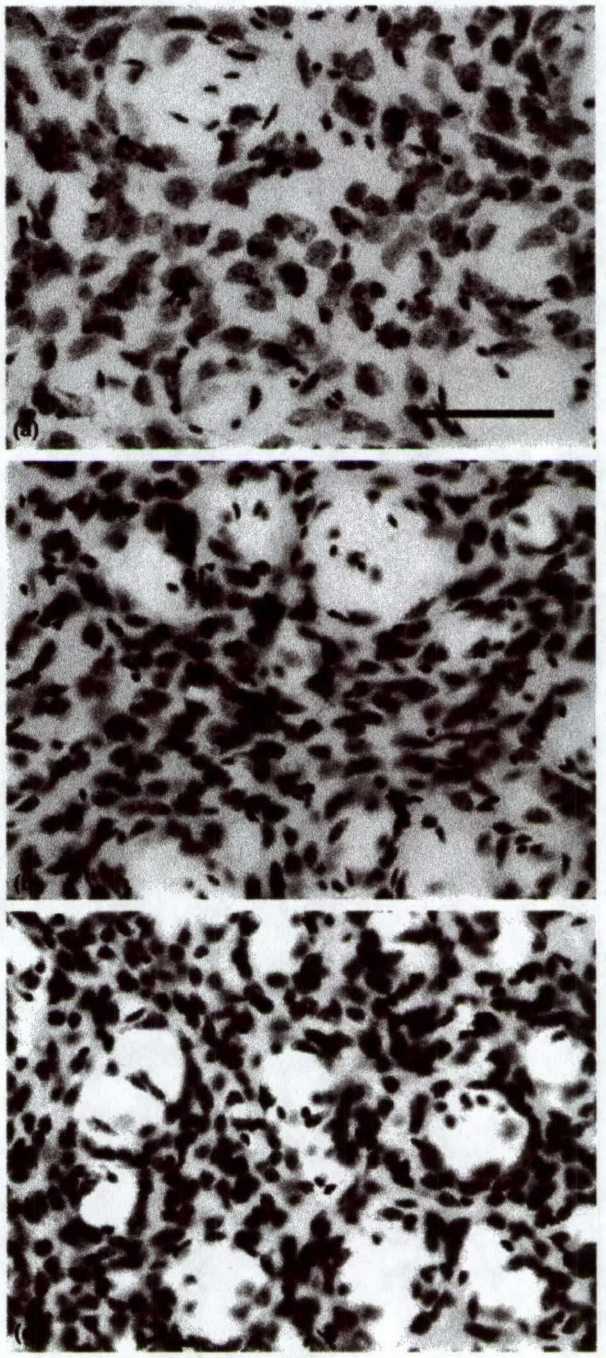

Fig. 3 Nissl-stained tissue sections from the dorso-medial aspect of the neostriatum at the level of the anterior commissure in a littermate wild-type control mouse (a), a BN8541-treated R6/2 mouse (b), and an untreated R6/2 mouse (c) at 10 weeks of age. There is marked neuronal atrophy in the untreated R6/2 mouse, with relative preservation of neuronal size in the BN8541-treated mouse, in comparison with the littermate control. Scale bar (shown in a): 100 μm.

90 days: wild-type littermate control: 114 ± 9.7 μm^2; BN82451-treated R6/2 mice: 79.5 ± 11.1 μm^2; unsupplemented R6/2 mice: 48.1 ± 17.2 μm^2; $p < 0.01$. Lastly,

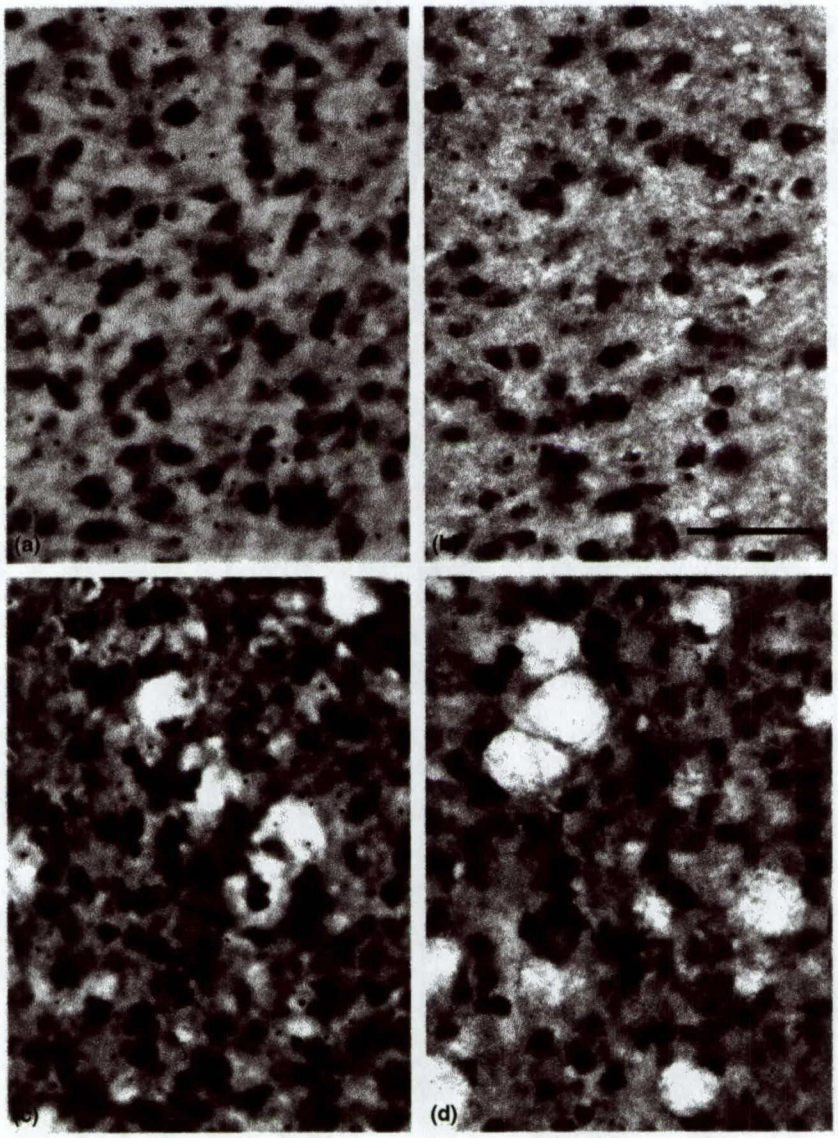

Fig. 4 Ubiquitin-immunostained tissue sections from the neocortex (a and b) and neostriatum (c and d) of untreated (a and c) and BN8541-treated (b and d) R6/2 mice at 10 weeks of age. While there were reduced numbers of ubiquitin-positive inclusions in both the neocortex and neostriatum of BN8541-treated mice, significance was only present in the neostriatum. Scale bar (shown in b): 100 μm.

administration of BN82451 significantly attenuated the numbers of striatal ubiquitin positive inclusions (Fig. 4). The number of aggregates at 90 days: BN82451-treated R6/2 mice: $1.16 \pm 0.43 \times 10^6$; unsupplemented R6/2 mice; $2.72 \pm 0.76 \times 10^6$, $p < 0.01$.

Discussion

The pathogenesis of neuronal degeneration in HD is an area of intense investigation. It has been demonstrated that huntingtin can directly bind to a number of transcription factors. These include the CREB binding protein (CBP) as well as Sp1 and several others (Steffan *et al.* 2000; Nucifora *et al.* 2001; Dunah *et al.* 2002; Li *et al.* 2002). Overexpression of either CBP or Sp1 can rescue cultured cells from the neurotoxicity of mutant huntingtin (Nucifora *et al.* 2001; Dunah *et al.* 2002). The precise mechanisms by which impaired gene transcription lead to cell death in HD, however, remain obscure. There is substantial evidence that both excitotoxicity and oxidative damage contribute to disease pathogenesis (Beal 1995). Transgenic mice with full length huntingtin expressed in a YAC construct show increased vulnerability to striatal excitotoxic lesions (Zeron *et al.* 2002). A secondary consequence of excitotoxicity is oxidative damage (Beal 1995). Expression of mutant huntingtin in neuronal and non-neuronal cells causes increased reactive oxygen species which contributes to cell death (Wyttenbach *et al.* 2002). A number of studies have demonstrated that there is increased oxidative damage in the R6/2 transgenic mouse model of HD. These mice show increased immunostaining for 3-nitrotyrosine, a marker of peroxynitrite-mediated oxidative damage (Tabrizi *et al.*

2000). They also show increased and progressive lipid peroxidation (Perez-Severiano *et al.* 2000). We recently examined concentrations of a marker of oxidative damage to DNA, 8-hydroxy-2-deoxyguanosine (Bogdanov *et al.* 2001). We found increased concentrations of 8-hydroxy-2-deoxyguanosine in the urine, plasma and striatal microdialysates of R6/2 HD mice. There were increased concentrations in isolated brain DNA at 12 and 14 weeks of age, and increased immunostaining in late stages of the illness.

There is also evidence that inflammation may contribute to disease pathogenesis in the R6/2 mice. Gene array studies show that there is increased expression of genes associated with inflammation at both 6 and 12 weeks of age in the R6/2 transgenic HD model (Luthi-Carter *et al.* 2000). There are increased concentrations of interleukin-1β, a pro-inflammatory cytokine (Ona *et al.* 1999). Inhibition of the interleukin-1β converting enzyme by crossing transgenic mice with a dominant-negative inhibitor of this enzyme into the R6/2 mice significantly extends survival (Ona *et al.* 1999). Lastly, minocycline, which is known to inhibit microglial activation, also shows neuroprotective effects in the R6/2 transgenic mice (Chen *et al.* 2000). Microglial activation is a prominent feature of the neuropathology of HD (Singhrao *et al.* 1999; Sapp *et al.* 2001).

In the present study, we therefore studied the effects of a novel compound which is an orally active brain permeable anti-oxidant, that not only acts as an inhibitor of lipid peroxidation but which also has potent anti-inflammatory effects (Chabrier *et al.* 2001). BN82451 has previously been shown to exert neuroprotective effects in animal models in which mitochondrial impairment was produced using malonate or MPTP (Chabrier *et al.* 2001). These models are associated with impaired ATP production as well as oxidative damage. Activated microglia may contribute to neuronal damage in these models, by secreting toxic substances, including free radicals, prostaglandins, inflammatory cytokines and proteolytic enzymes. BN82451 has both anti-oxidant effects, as well as anti-inflammatory activities, and blocking microglial activation and inhibiting cyclooxygenase enzymes following MPTP and malonate administration. *In vitro* BN82451 blocks lipid peroxidation of rat cerebral cortex homogenates with an IC_{50} of ~0.3 μm and it inhibits COX-1 and COX-2 with an IC_{50} of ~0.1 μm.

In the present experiments, we found that BN82451 produced significant improvements in survival and rotarod performance in the R6/2 transgenic mouse model of HD. Surprisingly, there were no effects on loss of body weight, suggesting that delay of weight loss does not necessarily accompany improved survival. It also significantly reduced striatal atrophy, neuronal atrophy and numbers of neuronal intranuclear inclusions. The improvement in survival of 15.3% is equivalent to the effects of co-enzyme Q10, and minocycline, although slightly less than the effects of creatine and cystamine (Chen *et al.* 2000; Ferrante *et al.* 2000; Dedeoglu *et al.* 2002; Ferrante *et al.* 2002). These findings, therefore, provide further evidence that both oxidative damage and inflammation may contribute to disease pathogenesis. They raise the possibility that agents which have anti-oxidative and anti-inflammatory activity may be useful as therapies to slow or halt the progression of neurodegeneration in HD. It is also possible that these agents might be useful in combination with other agents such as creatine, co-enzyme Q10, minocycline, and histone deacetylase inhibitors in producing additive therapeutic benefits for the treatment of HD.

Acknowledgements

Greta Strong and Sharon Melanson are thanked for secretarial assistance. This work was supported by NINDS grant NS39258, The Hereditary Disease Foundation and The Huntington's Disease Society of America.

References

Beal M. F. (1995) Aging, energy and oxidative stress in neurodegenerative diseases. *Ann. Neurol.* **38**, 357–366.

Bogdanov M., Brown R. H., Matson W., Smart R., Hayden D., O'Donnell H., Flint Beal M. and Cudkowicz M. (2000) Increased oxidative damage to DNA in ALS patients. *Free Radic. Biol. Med.* **29**, 652–658.

Bogdanov M. B., Andreassen O. A., Dedeoglu A., Ferrante R. J. and Beal M. F. (2001) Increased oxidative damage to DNA in a transgenic mouse model of Huntington's disease. *J. Neurochem.* **79**, 1–5.

Cha J. H. (2000) Transcriptional dysregulation in Huntington's disease. *Trends Neurosci.* **23**, 387–392.

Chabrier P. E., Roubert V., Harnett J., Cornet S., Delafotte S., Charnet-Roussillot C., Spinnewyn B. and Auguet M. (2001) New neuroprotective agents are potent inhibitors of mitochondrial toxins: *in vivo and in vitro* studies. *Soc. Neurosci. Abstr.* **27**, 530.

Chen M., Ona V. O., Li M., Ferrante R. J., Fink K. B., Zhu S., Bian J., Guo L., Farrell L. A., Hersch S. M., Hobbs W., Vonsattel J. P., Cha J. H. and Friedlander R. M. (2000) Minocycline inhibits caspase-1 and caspase-3 expression and delays mortality in a transgenic mouse model of huntington disease. *Nature Med.* **6**, 797–801.

Dedeoglu A., Jeitner T. M., Matson S. A., Kubilus J. K., Bogdanov M., Kowall N. W., Matson W. R., Cooper A. L., Ratan R. R., Beal M. F., Hersch S. M. and Ferrante R. J. (2002) Therapeutic effects of the transglutaminase inhibitor, cystamine, in a murine model of Huntington's disease. *J. Neurosci.* **22**, 8942–8950.

Dunah A. W., Jeong H., Griffin A., Kim Y. M., Standaert D. G., Hersch S. M., Mouradian M. M., Young A. B., Tanese N. and Krainc D. (2002) Sp1 and TAFII130 transcriptional activity disrupted in early Huntington's disease. *Science* **2**, 2.

Ferrante R. J., Andreassen O. A., Jenkins B. G., Dedeoglu A., Kuemmerle S., Kubilus J. K., Kaddurah-Daouk R., Hersch S. M. and Beal M. F. (2000) Neuroprotective effects of creatine in a transgenic mouse model of Huntington's disease. *J. Neurosci.* **20**, 4389–4397.

Ferrante R. J., Andreassen O. A., Dedeoglu A., Ferrante K. L., Jenkins B. G., Hersch S. M. and Beal M. F. (2002) Therapeutic effects of coenzyme Q10 and remacemide in transgenic mouse models of Huntington's disease. *J. Neurosci.* **22**, 1592–1599.

Li S. H., Cheng A. L., Zhou H., Lam S., Rao M., Li H. and Li X. J. (2002) Interaction of Huntington disease protein with transcriptional activator Sp1. *Mol. Cell Biol.* **22**, 1277–1287.

Luthi-Carter R., Strand A., Peters N. L., Solano S. M., Hollingsworth Z. R., Menon A. S., Frey A. S., Spektor B. S., Penney E. B., Schilling G., Ross C. A., Borchelt D. R., Tapscott S. J., Young A. B., Cha J. H. and Olson J. M. (2000) Decreased expression of striatal signaling genes in a mouse model of Huntington's disease. *Hum. Mol. Genet.* **9**, 1259–1271.

Mangiarini L., Sathasivam K., Seller M., Cozens B., Harper A., Hetherington C., Lawton M., Trottier Y., Lehrach H., Davies S. W. and Bates G. P. (1996) Exon 1 of the *HD* gene with an expanded CAG repeat is sufficient to cause a progressive neurological phenotype in transgenic mice. *Cell* **87**, 493–506.

Nucifora F. C. Jr, Sasaki M., Peters M. F., Huang H., Cooper J. K., Yamada M., Takahashi H., Tsuji S., Troncoso J., Dawson V. L., Dawson T. M. and Ross C. A. (2001) Interference by huntingtin and atrophin-1 with cbp-mediated transcription leading to cellular toxicity. *Science* **291**, 2423–2428.

Ona V. O., Li M., Vonsattel J. P., Andrews L. J., Khan S. Q., Chung W. M., Frey A. S., Menon A. S., Li X. J., Stieg P. E., Yuan J., Penney J. B., Young A. B., Cha J. H. and Friedlander R. M. (1999) Inhibition of caspase-1 slows disease progression in a mouse model of Huntington's disease. *Nature* **399**, 263–267.

Panov A. V., Gutekunst C. A., Leavitt B. R., Hayden M. R., Burke J. R., Strittmatter W. J. and Greenamyre J. T. (2002) Early mitochondrial calcium defects in Huntington's disease are a direct effect of polyglutamines. *Nat. Neurosci.* **1**, 1.

Perez-Severiano F., Rios C. and Segovia J. (2000) Striatal oxidative damage parallels the expression of a neurological phenotype in mice transgenic for the mutation of Huntington's disease. *Brain Res.* **862**, 234–237.

Sapp E., Kegel K. B., Aronin N., Hashikawa T., Uchiyama Y., Tohyama K., Bhide P. G., Vonsattel J. P. and DiFiglia M. (2001) Early and progressive accumulation of reactive microglia in the Huntington disease brain. *J. Neuropathol. Exp. Neurol.* **60**, 161–172.

Singhrao S. K., Neal J. W., Morgan B. P. and Gasque P. (1999) Increased complement biosynthesis by microglia and complement activation on neurons in Huntington's disease. *Exp. Neurol.* **159**, 362–376.

Steffan J. S., Kazantsev A., Spasic-Boskovic O., Greenwald M., Zhu Y. Z., Gohler H., Wanker E. E., Bates G. P., Housman D. E. and Thompson L. M. (2000) The Huntington's disease protein interacts with p53 and CREB-binding protein and represses transcription. *Proc. Natl Acad. Sci. USA* **97**, 6763–6768.

Tabrizi S. J., Workman J., Hart P. E., Mangiarini L., Mahal A., Bates G., Cooper J. M. and Schapira A. H. (2000) Mitochondrial dysfunction and free radical damage in the Huntington R6/2 transgenic mouse. *Ann. Neurol.* **47**, 80–86.

Wyttenbach A., Sauvageot O., Carmichael J., Diaz-Latoud C., Arrigo A. P. and Rubinsztein D. C. (2002) Heat shock protein 27 prevents cellular polyglutamine toxicity and suppresses the increase of reactive oxygen species caused by huntingtin. *Hum. Mol. Genet.* **11**, 1137–1151.

Zeron M. M., Hansson O., Chen N., Wellington C. L., Leavitt B. R., Brundin P., Hayden M. R. and Raymond L. A. (2002) Increased sensitivity to N-methyl-D-aspartate receptor-mediated excitotoxicity in a mouse model of Huntington's disease. *Neuron* **33**, 849–860.